1969

Partition of load in shingle joints

Ulise C. Rivera
Lehigh University

PARTITION OF LOAD IN SHINGLE JOINTS

by

Ulise C. Rivera

A Thesis

Presented to the Graduate Committee

of Lehigh University

in Candidacy for the Degree of

Master of Science

in

Civil Engineering

Lehigh University

1969

CERTIFICATE OF APPROVAL

This thesis is accepted and approved in partial fulfillment of the requirements of the degree of Master of Science.

May 16, 1969
(Date)

Dr. John W. Fisher
Professor in Charge

Dr. David A. VanHorn, Chairman
Department of Civil Engineering

ACKNOWLEDGMENTS

The present study was made at Lehigh University in the Fritz Engineering Laboratory as part of its civil engineering research. Dr. Lynn S. Beedle is Director of the Laboratory and Dr. David A. VanHorn is the Chairman of the Civil Engineering Department.

The study forms a part of Project 340: "Strength of Large Shingle Joints" sponsored financially by the Louisiana Department of Highways in cooperation with the U. S. Department of Transportation-Bureau of Public Roads. Technical guidance has been provided by the Research Council on Riveted and Bolted Structural Joints through an advisory committee under the chairmanship of Mr. T. W. Spilman.

Dr. J. W. Fisher supervised the work of this thesis. The author owes a special debt of gratitude to him for his advice, critical review, and encouragement.

The author wishes to express his appreciation for the help provided by a number of the research personnel at Fritz Engineering Laboratory. Thanks are extended to Dr. Roger G. Slutter, Director of the Operations Group and Mr. Joseph Corrado, Engineer of Tests for their advice. Mr. Kenneth Harpel, shop foreman and his staff were invaluable in their assistance during the performance of the testing. Thanks to Messrs. Hugh T. Sutherland

and Joseph Laurinitis for their advice in instrumentation; to Mr. Richard Sopko for the photography; to Mr. Jack Gera and Mrs. Sharon Balough for the drafting and to Miss Karen Philbin and Mrs. Shirley Labert for their care in typing this thesis. The help provided by his colleague on this project, Mr. Suresh Desai, is also sincerely appreciated.

TABLE OF CONTENTS

LIST OF TABLES

LIST OF FIGURES

ABSTRACT

This paper summarizes the results of tension tests of two large structural shingle joints of A572 steel. One joint was fastened with A325 bolts and the other with A502 Gr. 1 rivets. A theoretical analysis of the load partition is also described.

The ultimate strength and distribution of force in the joints was ascertained. The results of the two joints were compared since their joint geometry was the same. Only the type of fastener differed. The test results indicated that at every load level the riveted joint exhibited greater flexibility than the bolted joint. The tests also illustrated that there is more variation in the load carried by individual fasteners in the bolted joint than in the riveted joint although the bolted joint was 27% stronger than the riveted joint. The average shear strength of the bolted joint at ultimate load was 60% of the shear strength of a single bolt. The riveted joint failed when the average shear stress was 80% of the shear strength of a single rivet.

Hence, the study confirmed that the strength of large shingled bolted and riveted joints decreases with increasing joint length. The observed reductions were comparable to the reductions that were observed in previous studies on butt joints.

A theoretical elastic solution for the load partition in a shingle joint was extended to provide the stress resultants in all plate elements and at all fastener shear planes. Matrix notation is used to express the equilibrium and compatibility conditions. The experimental results were compared with the theoretical analysis and showed good agreement within the elastic region. The results also assisted in evaluating the boundary conditions that were assumed in the analysis.

1. INTRODUCTION

1.1 Shingle Joints

Shingle splices are usually used for connections where the main member consists of several plies of material, such as built-up box sections of chord members on a truss bridge. This type of connection provides a more gradual transfer of load throughout the joint. Figure 1 shows a schematic view of a typical triple-plate shingle joint. The figure shows graphically the transmission of force that is assumed to take place in this type of joint. The connection is used in order to minimize the joint thickness and may also facilitate the connection of the various bridge components in a truss bridge. For example, plate "A" may serve as a gusset for other members framing into the chord.

By terminating the main plates in stages at different locations, the continuation plate can serve as a cover plate over regions of the joint. The total joint load at each plate discontinuity within the joint is carried by the remaining plates at that location. If all main plates were to terminate at the same location, as is the case for butt joints, the joint thickness will be increased since all force must be transferred into the lap plates.

1.2 Summary of Previous Studies

Yoshida and Fisher[1] summarized the experimental work of Davis, Woodruff, and Davis,[2] and the theoretical studies on symmetrical butt joints by Armoulevic,[3] Batho,[4] Bleich,[5] Hrennikoff,[6] Vogt,[7] and Fisher and Rumpf.[8]

They reported on a series of five small butt joints (See Fig. 2) and two large shingle joints which simulated the real joint of a chord member from the Baton Rouge Interstate truss bridge. Four bolted and three riveted joints of A572 steel fastened with 7/8 in. A325 bolts or A502 Gr. 1 rivets respectively were tested. Table 1 summarizes the material properties of the joint components.

The results of the control butt joints are summarized in Table 2. The bolted joints gave a mean coefficient of slip of 0.36. The slip loads obtained from the two riveted joints indicated that the clamping force.

The large test joint dimensions of these joints are shown in Fig. 3. The geometry of the large test joints was governed by the length, cross section and load capacity limitations of the testing machine. The cross section of the test joint represented one half of the actual cross section of the chord member. Advantage was taken of the symmetry of the actual

splice (See Fig. 1) and only one half of the joint was chosen. Each test joint contained one half of the number of fasteners in the actual splice.

The overall behavior of the large bolted and riveted joints is summarized in Fig. 4. The figure compares the measured response of the bolted and riveted joints with the theoretical elastic stiffness of the joint. The response of rivets and bolts was comparable, although the overall deformations in the riveted joint always exceeded the deformations in the bolted joint at all levels of load including the working load of 3090 kips. The joint stiffness is due to all plates. The theoretical curves obtained using the net and gross cross section area bounded the measured behavior. The gross cross section area best represented the test results.

The slip behavior of the two large joints was in reasonable agreement with the small joints. The large bolted joint slipped at a load equivalent to a slip coefficient of 0.31. This was equal to the smallest value obtained from the small bolted joint tests. Large and complex bolted joints are unlikely to slip the full amount of the bolt hole clearance as was illustrated by these studies. The large bolted joint was observed to slip 0.035 inches, only 54% of the hole clearance. The large riveted joint also slipped at alload equivalent to the minimum slip load obtained from the small riveted joint tests.

1.3 Objective of this Study

The previous work[1] was limited to an evaluation of joint behavior up to and including slip. Also, it was not possible to compare the experimental results with theory because boundary conditions were not completely defined. The testing was terminated when the machine capacity was reached.

The study indicated that higher working shear stress appeared reasonable for working loads. The distribution of force to the individual plates was about the same whether or not load transfer was due to shear and bearing of fasteners or by friction on the faying surfaces.

The study also indicated that the currently used design concept of distributing only the force of the discontinuous plate into the lap plates is not realistic. The forces in each discontinuous plate element were transferred primarily into the adjacent plate elements.

The objectives of this study were:

(1) To observe joint behavior beyond slip.

(2) Ascertain the ultimate strength and distribution of force in the joints.

(3) Define boundary conditions more precisely.

(4) Extend the theoretical solution for the load partition in the elastic range.

(5) Compare experimental work with the theoretical elastic solution.

(6) Provide experimental evidence to assist in extending the theoretical solution into the inelastic region.

The experimental study consisted of the modification and retesting of the large joints previously tested.

All computations for the theoretical solution were programmed for computer solution.

2. DEVELOPMENT OF THEORETICAL SOLUTION

2.1 Introduction

The shear surfaces of a shingle joint are generally symmetric as shown in Fig. 5. In the development of the theoretical solution advantage is taken of the symmetry and only one-half of the joint is analyzed. The idealized joint used in this investigation is shown in Fig. 6. The part between where two plates are cut is defined as a portion of a shingle joint.

This study is concerned primarily with developing a solution for the load partition to the plates and fasteners within the elastic range. The theoretical solution suggested by Yoshida and Fisher is used as a foundation.[1]

The theoretical analysis consists basically of considering the joint as a statically indeterminate structure. The solution of the problem follows the well known methods of mechanics. Two basic conditions are formulated. One satisfies the condition of equilibrium and the other insures that continuity or compatibility will be maintained throughout the joint length. These conditions yield the solution of the problem.

2.2 Assumptions

The theoretical solution is based on the following assumptions:

(1) The hole pattern is assumed to be completely filled and the pitch is constant in a region but not necessarily throughout the joint.

(2) Even when slip has not developed, the transfer of force due to friction can be considered as restricted to the faying surface adjacent to the bolt. The same load-displacement relationship is assumed to hold regardless of the actual load transfer mechanism.

(3) The plate thickness remains constant within a region but may change throughout the joint. A constant plate stiffness is used to express elongations between fasteners as a function of gross area.

(4) The joint is divided into gage strips even when the fasteners of adjacent strips are staggered. No attempt is made to match the boundary conditions between strips.

(5) Figure 7 schematically shows the idealization of the joint used for the theoretical analysis. It is assumed that the plates separated by the principal slip plane will act as a unit and the joint will behave as an unsymmetrical butt joint. The unsymmetrical butt joint consists of three

components; (a) the top lap plate, (b) the main plate, and (c) the bottom lap plate. The plates have a different stiffness in each portion along the joint.

The longitudinal line of holes parallel to the axial load is called a line and the space between each hole is called a pitch. The transverse series of holes is called a row and the distance between transverse holes is called the gage (See Fig. 8). As was noted in assumption 4, the fasteners along each line need not align at each row. A staggered pattern can be evaluated in this manner.

2.3 Equilibrium and Compatibility Relationships

The equilibrium conditions can be visualized with the aid of Fig. 8. This figure shows a typical butt joint with three bolts. All three plates are assumed to have different stiffness. For purposes of analysis, the joint is divided into gage strips as shown. Forces between bolts J-1 and J in plates 1, 2, and 3 are classified as P_{1J}, P_{2J} and P_{3J} respectively. They are referred to as the plate forces in element J. The shear forces in bolt J at shear surfaces between plates 1 and 2, and 2 and 3 are classified as R_{1J} and R_{2J} respectively.

As was noted in assumption 2, the forces R_{ij} represent shear on the fastener or concentrated faying surface forces due to friction. The faying surface force can be considered as a fastener force for convenience. Therefore, the forces in each plate can be calculated from the applied load P_o and the force in the fastener R_{ij} from equilibrium considerations. The direction of the load transfer to the fastener on each shear surface of the joint was assumed not to change direction as load was increased.

Considering the absolute values of forces in fasteners, the force in the plates of the element J + 1 of Fig. 8 can be formulated from equilibrium as

$$P_{1,\ J+1} = P_{1,\ J} + R_{1,\ J}$$

$$P_{2,\ J+1} = P_{2,\ J} - R_{1,\ J} - R_{2,\ J}$$

$$P_{3,\ J+1} = P_{3,\ J} + R_{2,\ J}$$

In matrix form, the plate forces are

$$\begin{bmatrix} P_{1,\ J+1} \\ P_{2,\ J+1} \\ P_{3,\ J+1} \end{bmatrix} = \begin{bmatrix} P_{1,\ J} \\ P_{2,\ J} \\ P_{3,\ J} \end{bmatrix} + \begin{bmatrix} 1 & 0 \\ -1 & -1 \\ 0 & 1 \end{bmatrix} \begin{bmatrix} R_{1,\ J} \\ R_{2,\ J} \end{bmatrix}$$

or

$$\overline{P}_{J+1} = \overline{P}_J + \overline{E}\,\overline{R}_J \qquad (1)$$

where P_J, P_{J+1}, and $\overline{R}_J$ are force vectors for the plate elements J and J + 1 and fastener J respectively. $\overline{E}$ is a coefficient matrix for plate forces.

The compatibility conditions described hereafter assume that the fasteners in the joint are in contact with the plate. Justification for this assumption is given in Ref. 8.

For a joint which deforms in the manner suggested, one may write the compatibility equations for displacements of the fasteners and the connected parts. Consider first the compatibility equation between plates 1 and 2. This is illustrated schematically in Fig. 9(a). As load is applied to the joint the deformations are considered within the joint at points J and J + 1 between plates 1 and 2. Due to the applied load plate 1 will have elongated so that distance between holes in plate 1 is $p + e_{J+1}$. Plate 2 will have elongated and its distance will be given by $p + e'_{J+1}$. From Fig. 9(a) it can be seen that

$$\Delta_J + p + e_{J+1} = \Delta_{J+1} + p + e'_{J+1}$$

or

$$\Delta_J + e_{J+1} = \Delta_{J+1} + e'_{J+1} \qquad (2)$$

where

P = the fastener pitch

Δ_J = apparent deformation at fastener J

Δ_{J+1} = apparent deformation at fastener J + 1

e_{J+1} & e'_{j+1} = elastic deformation of plates 1 and 2 in element J + 1

The fastener deformations include the effects of friction, shear, bending, and bearing of the fastener and the localized effect of bearing on the plates. It is assumed that the fastener diameter does not change due to applied load.

If the plate elongation and fastener deformations are expressed as functions of the loads in the plates and fasteners, Eq. 2 can be written as

$$\Delta(R_J) + e(P_{J+1}) = \Delta(R_{J+1}) + e'(P_{J+1})$$

or

$$\Delta(R_{J+1}) = \Delta(R_J) + e(P_{J+1}) - e'(P_{J+1}) \qquad (3)$$

where $\Delta(R_J)$, $\Delta(R_{J+1})$ are bolt deformations and $e(P_{J+1})$, $e'(P_{J+1})$ are the elongations of plates 1 and 2.

In the elastic range they can be expressed

$$e(P_{J+1}) = \frac{P_{1,\,J+1} \cdot p}{EA_1}$$

$$e'(P_{J+1}) = \frac{P_{2,\,J+1} \cdot p}{EA_2} \qquad (4)$$

$$\Delta(R_J) = \frac{R_{1,\,J}}{K}$$

$$\Delta(R_{J+1}) \equiv \frac{R_{1,\,J+1}}{K}$$

where

E = modulus of elasticity

p = pitch

A_1, A_2 = gross area of plate 1 and 2 respectively

K = elastic constant

The elastic constant K was derived for bolts in bolted joints by Tate and Rosenfeld.[13] The solution was compared by Fisher with experimental data and yielded reasonable agreement within the elastic range.[9]

For shear: $K_s = \frac{t_1 + t_2}{3 G_b A_b}$

For bending: $K_b = \frac{t_1^3 + 4t_1t_2^2 + 4t_1^2t_2 + t_2^3}{192EI_b}$ (5)

For bearing: $K_r = \frac{2(t_1 + t_2)}{Et_1t_2}$

and the constant K was evaluated as

$$K = \frac{2}{K_s + K_b + 2K_r} \qquad (6a)$$

where E = modulus of elasticity .

G_b = shear modulus

A_b = fastener area

I_b = moment of inertia of a fastener

t_1 and t_2 = thickness of the plate

Fisher described the elastic constant K in the elastic range as

$$K = \mu \tau \tag{6b}$$

where μ and τ are regression coefficients. The coefficient τ was found to be equal to the ultimate shear strength in kips of the fastener. The coefficient μ can be related to the physical and geometrical properties of the plate and bolt. For 7/8 in. A325 bolts tested in high strength steel plates a value of 23 was suggested. For rivets the coefficient μ was found to be 19.[9]

Two different types of shear jigs were prepared to simulate the conditions in the full size joints. The ultimate strength and load-deformation characteristics shear jigs are shown in Fig. 9(b). The ultimate shear strength was 92 kips in the bolted shear jig and 56 kips in the riveted shear jig. This yielded elastic constant K equal to 1064 for A502 Gr. 1 rivets and 2116 for A325 bolts.

By substituting Eq. 4 into Eq. 3, the general compatibility equation for internal J can be expressed in terms of the forces in the plates and fasteners as

$$\frac{R_{1,\,J+1}}{K_1} = \frac{R_{1,\,J}}{K_1} + \frac{P_{1,\,J+1}\cdot p}{EA_1} - \frac{P_{2,\,J+1}\cdot p}{EA_2}$$

or

$$R_{1,\,J+1} = R_{j,\,J} + \frac{K_1\cdot p}{E}\,\frac{P_{1,\,J+1}}{A_1} - \frac{P_{2,\,J+1}}{A_2} \qquad (7)$$

where K_1 is the elastic constant defined by Eq. 6.

Similarly, the compatibility equation between plates 2 and 3 can be expressed as

$$R_{2,\,J+1} = R_{2,\,J} + \frac{K_2\cdot p}{E}\,\frac{-P_{2,\,J+1}}{A_2} + \frac{P_{3,\,J+1}}{A_3} \qquad (8)$$

Letting

$$C_1 = 1$$

$$A = A_1$$

$$C_2 = \frac{A_2}{A_1}$$

$$C_3 = \frac{A_3}{A_1}$$

$$\overline{K}_1 = \frac{K_1\cdot p}{EA}$$

$$\overline{K}_2 = \frac{K_2\cdot p}{EA}$$

Equations 7 and 8 can be written as

$$R_{1,\,J+1} = R_{1,\,J} + \overline{K}_1\left[\frac{P_{1,\,J+1}}{C_1} - \frac{P_{2,\,J+1}}{C_2}\right] \qquad (9)$$

$$R_{2,\,J+1} = R_{2,\,J} + \overline{K}_2\left[\frac{-P_{2,\,J+1}}{C_2} + \frac{P_{3,\,J+1}}{C_3}\right] \qquad (10)$$

or in matrix form

$$\begin{vmatrix} R_{1,\ J+1} \\ R_{2,\ J+1} \end{vmatrix} = \begin{vmatrix} R_{1,\ J} \\ R_{2,\ J} \end{vmatrix} + \begin{vmatrix} \frac{\bar{K}_1}{C_1} & -- & \frac{\bar{K}_1}{C_2} & 0 \\ 0 & - & \frac{\bar{K}_2}{C_2} & + & \frac{\bar{K}_3}{C_3} \end{vmatrix} \begin{vmatrix} P_{1,\ J+1} \\ P_{2,\ J+1} \\ P_{3,\ J+1} \end{vmatrix}$$

or

$$\bar{R}_{J+1} = \bar{R}_J + \bar{S}\,\bar{P}_{J+1} \tag{11}$$

where $\bar{R}_j$, $\bar{R}_{J+1}$, and $\bar{P}_{J+1}$ are the fastener forces for fastener number J and J + 1 and plate element J + 1 respectively. $\bar{S}$ is a coefficient matrix for fastener forces and is a function of the different rigidities at each portion.

2.4 Solution of Equilibrium and Compatibility Equations

The theoretical solution of a joint with multiple main plates can be obtained by consideration of the schematic shown in Fig. 7. It is assumed that the plates reported by the principal slip plane will act as a unit and the joint will behave as an unsymmetrical butt joint. The top, middle, and bottom part of the joint are assumed to act as solid bodies with appropriate rigidities within each portion. Equilibrium and compatibility equations, (Eqs. 1 and 11) can be developed for each element. By applying suitable boundary conditions the fastener forces along the principal shear surface and the plate forces for the top, middle, and bottom plates can be obtained from the solution of the equations.

The unknown fastener force at element i are R_{1i} and R_{4i}, (i = 1, 2, 3,..., 16). Thirty-two unknown fastener forces

can be expressed as a function of the initial plate force P and the bolts forces $R_{1,1}$ and $R_{4,1}$. To assist in determining the unknown bolt forces $R_{1,,}$ and $R_{4,1}$, the boundary conditions at the end of the joint will be used. That is,

$$\bar{P}_{17} = \begin{vmatrix} P_{1,\,17} \\ P_{2,\,17} \\ P_{3,\,17} \end{vmatrix} = \begin{vmatrix} \alpha\, P \\ 0 \\ (1-\alpha)\, P \end{vmatrix}$$

The coefficient α varies between 0 and 1. Its value can be arbitrarily established or assumed on the basis of a rationale such as being proportional to the plate area.

Initial Values of Plates or Fasteners

The plate and fastener forces at the joint boundary can be expressed in matrix form as

$$\bar{P}_1 = \begin{vmatrix} P_{11} \\ P_{21} \\ P_{31} \end{vmatrix} = \begin{vmatrix} 0 & 0 & 0 \\ 1 & 0 & 0 \\ 0 & 0 & 0 \end{vmatrix} \begin{vmatrix} P \\ R_{11} \\ R_{41} \end{vmatrix}$$

or $$\bar{P}_1 = \bar{A}\,\bar{U}$$

$$\bar{R}_1 = \begin{vmatrix} R_{11} \\ R_{41} \end{vmatrix} = \begin{vmatrix} 0 & 1 & 0 \\ 0 & 0 & 1 \end{vmatrix} \begin{vmatrix} P \\ R_{11} \\ R_{41} \end{vmatrix}$$

or $$\bar{R}_1 = \bar{D}\,\bar{U}$$

In the vector, $\bar{U}$, the unknown forces are R_{11} and R_{41}. P is the magnitude of applied load. The forces in plate and fasteners can be evaluated from Eqs. 1 and 11

$$\bar{P}_{J+1} = \bar{P}_j + \bar{E}\,R_J \qquad (1)$$

$$\bar{R}_{J+1} = \bar{R}_j + \bar{S}\,\bar{P}_{J+1} \qquad (11)$$

For example, the forces in the plate element 2 are:

$$\begin{aligned}\bar{P}_2 &= \bar{P}_1 + E\bar{R}_1 \\ &= \bar{A}\,\bar{U} \pm \bar{E}\,\bar{D}\,\bar{U} \\ &= [\bar{A} + \bar{E}\,\bar{D}]\bar{U} \\ &= \bar{F}_2\bar{U}\end{aligned}$$

The forces on fastener 2 are

$$\begin{aligned}\bar{R}_2 &= \bar{R}_1 + \bar{S}\,\bar{P}_2 \\ &= \bar{D}\,\bar{U} + \bar{S}\,\bar{F}_2\bar{U} \\ &= [\bar{D} + \bar{S}\,\bar{F}_2]\bar{U} \\ &= \bar{H}_2\bar{U}\end{aligned}$$

The calculation procedures can be repeated until the end of the joint is reached and $\bar{P}_{17}$ is evaluated. The boundaries conditions provide three simultaneous equations and permit the determination of the two initial fastener forces R_{11} and R_{41}. Two of

these equations are linearly dependent. Therefore, solving two simultaneously equations for the two unknowns yield the fastener forces R_{11} and R_{41}. All other forces in plate and fastener are to be obtained as a function of these two initial fastener forces.

Lap Plate Solution

The solution of the unsymmetrical butt splice during the first stage of the analysis yields the fastener forces on the principal shear surface and the total plate force within each element. The second stage of the analysis is to determine the force in each individual plate element and the shear at each fastener shear surface.

The second stage of the solution for the remaining unknowns will be illustrated with the aid of Fig. 10. The discontinuous middle plate can be evaluated by the methods described in Ref. 1.

The shear forces on the external faces of the main plate are known from the first stage of the analysis. The known fastener forces are $R_{k,\,i}$, $(i = 1, 2, 3, 4, 5)$, $R_{2,\,J}$, $(i = 6, 7, 8, 9, 10)$, $R_{3,\,k}$, $(k = 11, 12, 13, 14, 15, 16)$, and $R_{4,\,i}$, $(i = 1,\ldots, 16)$. Considering the calculation procedure described previously only R_{21} and R_{31} are considered unknowns. At each element, i, the forces in each plate can be expressed as a function of the initial plate force P, the known fastener force $R_{1,\,i}$ and $R_{4,\,i}$ and the unknown bolt forces R_{21} and R_{31}. To determine

the unknown bolt forces R_{21} and R_{31}, the boundary conditions $P_{1,\ 6} = 0$ and $P_{2,\ 11} = 0$ will be used.

Coefficient Matrices $\overline{B}$ and $\overline{C}$

Using the same approach as that used in Ref. 1, coefficient matrices B and C can be written for each portion of the joint.

Matrix B

Considering the absolute values of forces in fasteners, the forces in the plate of the element J + 1 of Fig. 10 can be formulated from equilibrium as

$$\begin{aligned} P_{1,\ J+1} &= P_{1,\ J} - R_{1,\ J} - R_{2,\ J} \\ P_{2,\ J+1} &= P_{2,\ J} + R_{2,\ J} - R_{3,\ J} \\ P_{3,\ J+1} &= P_{3,\ J} + R_{3,\ J} - R_{4,\ J} \end{aligned} \tag{16}$$

In matrix form, the plate forces are

$$\begin{vmatrix} P_{1,\ J+1} \\ P_{2,\ J+1} \\ P_{3,\ J+1} \end{vmatrix} = \begin{vmatrix} P_{1,\ J} \\ P_{2,\ J} \\ P_{3,\ J} \end{vmatrix} + \begin{vmatrix} -1 & -1 & 0 & 0 \\ 0 & 1 & -1 & 0 \\ 0 & 0 & 1 & -1 \end{vmatrix} \begin{vmatrix} R_{1,\ J} \\ R_{2,\ J} \\ R_{3,\ J} \\ R_{4,\ J} \end{vmatrix} \tag{17}$$

or $$\overline{P}_{J+1} = \overline{P}_J + B^I.\overline{R}_J \tag{18}$$

Similarly, considering the direction of forces in portion 2, coefficient matrix B^{II} can be defined as

$$B^{II} = \begin{vmatrix} 0 & 0 & 0 & 0 \\ 0 & -1 & -1 & 0 \\ 0 & 0 & 1 & -1 \end{vmatrix} \tag{19}$$

Hence, the equilibrium condition for portion 2 can be expresses as

$$\overline{P}_{J+1} = \overline{P}_J + B^{II} R_J \tag{20}$$

The plate forces in portion III can be calculated directly from the known shear forces.

Matrix C

Considering the direction of the deformations of the fasteners in portion 1, the compatibility equation can be expressed in terms of the forces in plate and fasteners as

$$\begin{aligned} R_{1,\,J+1} &= R_{1,\,J+1} \quad \text{(Known value)} \\ R_{2,\,J+1} &= R_{3,\,J} + \overline{K}\left[-P_{2,\,J+1} + P_{3,\,J+1}\right] \\ R_{3,\,J+1} &= R_{3,\,J} + \overline{K}\left[-P_{3,\,J+1} + P_{4,\,J+1}\right] \\ R_{4,\,J+1} &= R_{4,\,J+1} \quad \text{(Known value)} \end{aligned} \tag{21}$$

Using matrix notation, the bolt forces in portion I are

$$\begin{vmatrix} R_{1,\,J+1} \\ R_{2,\,J+1} \\ R_{3,\,J+1} \\ R_{4,\,J+1} \end{vmatrix} = \begin{vmatrix} 0 \\ R_{2,\,J} \\ R_{3,\,J} \\ 0 \end{vmatrix} + \overline{K} \begin{vmatrix} 0 & 0 & 0 \\ -1 & 1 & 0 \\ 0 & -1 & 1 \\ 0 & 0 & 0 \end{vmatrix} \begin{vmatrix} P_{1,\,J+1} \\ P_{2,\,J+1} \\ P_{3,\,J+1} \end{vmatrix} \tag{22}$$

or

$$\bar{R}_{J+1} = \bar{R}_J + \bar{K} C^I \bar{P}_{J+1} \tag{23}$$

where C^I is a coefficient matrix for fastener forces in portion I. Similarly, considering the directions of deformations of the fasteners in portion II we obtain coefficient matrix C^{II} as

$$C^{II} = \begin{vmatrix} 0 & 0 & 0 \\ 0 & 0 & 0 \\ 0 & -1 & 1 \\ 0 & 0 & 0 \end{vmatrix} \tag{24}$$

Hence, the compatibility equation for portion II can be expressed as

$$\bar{R}_{J+1} = \bar{R}_J + K C^{II} P_{J+1} \tag{25}$$

Initial Values of Plates or Fastener

In matrix form

$$\begin{vmatrix} P_{11} \\ P_{21} \\ P_{31} \end{vmatrix} = \begin{vmatrix} 1/3 & 0 & 0 & 0 & 0 \\ 1/3 & 0 & 0 & 0 & 0 \\ 1/3 & 0 & 0 & 0 & 0 \end{vmatrix} \begin{vmatrix} P \\ 1 \\ R_{21} \\ R_{31} \\ 1 \end{vmatrix} \tag{26}$$

or

$$\bar{P}_1 = \bar{A}\,\bar{U} \tag{27}$$

$$\begin{vmatrix} R_{11} \\ R_{21} \\ R_{31} \\ R_{41} \end{vmatrix} = \begin{vmatrix} 0 & R_{11} & 0 & 0 & 0 \\ 0 & 0 & 1 & 0 & 0 \\ 0 & 0 & 0 & 1 & 0 \\ 0 & 0 & 0 & 0 & R_{41} \end{vmatrix} \begin{vmatrix} P \\ 1 \\ R_{21} \\ R_{31} \\ 1 \end{vmatrix} \qquad (28)$$

or

$$\bar{R}_1 = \bar{D}\,\bar{U} \qquad (29)$$

where in the unknown vector $\bar{U}$ the real unknowns are R_{21} and R_{31}. The second (1) and fifth (1) element correspond to the known values on the principal shear surfaces. P is the applied load. The forces in plates and fasteners are calculated by means of Eqs. 18 and 23 in portion I and Eqs. 20 and 25 in portion II.

The same calculation procedures as described in section 2 were repeated until $\bar{P}_{11}$ and applying the boundaries conditions gave a two order simultaneous equation to determine the two initial fastener forces R_{21} and R_{31}. All other forces in plate and fastener are to be obtained as function of the initial fastener forces.

Similarly, the same procedure is followed to obtain the forces in plate and fastener for the top plate.

3. EXPERIMENTAL INVESTIGATION

3.1 Introduction

The tests on large shingle joints (see Fig. 3) were loaded up to the capacity of the 5,000,000 lb. testing machine.[1] Except for slip, no marked non-linear behavior was observed in the joints and it was not possible to determine the joint strength. Therefore, it was decided to reduce the net cross sectional area of the joints so that failure could occur within the machine's capacity. Since the tensile strength of the plate material was 88 ksi, the net area of 101.6 in^2 had to be reduced.

Three major factors were considered when developing the joint modifications:

(1) The results of the modified joint test were to be correlated with the test results of the original joint. Therefore, it was important that the ratio of the net plate area to the fastener shear area be maintained.

(2) It was desirable to modify the joint without disassembling it in the test portion. Major slippage had already occurred throughout the joint length and the fasteners were bearing against the plates. The intent of subsequent testing was to continue the loading until failure, in order to observe joint behavior and strength.

(3) The joint should fail in the test portion and not in the loading grips. The grip areas of the joints had to be reinforced because some of the plates in this area had cracked during the earlier test and most of the rivets had sheared off.

A sketch of the modified joint is shown in Fig. 11. Figure 12 shows the joint shear planes and the net areas in the original and the modified joints.

3.2 Fabrication

The fasteners in the grip areas were removed in both joints so that additional plates could be added. None of the fasteners in the test portion were disturbed. A514 and A572 high strength steel plates were added at both ends of each joint and drilled to match the existing hole patterns. The original drilled holes were distorted due to the prior loading, and it was necessary to ream the resulting plate assembly so that 1 in. A490 bolts could be installed.

The cross sectional area in the test portion was reduced by removing the existing angles and two lines of fasteners on each side which reduced the width of the joint plates as well as the number of fasteners. The reduction in plate area was accomplished while the shingle joints were still assembled. A line of holes was drilled through all plates along each edge of the

joint for ease of cutting off the remaining plate area with an acetylene torch. The rough finish was then milled until the desired reduction in area was obtained, and all surfaces milled until smooth to provide a uniform width and remove any damaged material.

3.3 Instrumentation

As in the previous tests the joints were instrumented to assist in the evaluation of joint strength and to provide information for extending theoretical studies into the non-linear region.

The modified joints were instrumented to record:

(1) Distribution of plate forces. Previous measurements were not extensive enough to permit satisfactory evaluation of plate forces throughout the joint.

(2) Overall joint elongation which gave a measure of the joint stiffness.

(3) Fastener Forces. No technique has been developed to measure fastener shear forces directly, but by measuring the hole offsets of the fastener, the fastener force can be determined from calibration curves.[9]

The plate forces were measured at various locations with 144 electrical resistance strain gages placed on each joint as shown in Fig. 13.

Overall joint elongation was measured in each joint with both dial gage (see Fig. 14a) and cantilever gage (see Fig. 14b). The elongations were measured at the center line of each face over a length of ten feet, as indicated in Fig. 15 by gages 21 and 22.

Local joint deformations were measured with dial gages on one side and cantilever gages on the opposite side at ten differnet levels on each edge of the bolted joint. The selected locations were at points where one of the main plates or lap plates were cut and midway between them as illustrated in Fig. 15.

In addition to the dial and cantilever, lines were scribed across all six plates at eighteen differnet levels on each edge of both joints. The selected locations were at points on the edges corresponding to the outside line of fasteners as shown in Fig. 16.

3.4 Test Procedure

Both joints were loaded in static tension using a 5,000,000 lb. univeral testing machine with pin grips as illustrated in Fig. 17. The procedure used for the bolted joint, as described herewith, was also followed for the riveted joint.

The dials, cantilever gages, and strain gages were all read before load was applied. The joint was then loaded in increments of 300 kips up to the inception of non-linear behavior and then increments of 100 kips until the ultimate load was reached.

Total joint elongations, local deformations, and the distribution of plate forces were recorded at every other load increment in the elastic region and at each load increment in the inelastic region. The hole offsets from the scribed lines were recorded at every load increment as soon as they were noticeable.

3.5 Test Results

1. Bolted Joint

The test of the bolted joint was terminated when the bottom row of fasteners at the most flexible end failed by shearing off due to the unbuttoning or long joint effect. This occurred at a load level of 3,550 kips and coresponds to a load equivalent to 75% of the tensile strebgth at the net section.

The unbuttoning failure of the bolted joint is shown in Fig. 18. The figure shows the holes at the location where the bølts were sheared off. The average ultimate shear strength was 46 ksi which is 60% of the shear strength of a single bolt. This type of behavior has been observed in previous tests of long bolted and riveted butt joints where the strength also decreased with increasing joint length.[10,11]

The overall bolted joint elongation is shown in Fig. 19. No slip was evident at any stage of loading because of the previous test history (See Fig. 4). The average stress at the net section was 70.0 ksi and 62.0 ksi on the gross section at the maximum load.

As was noted, the joints were modified so that the earlier tests and the retests could correlated. For this reason, the fasteners were not removed during the modifications and the geometric proportions of the joint were maintained. Since the area was reduced by a factor of one-half, the test load for the retest was factored by two and the results were compared with the initial test results. Figure 20 compares the load-deformation curve of the factored retest with the unloading curve of the original test. It is readily apparent that the original and modified joint had about the same stiffness.

The results of the local deformations measurements are summarized in Fig. 21. The location of the local deformation gages are shown in Fig. 15. The results clearly indicate that there is a substantial variation in the load carried by individual fasteners as evidenced by the variations in hole offsets along the joint length. Equalization of load among all bolts did not occur. The end fasteners were critical, (See locations 1 and 11 and 10 and 20 in Fig. 21a). Although the interior fasteners have considerable reserve in shear strength, this reserve cannot be developed because of the controlling action of the end fasteners.

This is also illustrated by the displacements of the scribe lines along the joint length. Figure 22 summarizes the hole offsets in inches at the ultimate load of 3550 kips. The values in the columns refer to the relative movement between the outside lap plate and the nearest main plate. These values confirm that the principal shear planes are the critical ones. This is evidenced by the variation in hole offsets along the joint length.

These measurements also show that the end of the joint is the critical area. Note the large offsets at the end of the joint and how rapidly they decrease as one moves up the joint. Bolts at the joint end were sheared off as indicated. An examination of the fasteners after the test indicated that failure was imminent at the other critical shear plane. Fasteners beyond the first plate termination were not significantly affected and little load was able to be distributed to them on the shear plane (See Figs. 21c and 21d).

Figures 23 and 24 are photographs of the scribe lines that were used to determine the relative plate movements. The bottom photo (Fig. 23) shows the offset at the row where fastener failure occurred. The bolts were sheared off between the plates marked with strain gages 1 and 2. This location showed the largest relative movement between plates throughout the joint, confirming the large force that was transferred into the bolts at this location.

The top photograph (Fig. 23) shows the scribe lines just below the main plate termination. Note that the hole offsets on each side of the plate are substantially less than the offsets observed at the end of the joint. The largest relative movement at this location occurred between the plates marked with strain gages 19 and 20. This was the more critical shear plane. The offset between plates 20 and 21 are obviously less.

Hole offsets at other locations along the joint are illustrated in Fig. 24. They show the offsets at the termination of the two remaining main plates. It is apparent that the termination of these plates had substantially less effect than at the more flexible joint end. The largest relative movement at middle plate termination occurred between the plates marked 51 and adjacent plates identified by strain gages 50 and 52.

The top picture (Fig. 24) shows the scribe line at the last plate termination. Note that at this location almost no relative movements between plates have taken place, indicating that very little force was being transferred into adjacent plates.

Referring to Figs. 22, 23 and 24, one sees that the prevailing trend for the relative movement between plates at different locations throughout the joint are generally the same as was assumed in the development of the theoretical solution. This confirms and justifies the choice of boundary conditions that were assumed in the idealized joint.

The strain measurements provided a means of evaluating the assumed load distribution that is used in design. Figure 25 shows the plate forces computed from the measured strains and compared with the assumed design plate forces at the design load of 1524 kips. It is apparent that the load was transferred from all three main plates into the lap plates as these elements progressed into the joint.

Figure 26 and 27 summarizes the measured load distribution at a load level of 1524 and 2080 kips respectively. It is apparent that the forces in each discontinuous plate element were transferred primarily into the adjacent plate elements. This was confirmed by the measured hole offsets. As expected, the load was about evenly distributed to all plates near the middle of the joint. This is apparent from the measured forces that existed in each plate element between fasteners 8 and 9.

2. Riveted Joint

The test of the rivited joint was terminated when all the rivets in regions I and II were simultaneously sheared off. At rupture the shank, manufacture head, and driven head of the rivets remained lodged in the plates. This occurred at a load level of 2800 kips and corresponds to a load equivalent to 63% of the tensile strength at the net section.

Figures 28, 29, 30 and 31 are photographs of the riveted joint after failure. The photo in Fig. 28 shows the head of the rivets lodged in the lap plate in portion I. The photo

in Fig. 29 shows the most flexible end of the joint, portion I. All rivets were sheared off a long both major shear surface. Figure 30 shows portion II. The rivets were also sheared off at the critical shear surface in this portion. Figure 32 shows portion III. It is apparent that the termination of last main plate has substantially less effect than at the other two plate terminations. It is also apparent that in portion III very little relative movements between plates have taken place, indicating that the force variations was not as great. Again, these results show that the flexible end of the joint is the critical area.

The overall riveted joint elongation is shown in Fig. 32. The figure compares the measured response of the bolted and riveted joints with the theoretical stiffness of the joint. The theoretical curves obtained using the net and gross section areas bounded the measured behavior in the elastic range. The gross cross section predicts closely the bolted joint stiffness whereas the net section area predicted the riveted joint stiffness in the elastic range. The figure illustrated that at every load level the riveted joint elongation was greater than the bolted joint. No slip was evident at any stage of loading because of the previous test history (See Fig. 4).

The average stress in the riveted joint at the net section was 55.5 ksi which is below the yield strength (See Table 1). The average ultimate shear strength was 36.2 ksi which was 80% of the shear strength of a single rivet. The average

ultimate shear strength in the bolted joint was 60% of the strength of a single bolt. These results indicate that there is less variations in the load carried by individual fasteners in large riveted joints than in large bolted joints. Although the bolted joint was 27% stronger than the riveted joint.

Figures 33 and 34 summarize the measured load distribution at load levels of 1524 and 2080 kips. As in the bolted joints, the load was transferred from all three main plates into the lap plates as these elements progressed into the joint. The load was about evenly distributed to all plates in portion III of the joint. This is apparent from the measured forces that existed in each plate element between fasteners 14 and 15. This helped to explain why the fasteners in this portion were not sheared off since the magnitude of the force in the plates is about half the force that exists at the other end of the joint in Portion I. In addition the uniformity in plate forces tends to produce a more uniform distribution in the fasteners force.

The measured results from the previous tests and the test reported herein will be compared in the following section with results from the theoretical solution.

4. COMPARISON OF THEORETICAL SOLUTION WITH EXPERIMENTAL RESULTS

4.1 Partition of Load in Simulated Bridge Joint

The theoretical elastic load partition in a shingle joint requires an evaluation of the various assumptions made in its development. This can be accomplished by comparing the theoretical solution with the plate forces reported by Yoshida and Fisher[1] as well as the initial stages of loading of the tests reported herein.

The idealized joint was partitioned into gage strips and the theoretical solution is based on the solution of a single gage strip. Previous tests on butt joints with regular hole patterns showed that the unit strains did not vary across the joint from edge to edge.[12] It was important to evaluate the suitability of a single gage strip in joints with staggered hole patterns.

Strain distribution was determined from SR-4 gages which were located at eight different cross sections. These measurements demonstrated that the unit strain variations across the joint was very small at all stages of loading. Figure 35 shows the strain distribution across the top lap plate at about mid-point of the bolted joint for several load levels. The dashed lines indicate the average strain at this point for the given loads. The figure illustrates that the unit strains were nearly

uniform across the joint from edge to edge irregardless of the fastener pattern. The same behavior was observed at other locations along the length of the bolted and riveted joints. The results indicate that each gage strip behaves about the same.

Since the edge angles were cut at the same point as the third main plate (See Fig. 3) their area was averaged and distributed to the third main plate.

One of the assumptions made in the development of the theoretical solution was that the plates separated by the principal slip plane act as a unit. This idealized joint will behave as an unsymmetrical butt joint. The unsymmetrical butt joint consisted of three components as shown in Fig. 6. In order to check this assumption the plate forces measured in each individual plate were integrated as appropriate. Figure 36 shows the resulting measured plate forces for both the bolted and riveted joints when the applied joint load was 3100 kips. These forces were obtained by adding the individual plate forces in each plate element. The force in the edge angles was added to the middle portion.

One interesting result that is apparent from Fig. 36 is that the value of α is about one-half. Since α was taken as the ratio of the force carried by the top lap plate to the applied load, it was originally assumed that α was proportional to the contributing areas of the lap plates. This would yield a value

of α equal to 0.6. The test results indicated that the stress distribution at the interior of the joint was substantially different from this design assumption at all stages of the loading.

The load partition in the unsymmetrical butt joint was determined theoretically using a value of α equal to one-half. The results are summarized in Figs. 37 to 39 and compared to the experimental results. Figure 37 compares the theoretical and experimental results for the load carried by the top lap plate when the total applied load is 3100 kips. The integrated forces shown in Fig. 36 are plotted in Fig. 37 for both the bolted and riveted joints. Figure 38 shows similar comparisons of the load partition for the middle plate and Fig. 39 for the bottom plate.

It is apparent from Figs. 37 to 39 that there is good overall agreement between the theoretical and experimental results. The measured force in each plate element followed the trend predicted by the theoretical analysis. There were insufficient measurements along the joint length to permit a more detailed evaluation. The observed deviations between the theoretical results and the measured plate forces in the bottom lap plate are in part due to (1) the effect of the angles, (2) the assumptions of a single gage strip, (3) the value of α, and (4) lack of complete documentation of each plate force.

It should be emphasized that the comparisons are limited to the elastic region. No attempt was made to extend the solution in to the inelastic region.

4.2 Partition of Load in Modified Bolted Joints

The strain measurements during the original tests were not extensive enough along the joint length to permit a complete evaluation of the transfer of plate forces throughout the joint. In addition, as was noted in Article 4.1 other factors could influence the comparison between theory and test. The modified joint and the idealized joint were more nearly alike when the angles were removed. The plate strain were measured in each plate at seventeen different cross-sections along the joint. Figure 27 summarized the measured load that was observed in each element of the bolted joint at a load level of 2080 kips.

Figure 40 summarizes the total plate force in each major component that was obtained by adding the individual plate forces shown in Fig. 27. The value α is approximately equal to one half as was the case in the earlier work prior to the joint modifications. The measured force in each major component are compared with the theoretical solution in Figs. 41 to 43.

Figure 41 shows the comparison between the theoretical and the experimental load partition for the top lap plate. Figure 42 shows the comparison for the middle component and Fig. 43 for

the bottom lap plate. Note that the major deviations between theory and experiment occurs at locations where the regions change. The load was not transferred into the lap plate in this region as quickly as the theory would predict. Very little deviation occurs between theory and experiment in regions II and III. Except for the slight deviation in region I, the measured forces conformed to the predicted plate forces. It should be noted that the observed distribution of force to the lap plates at the interior was used in the theoretical analysis. In other words α was taken as 0.5 instead of proportional to the plate area. This is the reason for the convergence of the test data and the theoretical curve at location 16.

It seems probable that part of the reason for the slight deviations between theory and test is the addition of the individual gage strips.

The individual plate forces that were summarized in Fig. 27 are compared in graphical form with the theoretical results in Fig. 44. The comparison is for the middle or main plates of the joint. Major deviation is in the two plates adjacent to the lap plates. More force is being transferred from plate 2 than the other two plates. Note that at each plate discontinuity, there is a sudden pick up of load by the adjacent plates. The theoretical and the experimental load distribution results show very good agreement. Similar behavior was observed at other load levels.

5. SUMMARY AND CONCLUSIONS

The conclusions are based on the results of theoretical elastic studies of load distribution in shingle joints and two tests of large shingle joints of A572 steel. One fastened with 7/8 in. A325 bolts and the other with 7/8 in. A502 Gr. 1 rivets.

1. The gross cross sectional area best represented the joint stiffness in the bolted joint. And, the net cross sectional area best represented the joint stiffness in the riveted joint.

2. The ultimate load in the bolted joint was 3550 kips which corresponds to a load equivalent to 75% of the tensile strength at the net section. The ultimate load in the riveted joint was 2800 kips which corresponds to a load equivalent to 63% of the tensile strength at the net section. The bolted joint was 27% stronger than the riveted joint.

3. At every load level the deformation of the riveted joint was greater than the bolted joint.

4. At the ultimate test load, there was substantial variation in the load carried by individual fasteners in the large bolted joint. The average ultimate shear strength in the bolted joint was

60% of the shear strength of a single bolt. The end of the shingle joint with the most heavily loaded plates is the critical area. The end fasteners at this joint end failed by unbuttoning.

5. At the ultimate test load there was less variation in the load carried by individual fasteners in the large riveted joint than in the large bolted joint. The average ultimate shear strength in the riveted joint was 80% of the shear strength of a single rivet.

6. The average ultimate shear strength was 46 ksi in the bolted joint and 36.2 ksi in the riveted joint.

7. The ultimate strength tests indicated that shingle joints did not produce satisfactory distribution of forces to the fasteners. The fasteners in Region I were forced to resist substantially higher loads than assumed and resulted in premature joint failure. Although a shingle joint does produce a reasonable flow of force in the plates it leads to very long joints and a resulting decrease in strength of the fasteners.

8. The forces in each discontinuous plate element were transferred primarily into the adjacent plate elements.

9. A theoretical elastic solution for the stress resultants in the various components of a shingle joint was found to be in good agreement with the experimental results within the elastic range.

10. The study also indicated that the effectiveness of the plates at the joint interior was not proportional to their area. This deviation was greatest for the bolted joint. Apparently, the greater stiffness of the bolt distributes the load about equally to the lap plates even though their areas differ. This tendency was not as great for the riveted joint.

TABLES

TABLE 1

SUMMARY OF MATERIAL PROPERTY CALCULATIONS

Specimens	Type of Test	Number of Test	Yield Stress (ksi)	Standard Deviation (ksi)	Ultimate Strength (ksi)
A325 Bolt	Direct Tension	6	93	1.60	98
	Torqued Tension	6	82	1.56	86
	Shear Jig	2	42	1.80	76
A502 Gr. 1 Rivet	Tension Coupon	6	53	1.75	65
	Shear Jig	6	27	1.80	45
V55 Plate	Tension Coupon	9	59	1.40	88

TABLE 2

SUMMARY OF TESTS OF CONTROL JOINTS

Specimen	Clamping Force (kips)	Slip Load (kips)	Slip Coefficient	Ultimate load (kips)	Failure Mode
CBJ-1	432	361	0.42	518	Plate
CBJ-2	429	263	0.35	500	Plate
CBJ-3	430	324	0.31	492	Plate
CRJ-1	-	190	-	475	Rivet Shear
CRJ-2	-	169	-	481	Rivet Shear

FIGURES

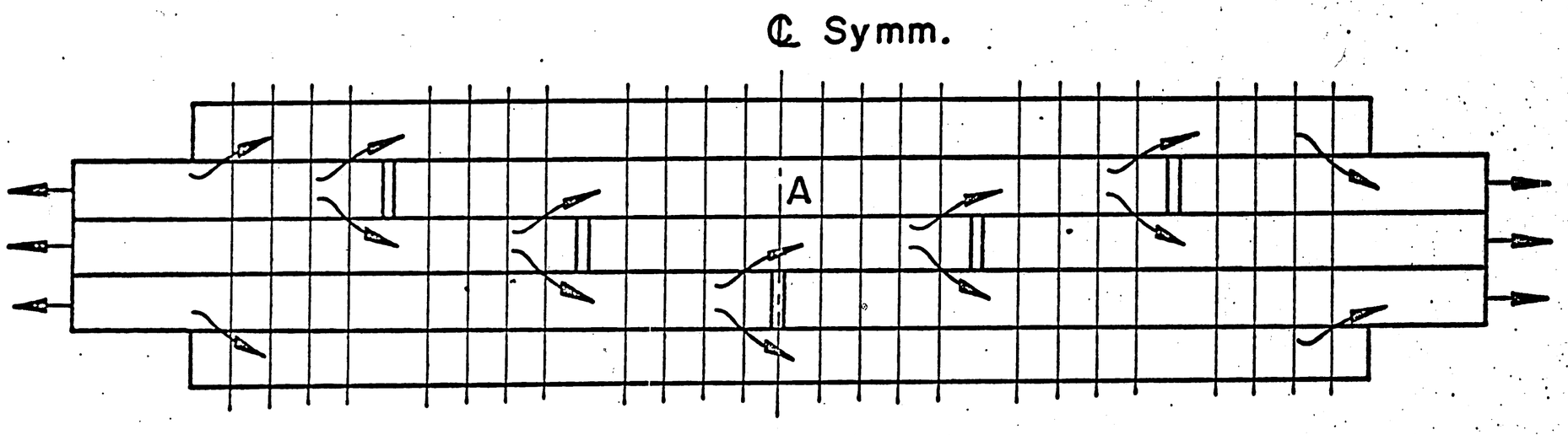

FIG. 1 TYPICAL TRIPLE-PLATE SHINGLE JOINT

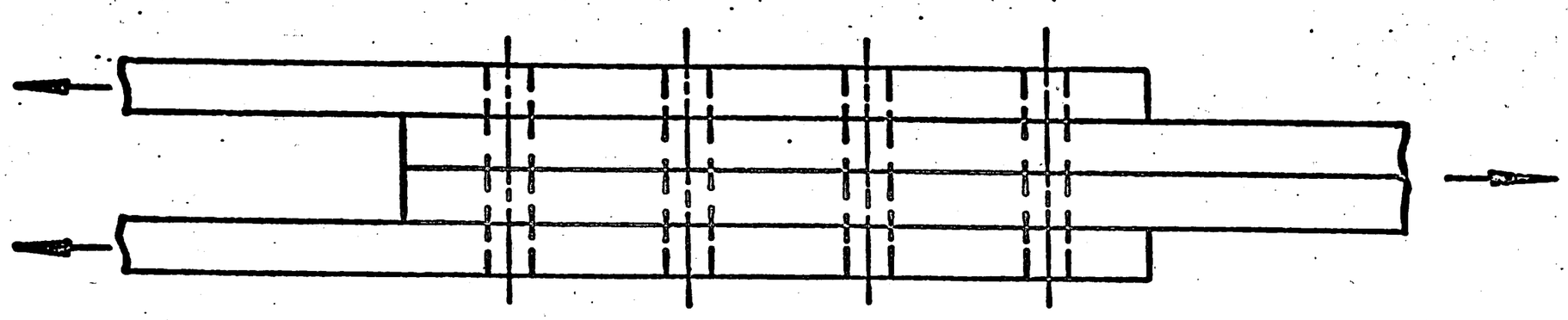

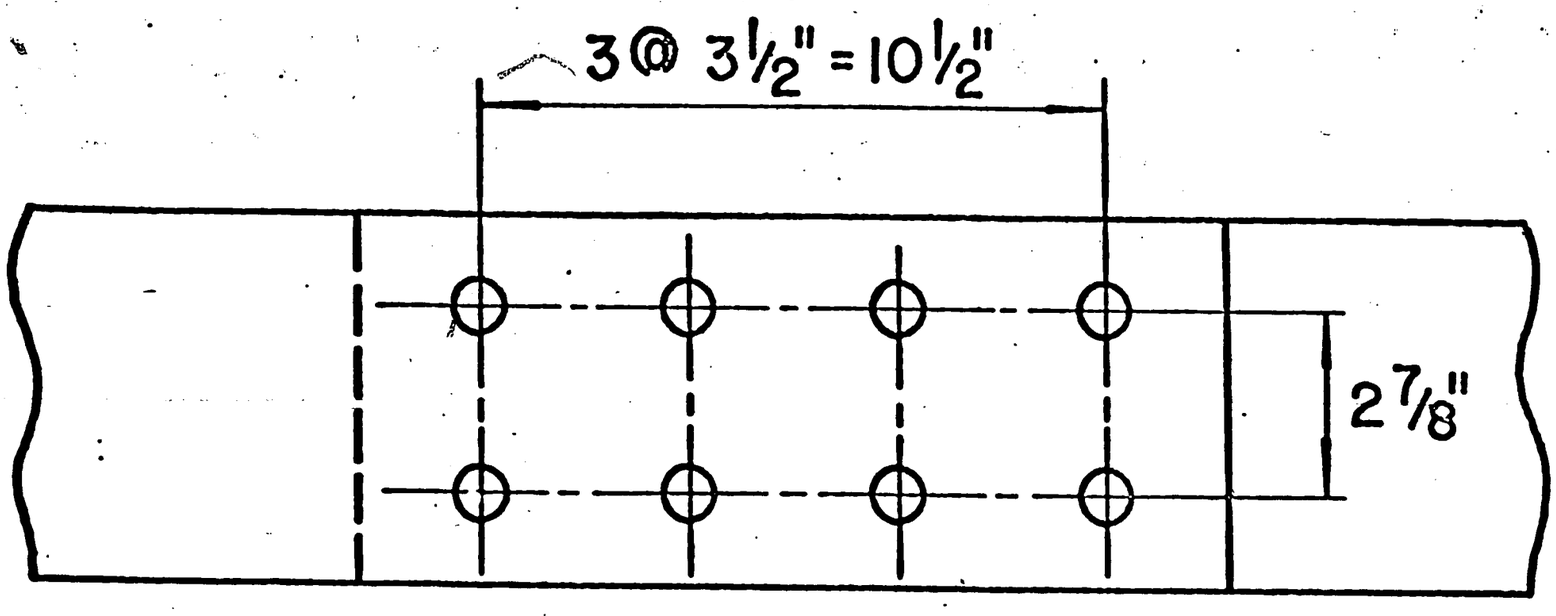

V55 STEEL PLATES

⅞" ϕ A325 BOLTS OR A502 Gr. 1 RIVETS

FIG. 2 CONTROL TEST SPECIMENS

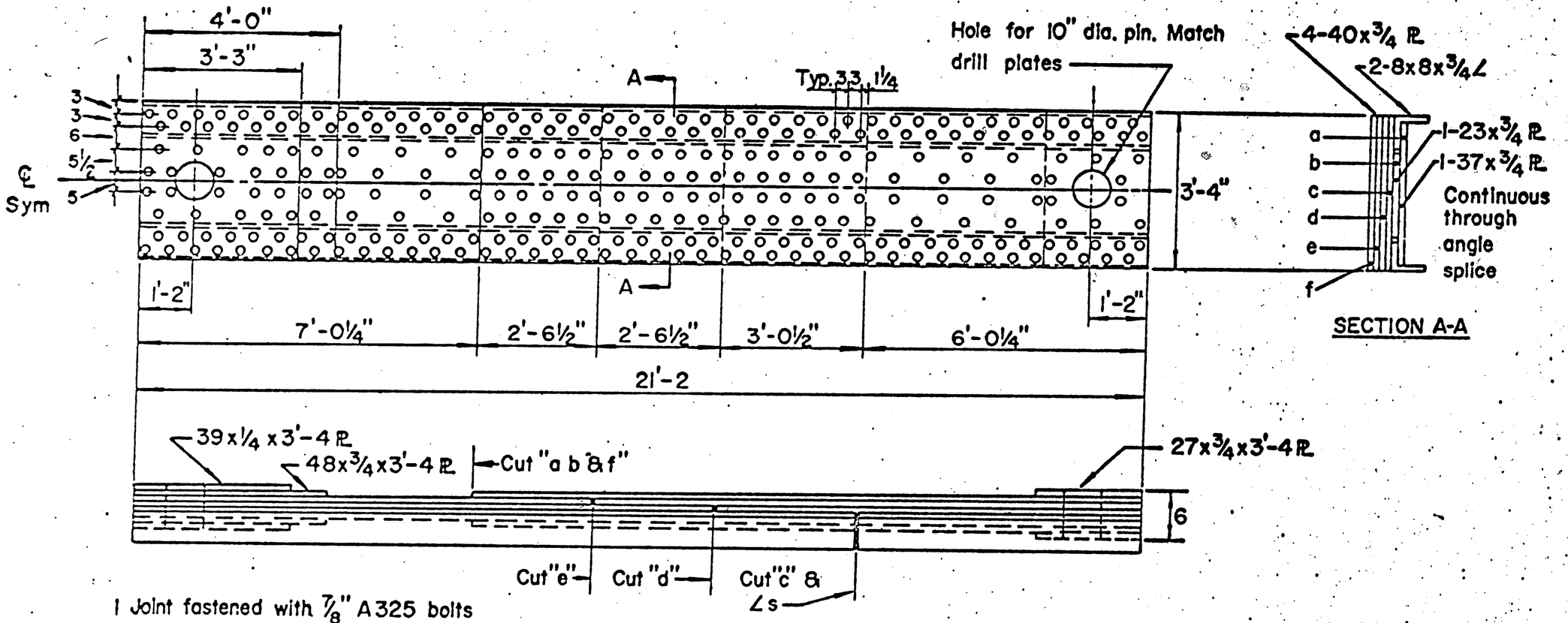

I Joint fastened with ⅞" A325 bolts

" " " " " A502 Gr:1 rivets

LARGE TEST JOINTS

Scale- ½"=1'-0"

FIG. 3 SCHEMATIC OF FULL SIZE SIMULATED JOINT SPECIMEN

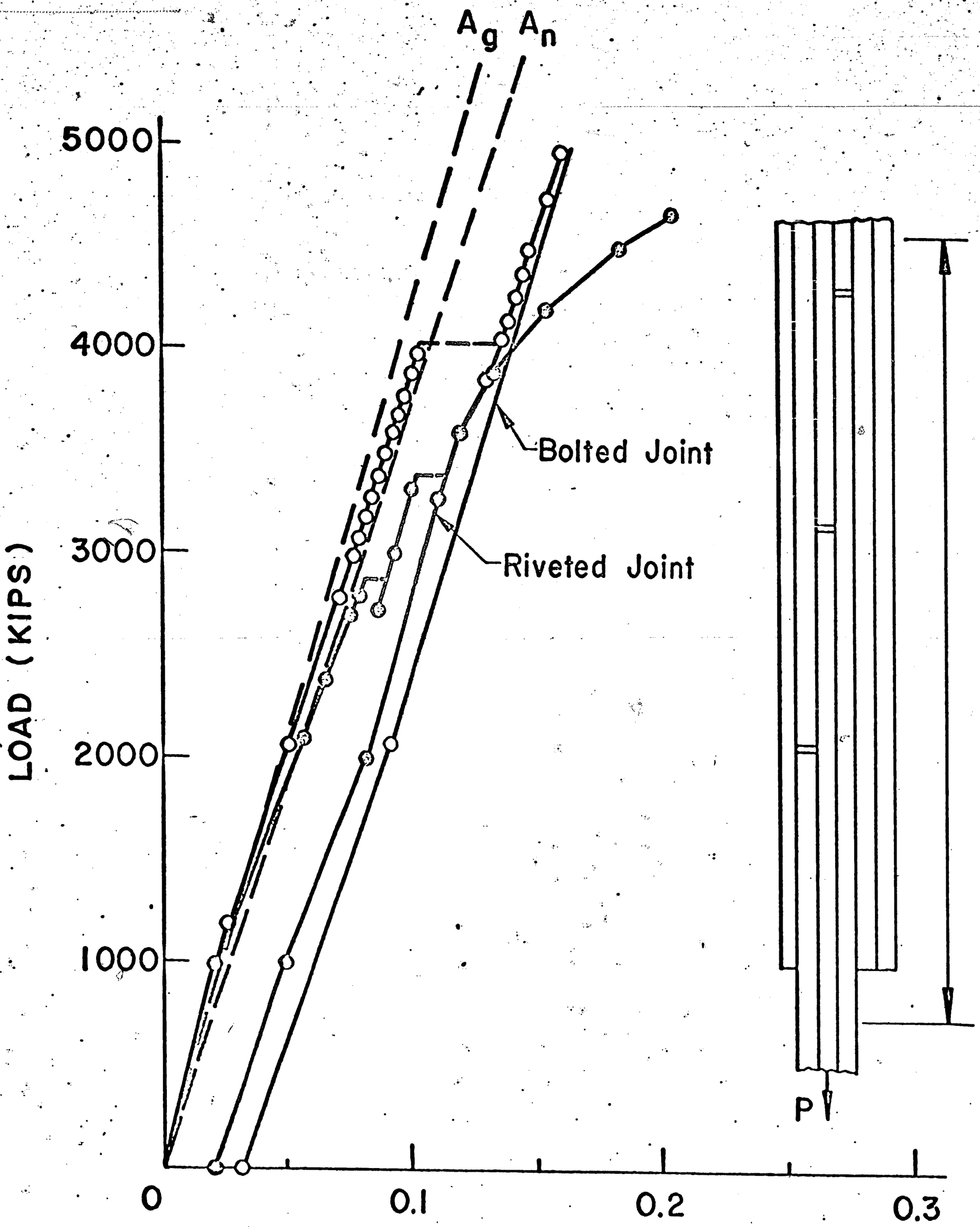

FIG. 4 COMPARISON OF LOAD-DEFORMATION CURVES OF BOLTED AND RIVETED SIMULATED BRIDGE JOINT

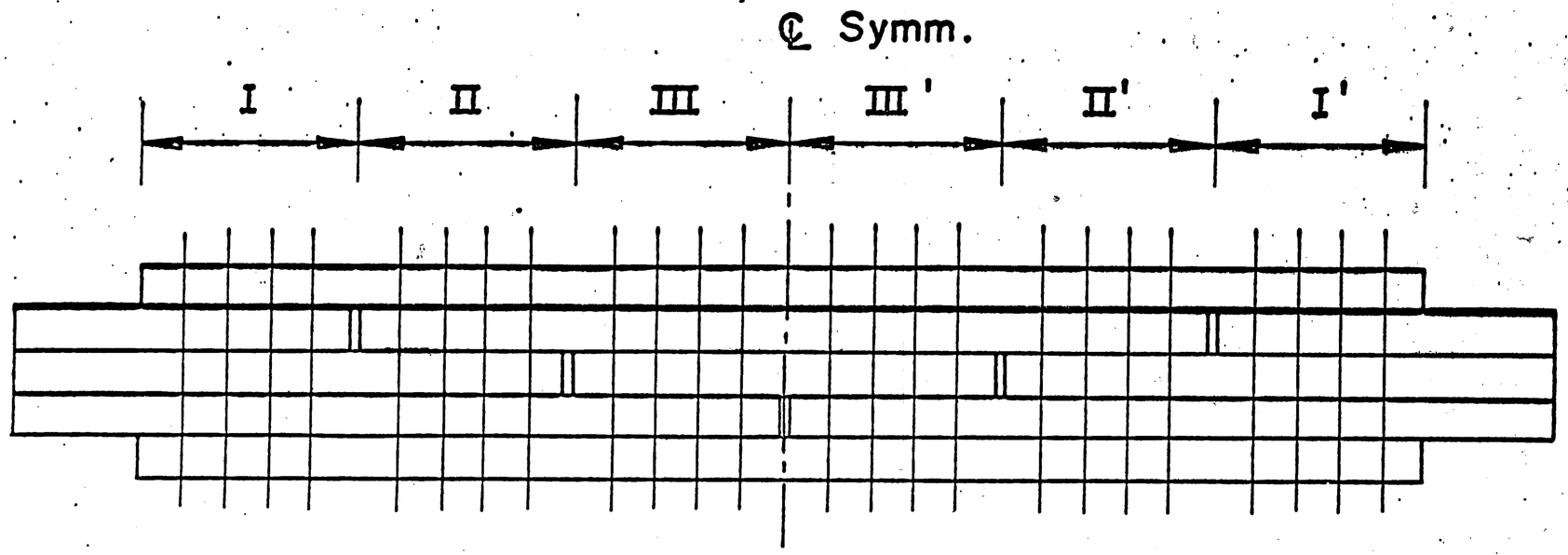

FIG. 5 TYPICAL SHINGLE JOINT

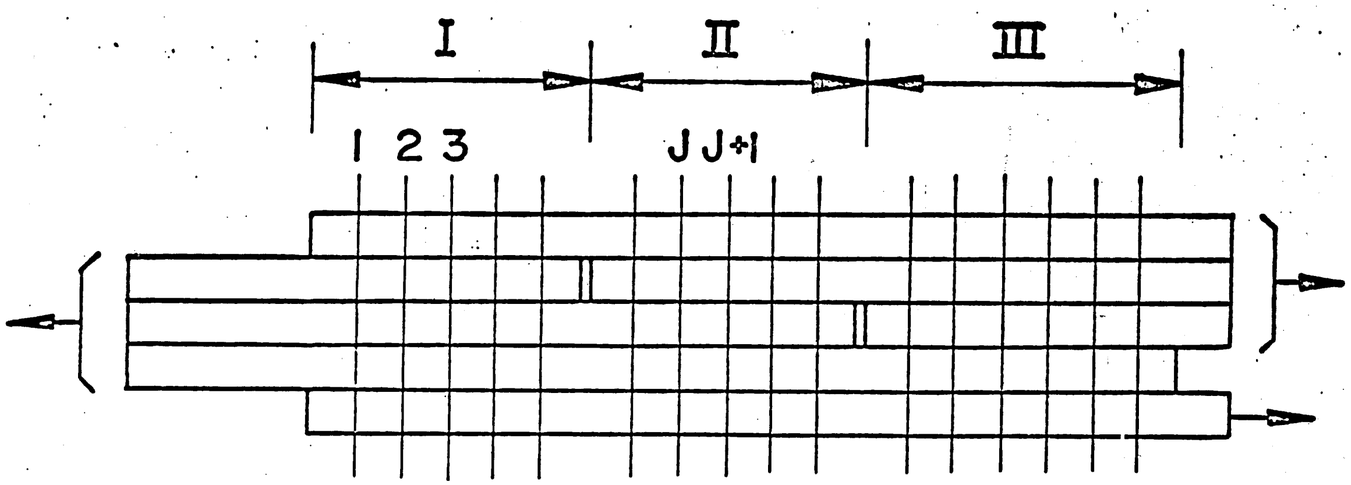

FIG. 6 SCHEMATIC OF IDEALIZED JOINT

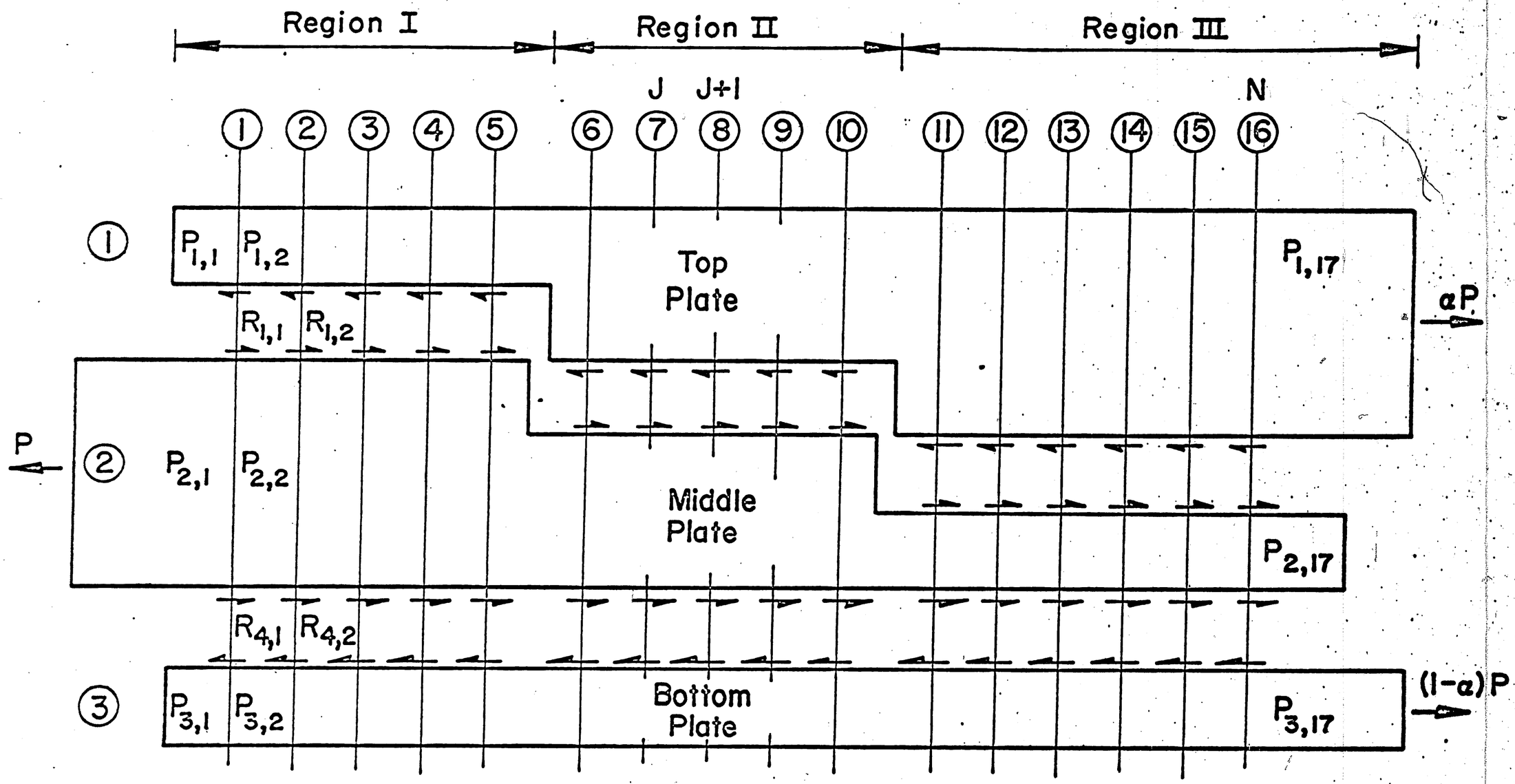

FIG. 7 IDEALIZED MODEL FOR FIRST STAGE OF ANALYSIS

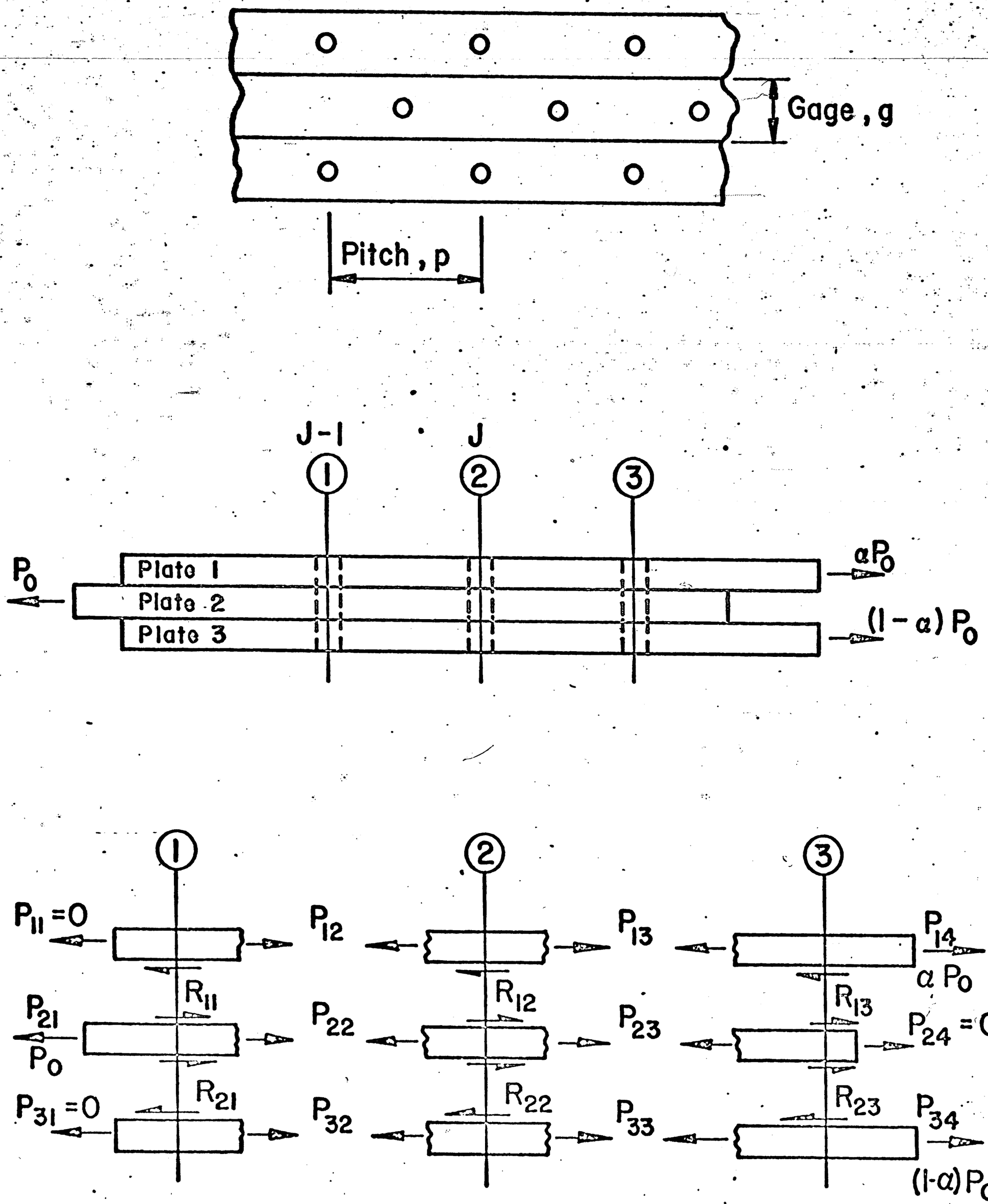

FIG. 8 UNSYMMETRICAL BUTT SPLICE

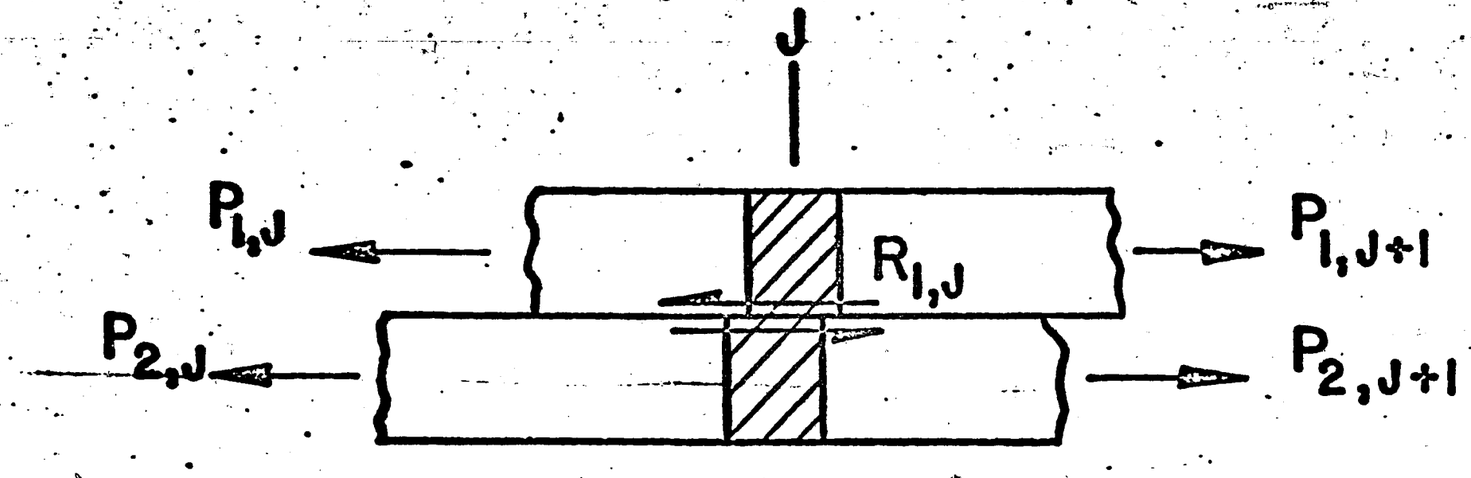

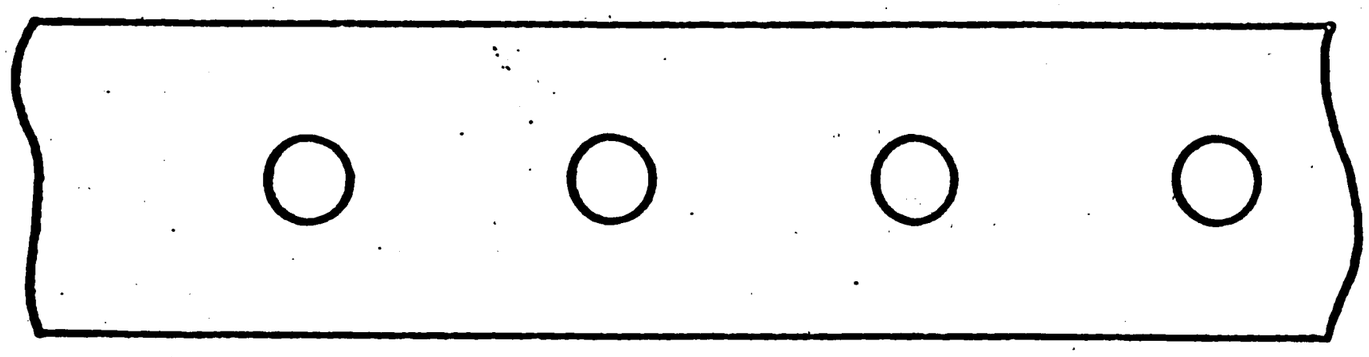

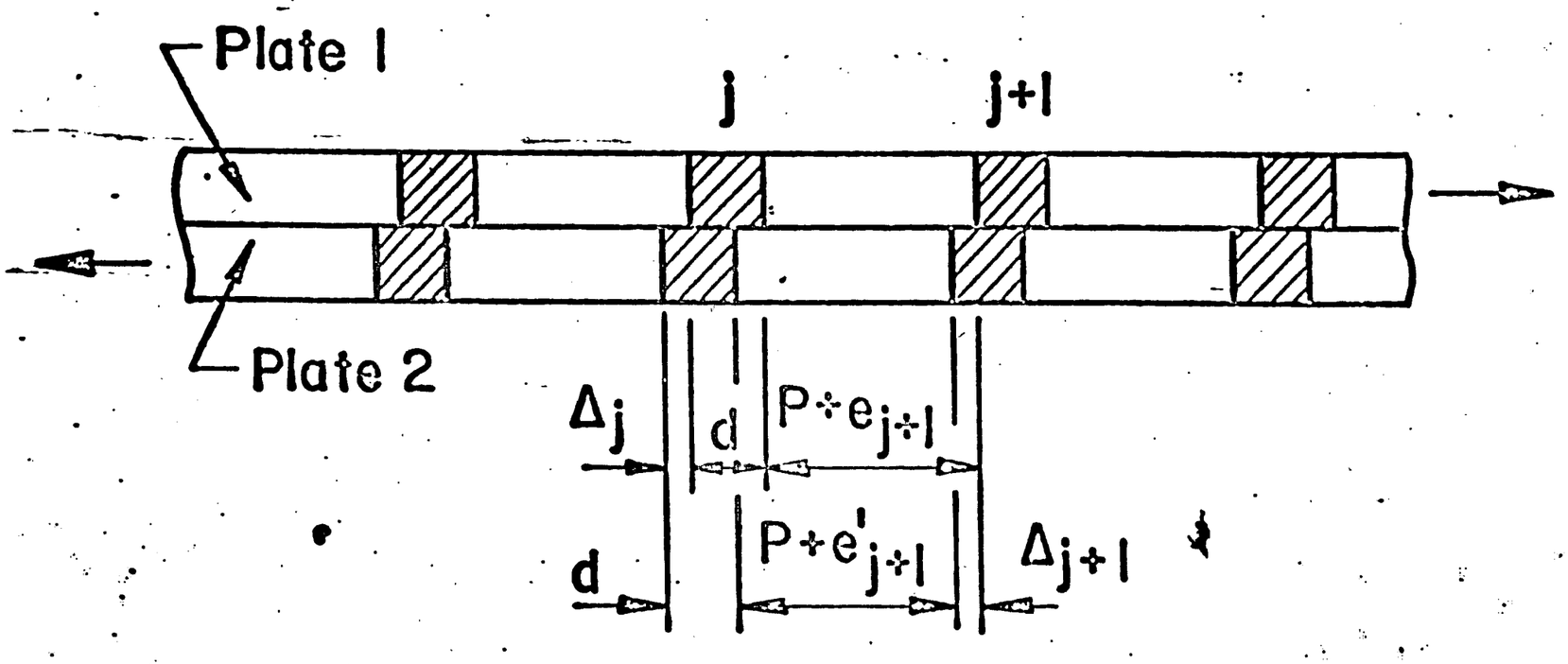

FIG. 9(a) DEFORMATIONS IN FASTENERS AND PLATES

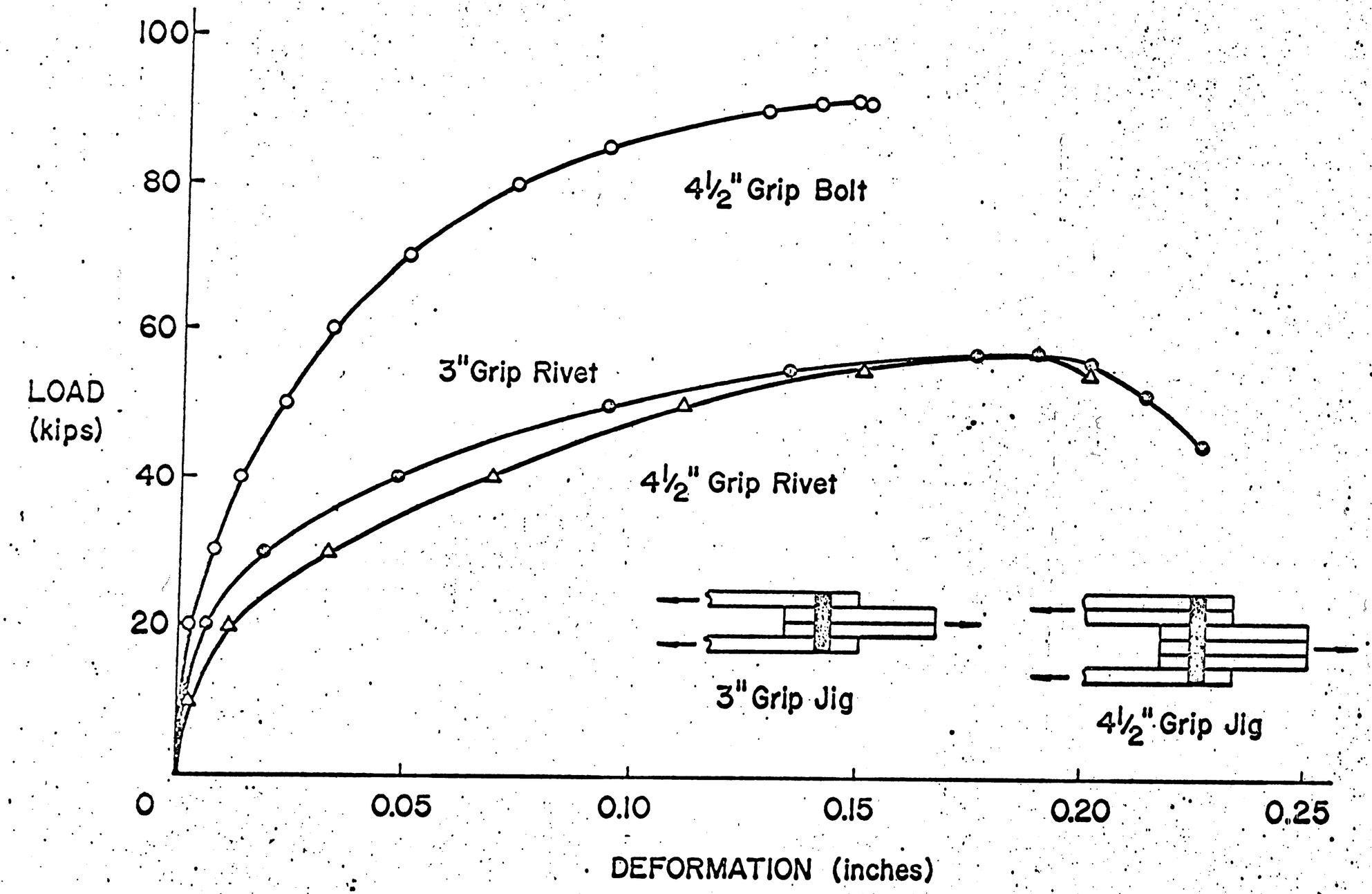

FIG. 9(b) SHEAR DEFORMATION BEHAVIOR OF SINGLE FASTENERS

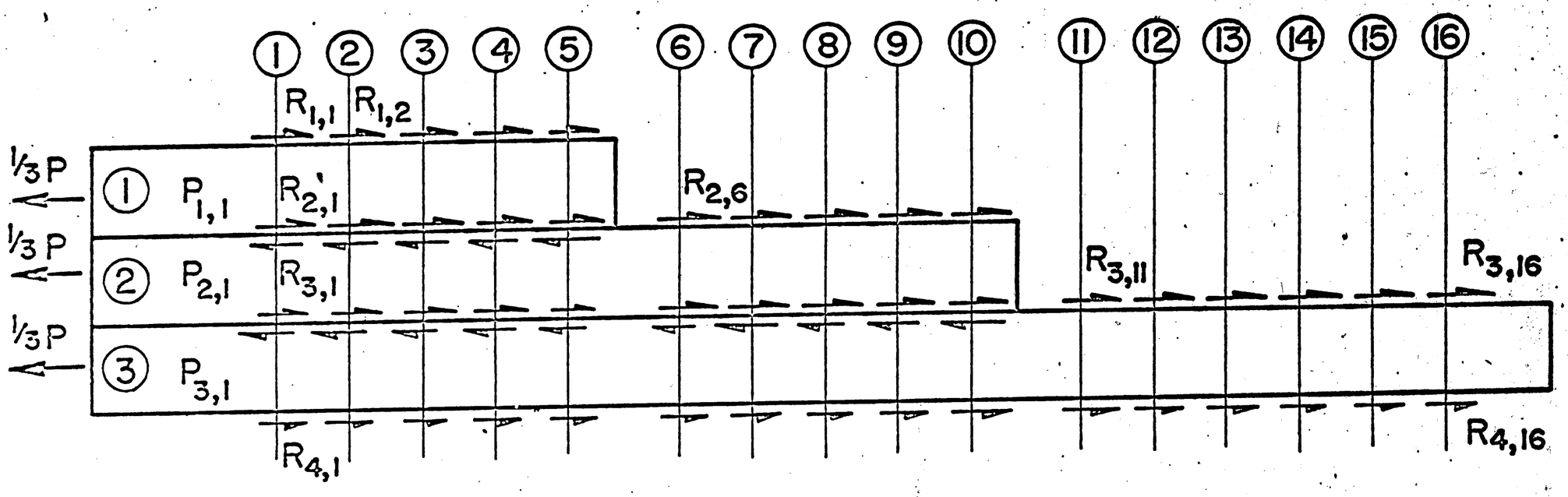

UNKNOWNS	B.C. : $P_{1,6} = 0$	B.C. : $P_{2,11} = 0$
$R_{2,1}$ & $R_{3,1}$		

FIG. 10 PORTION OF JOINT FOR SECOND STAGE OF ANALYSIS

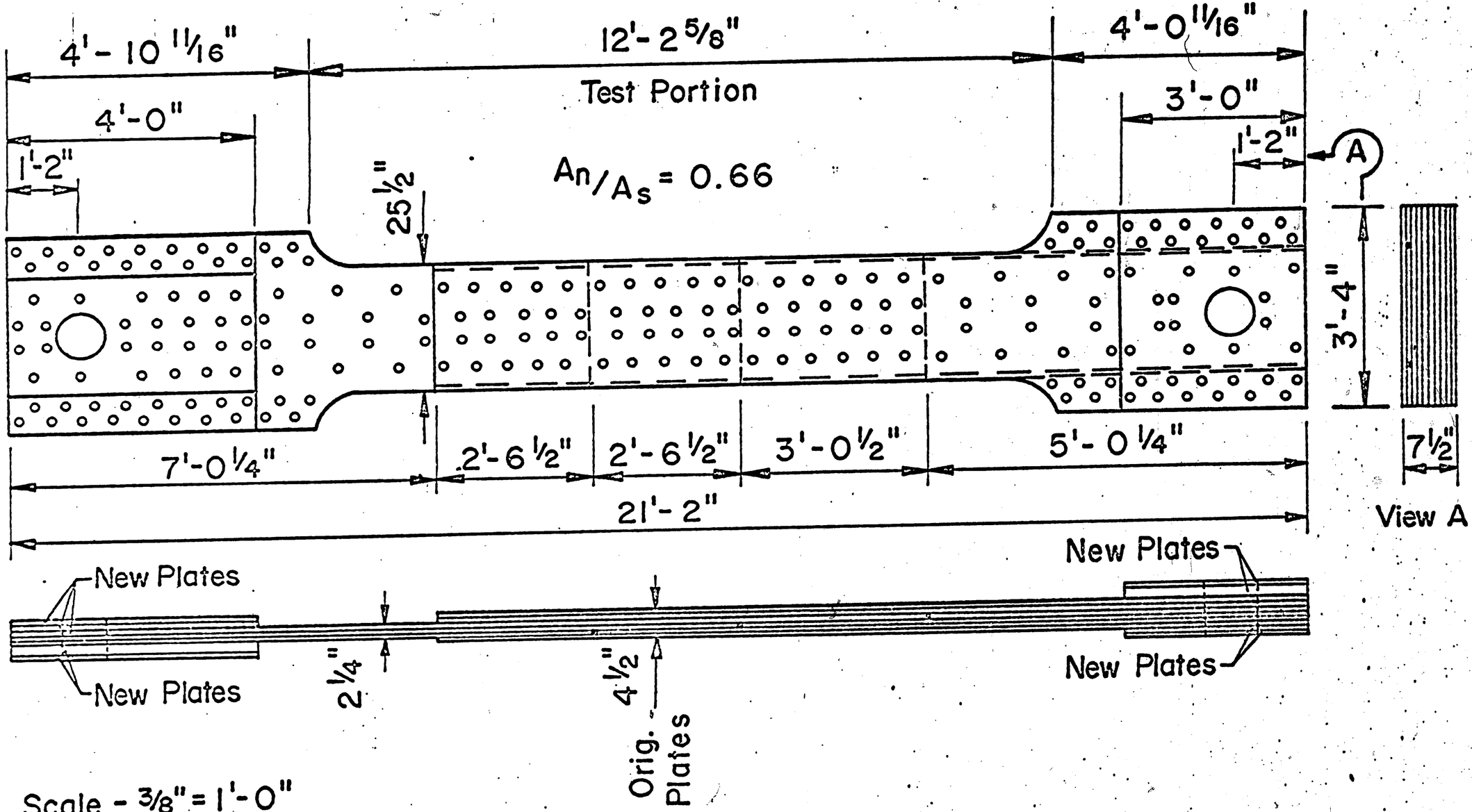

Scale - 3/8" = 1'-0"

FIG. 11 MODIFIED TEST JOINTS

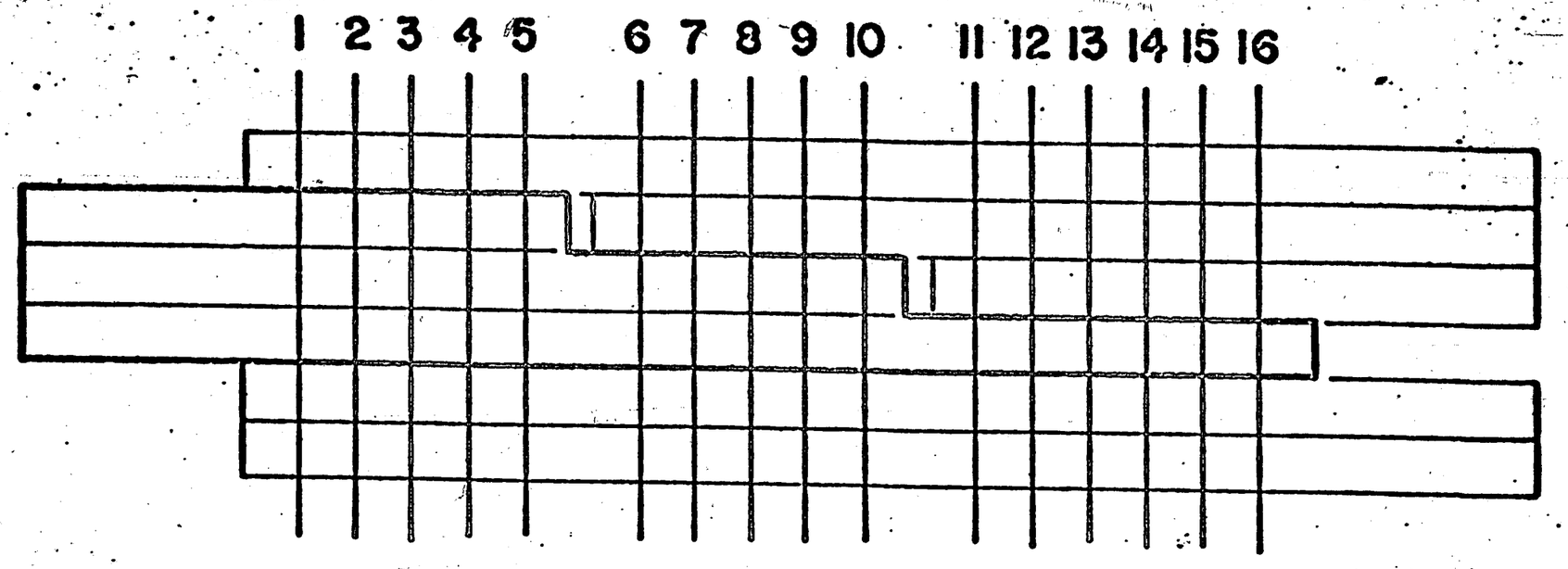

FIG. 12 SHEAR AND NET AREAS IN ORIGINAL AND MODIFIED JOINTS

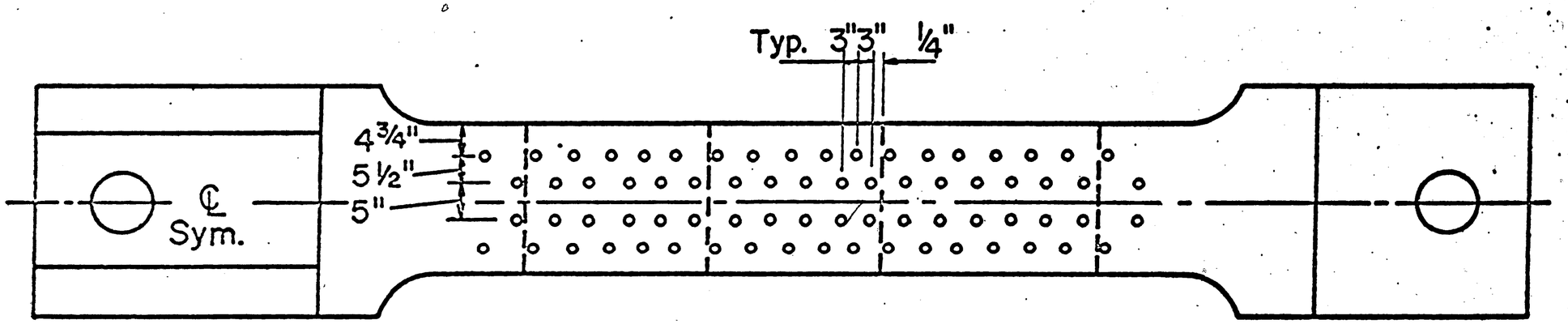

FIG. 13 POSITION OF SR4 STRAIN GAGES ON MODIFIED JOINTS

a) Mechanical Dial Gages

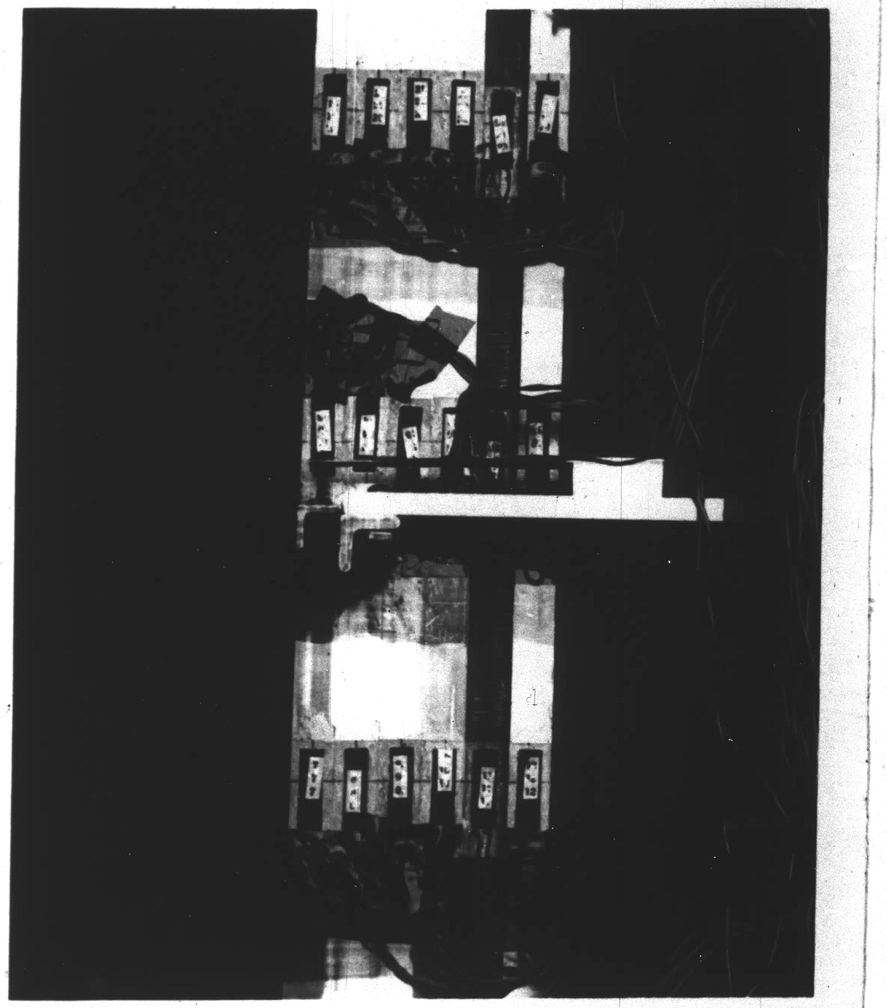

b) Cantilever Gages

FIG. 14 INSTRUMENTATION OF BOLTED JOINT

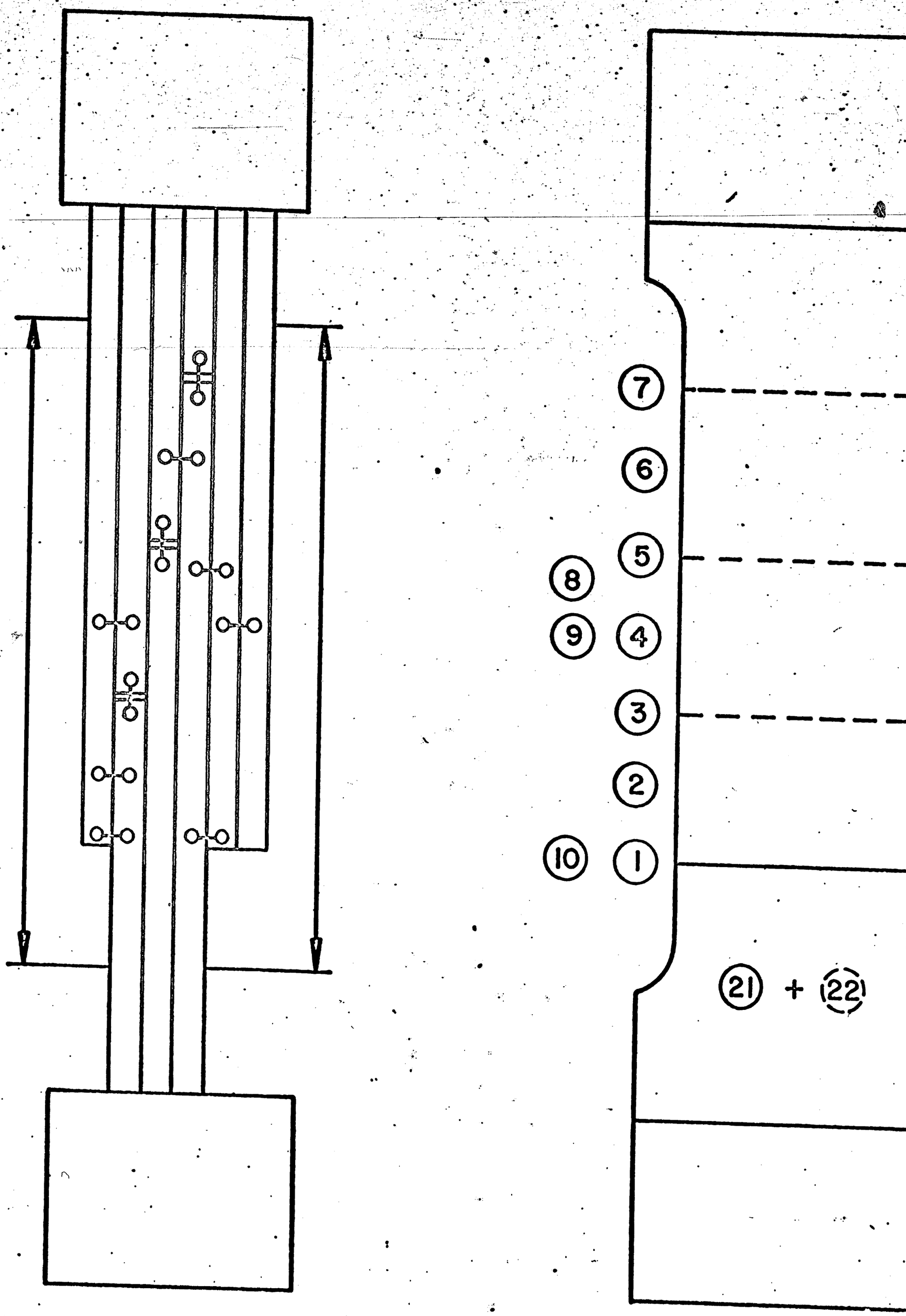

FIG. 15 LOCATION OF LOCAL AND OVERALL JOINT ELONGATIONS IN MODIFIED JOINTS

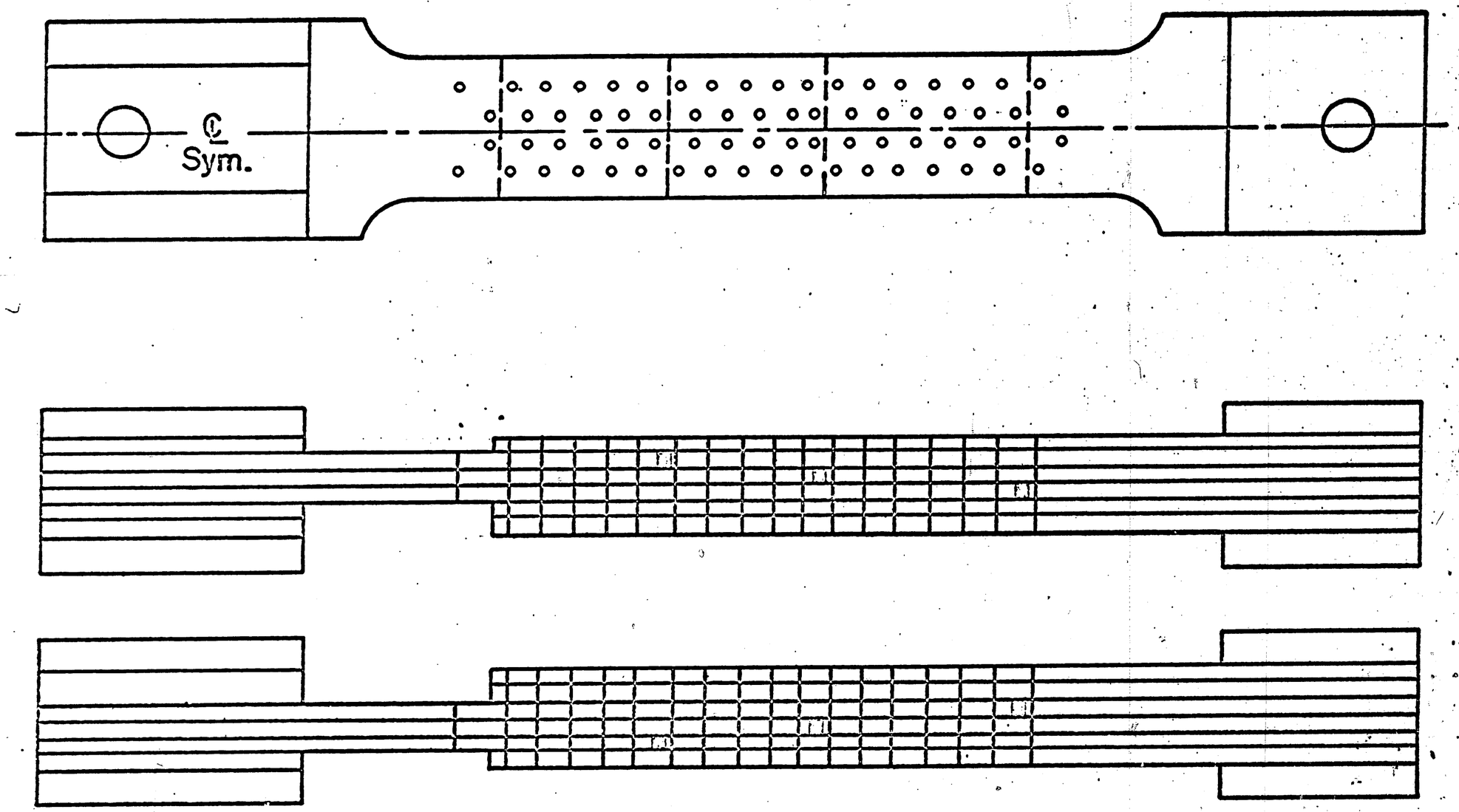

FIG. 16 SCRIBE LINES FOR MEASURING HOLE OFFSET IN MODIFIED JOINTS

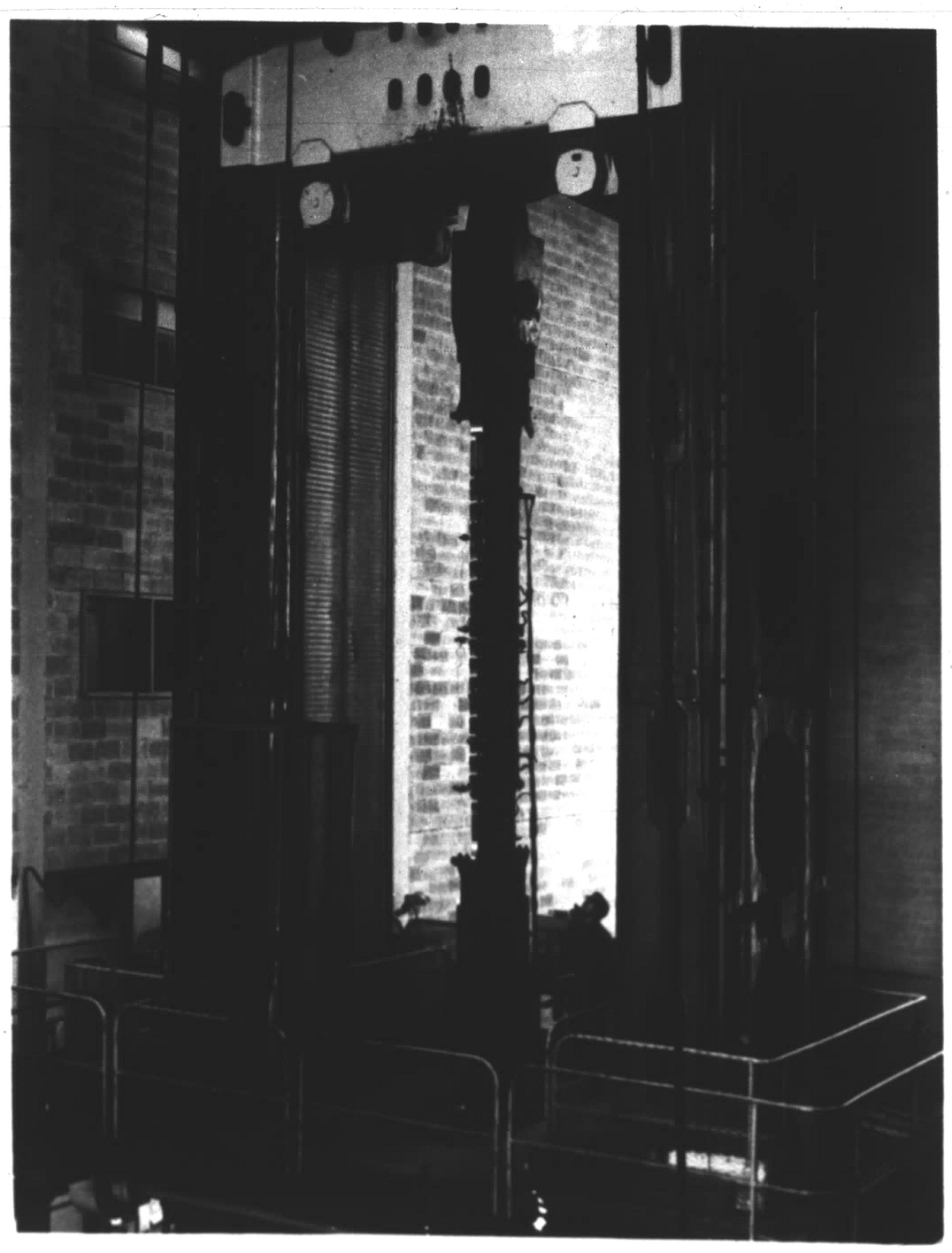

FIG. 17 MODIFIED TEST JOINT IN 5,000,000 lb. MACHINE

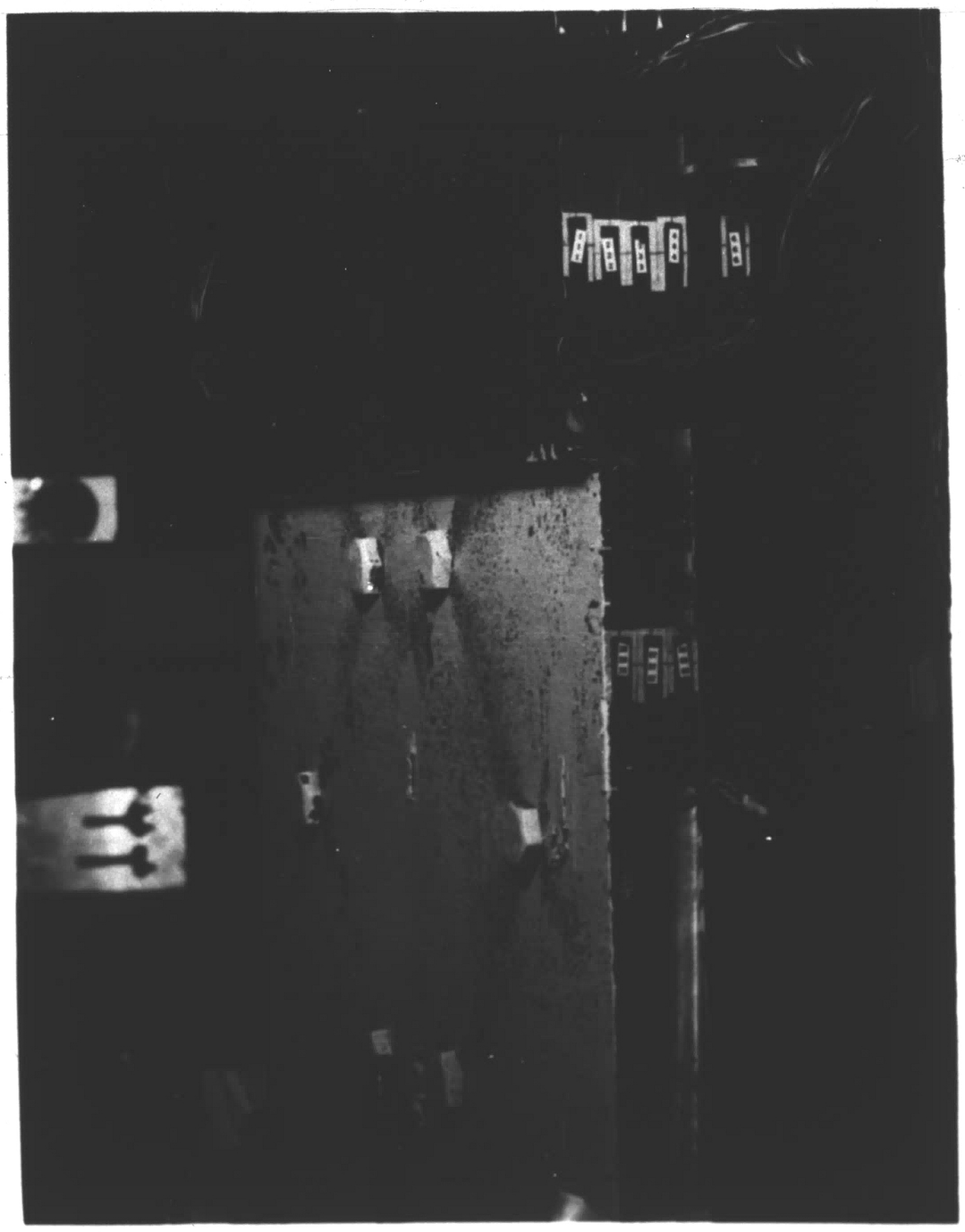

FIG. 18 "UNBUTTONING" FAILURE OF LARGE BOLTED JOINT

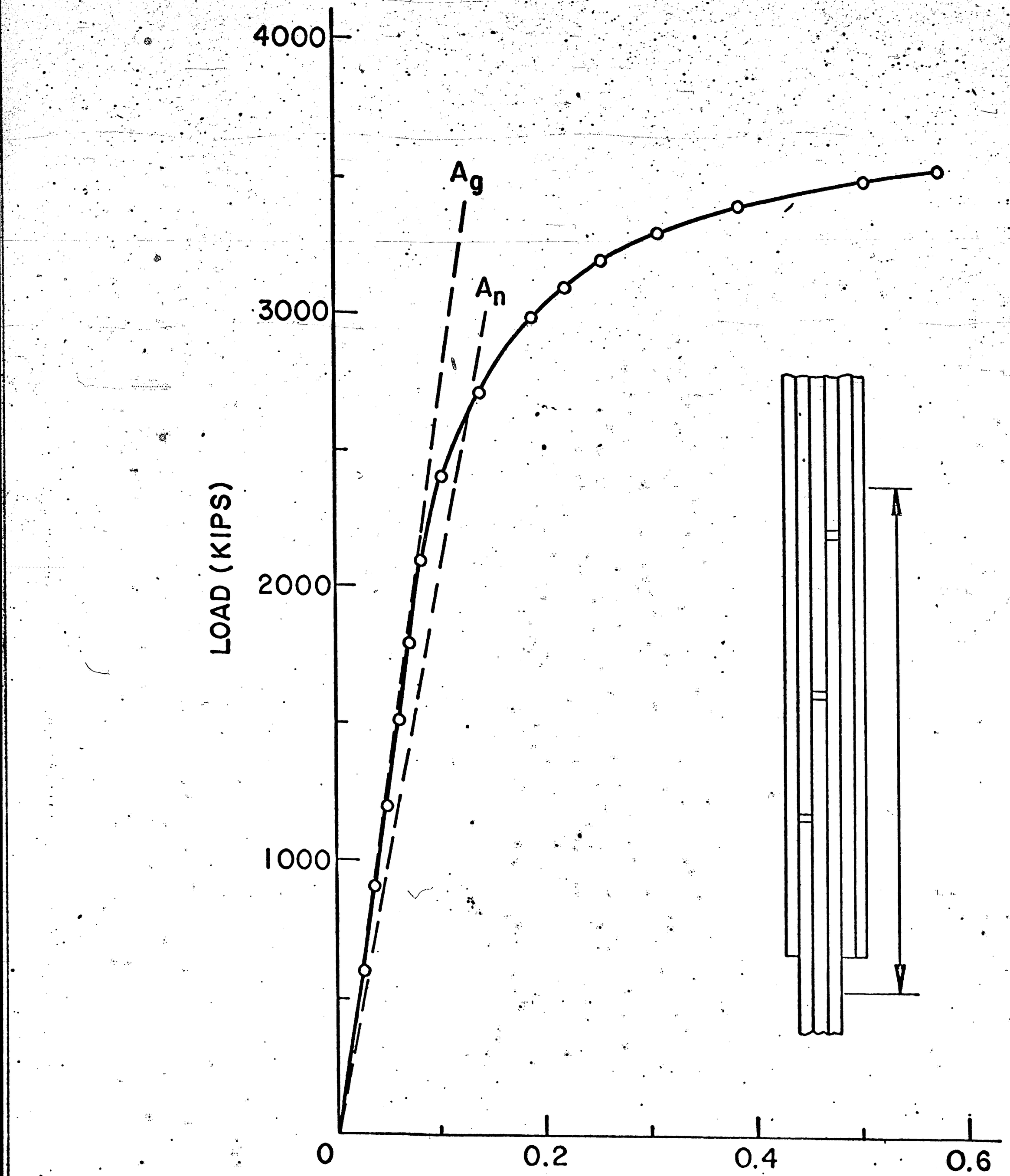

FIG. 19 LOAD-ELONGATION CURVE FOR MODIFIED BOLTED JOINT

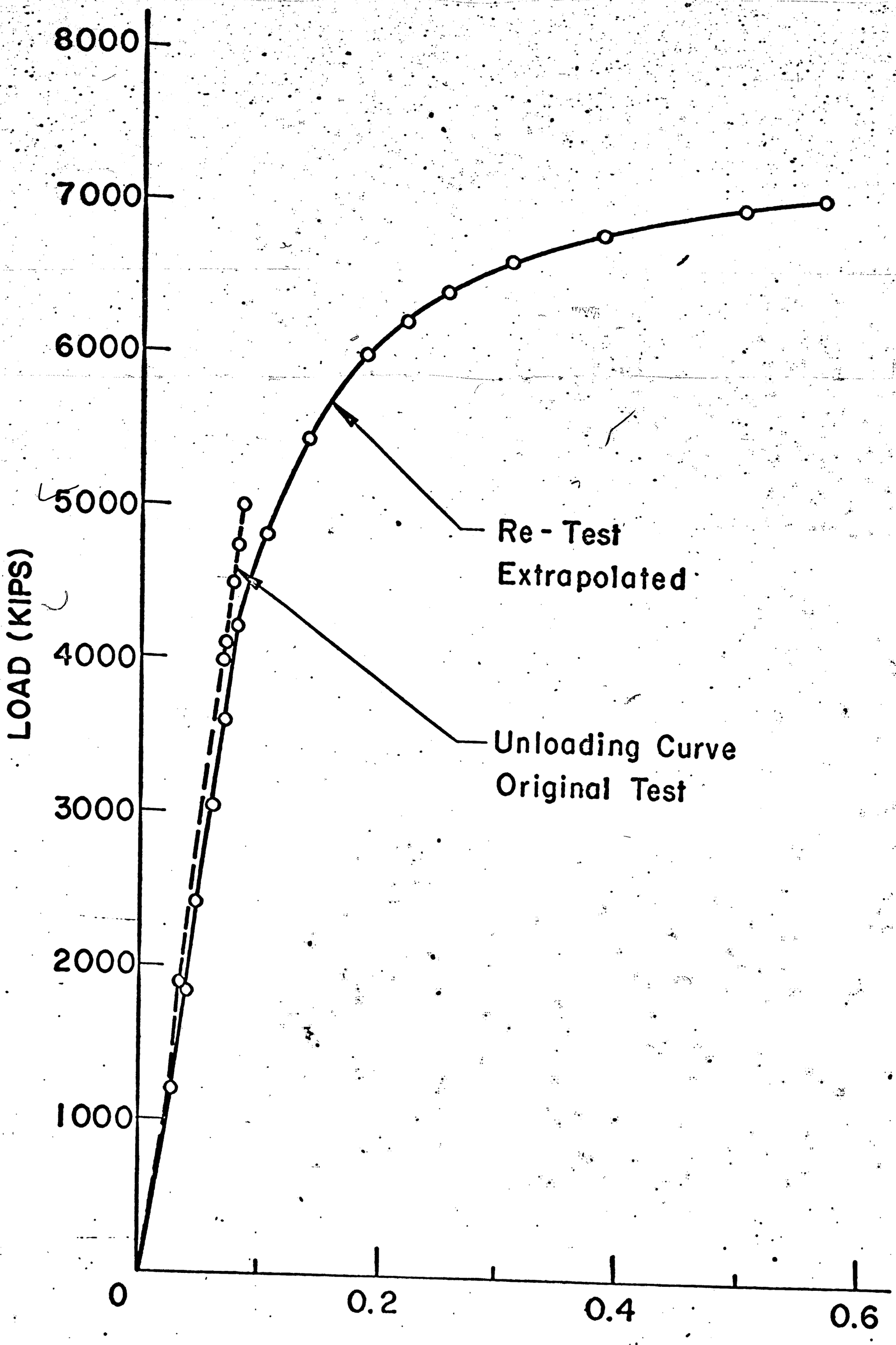

FIG. 20 COMPARISON OF LOAD-DEFORMATION CURVES FOR THE ORIGINAL TEST AND THE RE-TEST OF BOLTED JOINT

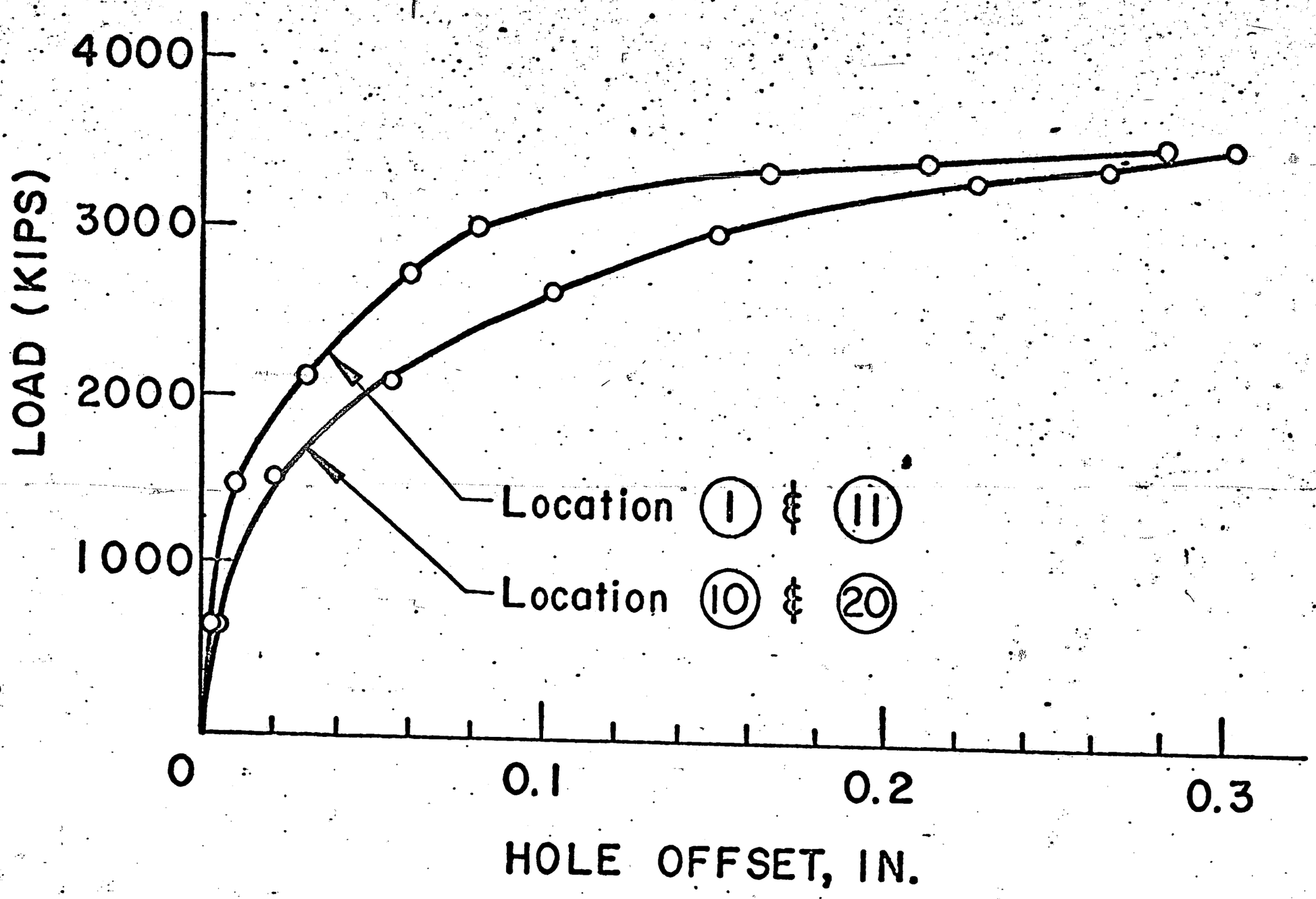

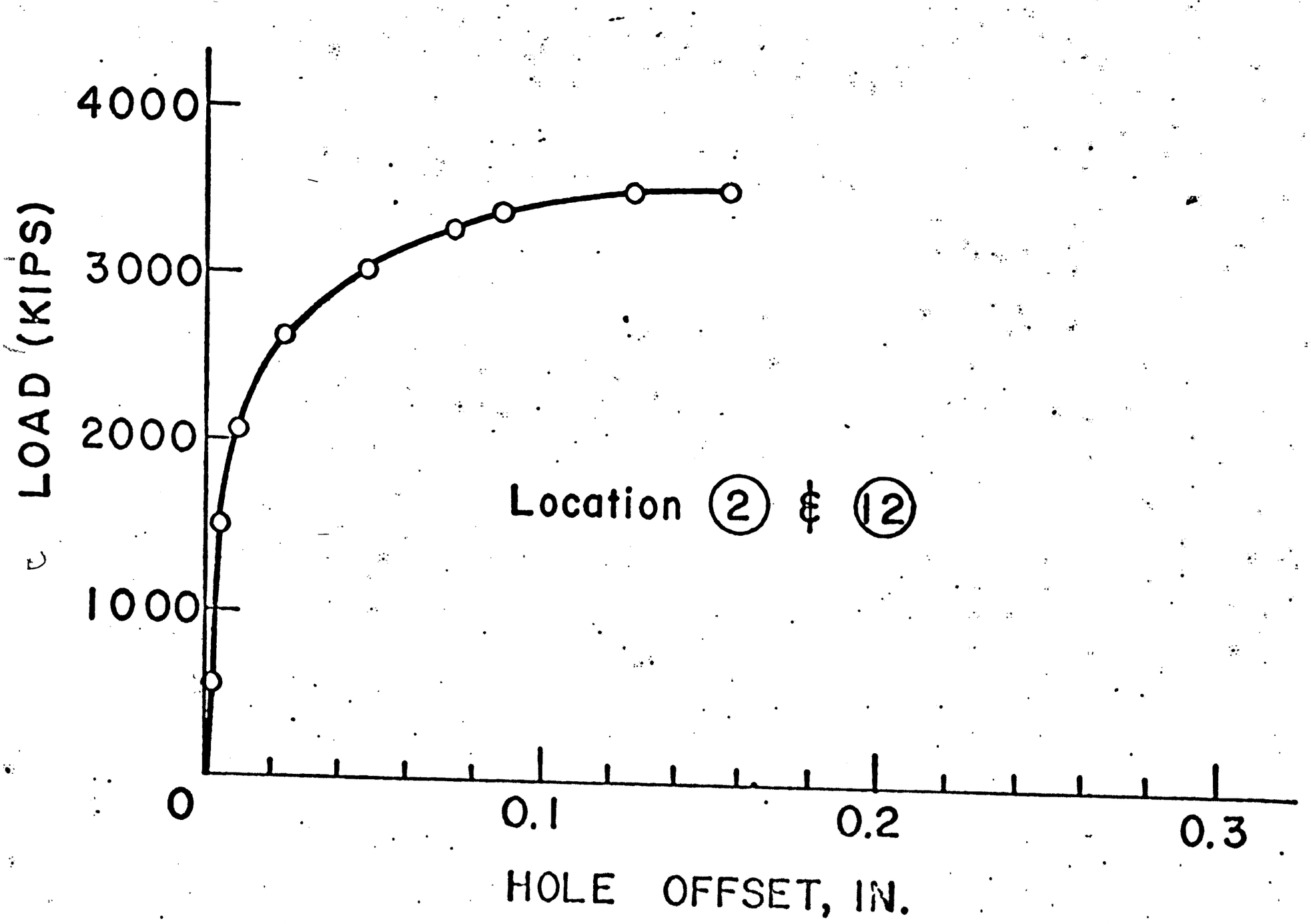

FIG. 21(a) LOCAL DEFORMATION OF LARGE BOLTED JOINT

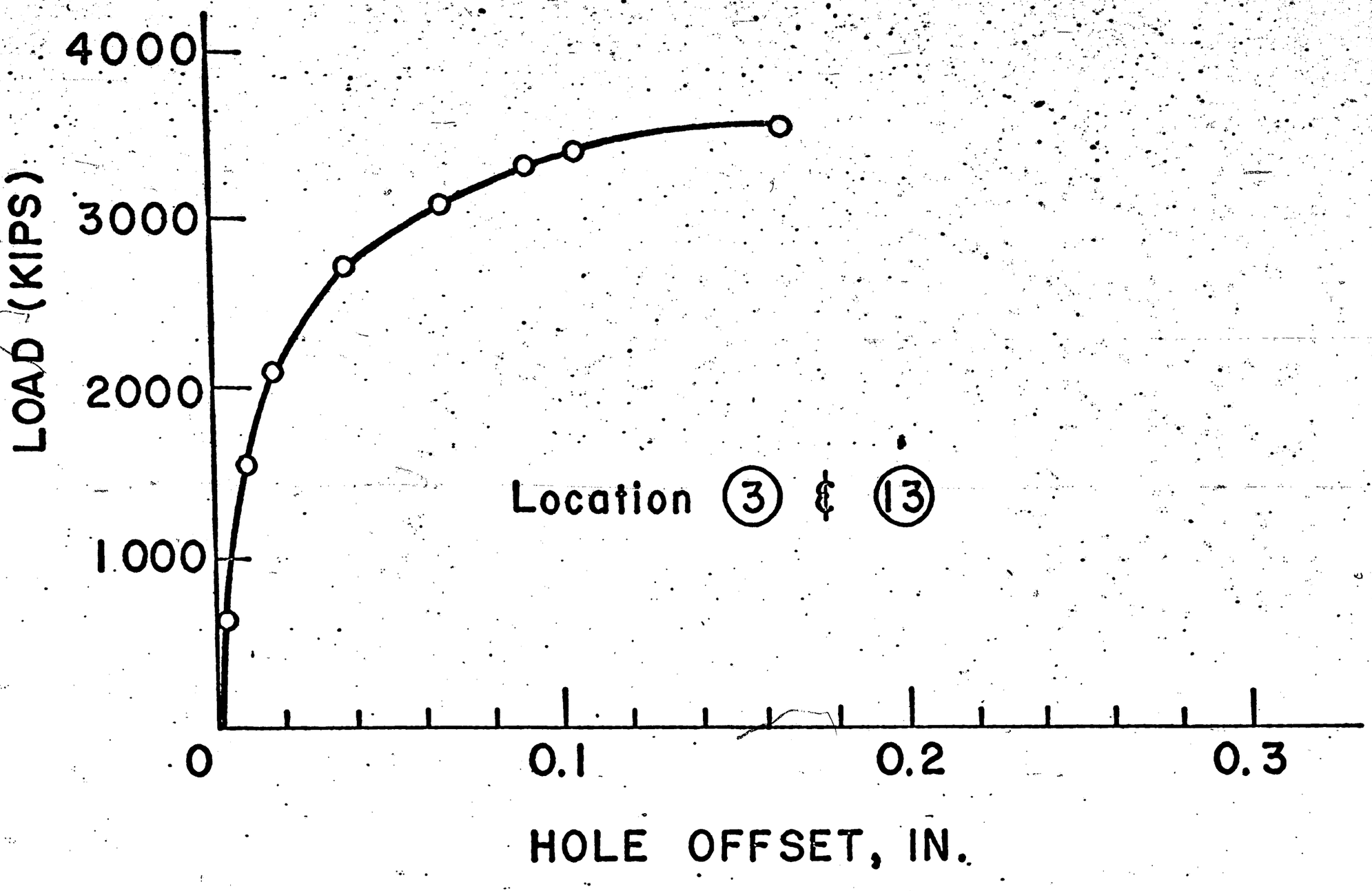

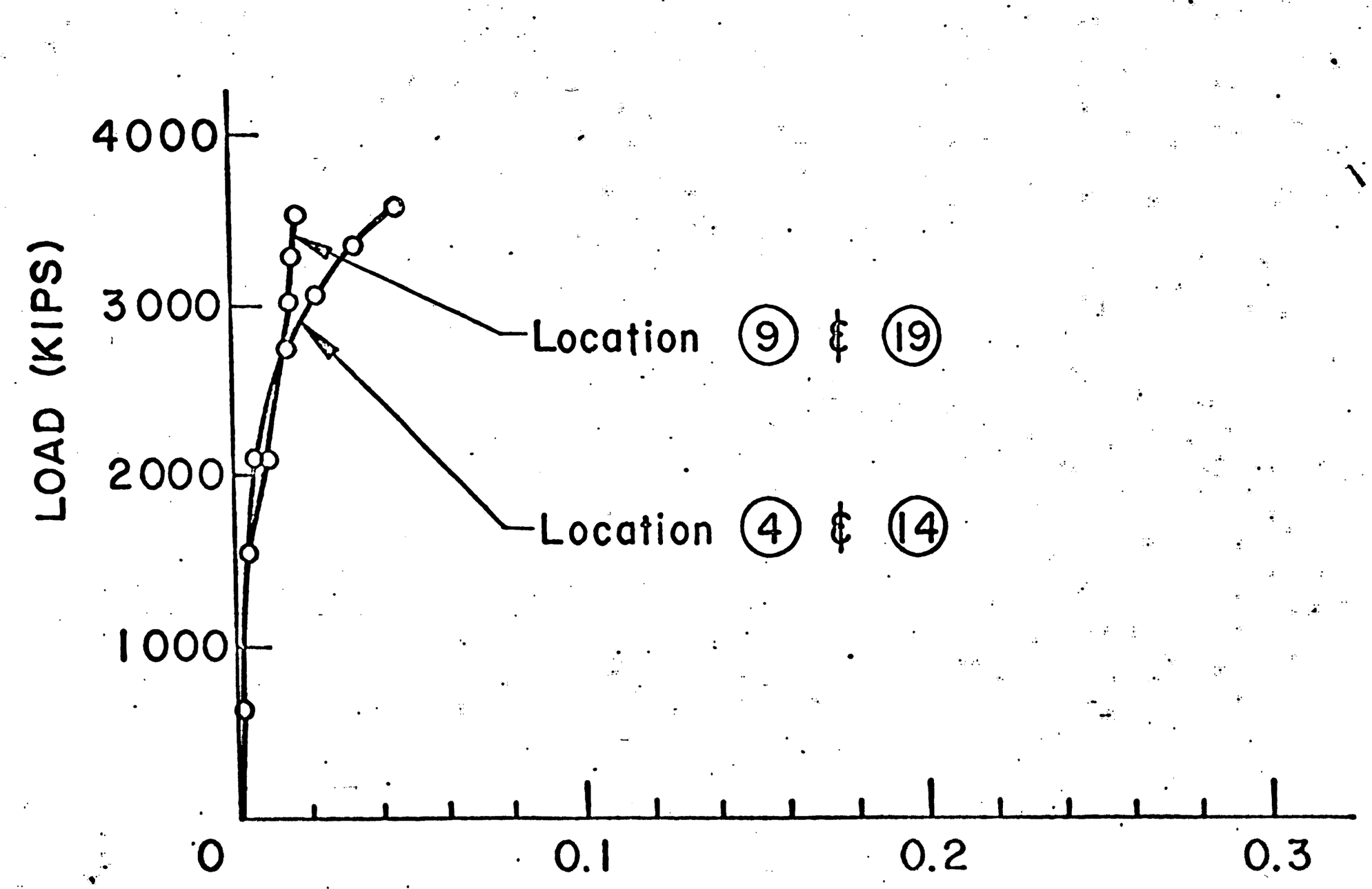

FIG. 21(b) LOCAL DEFORMATION OF LARGE BOLTED JOINT

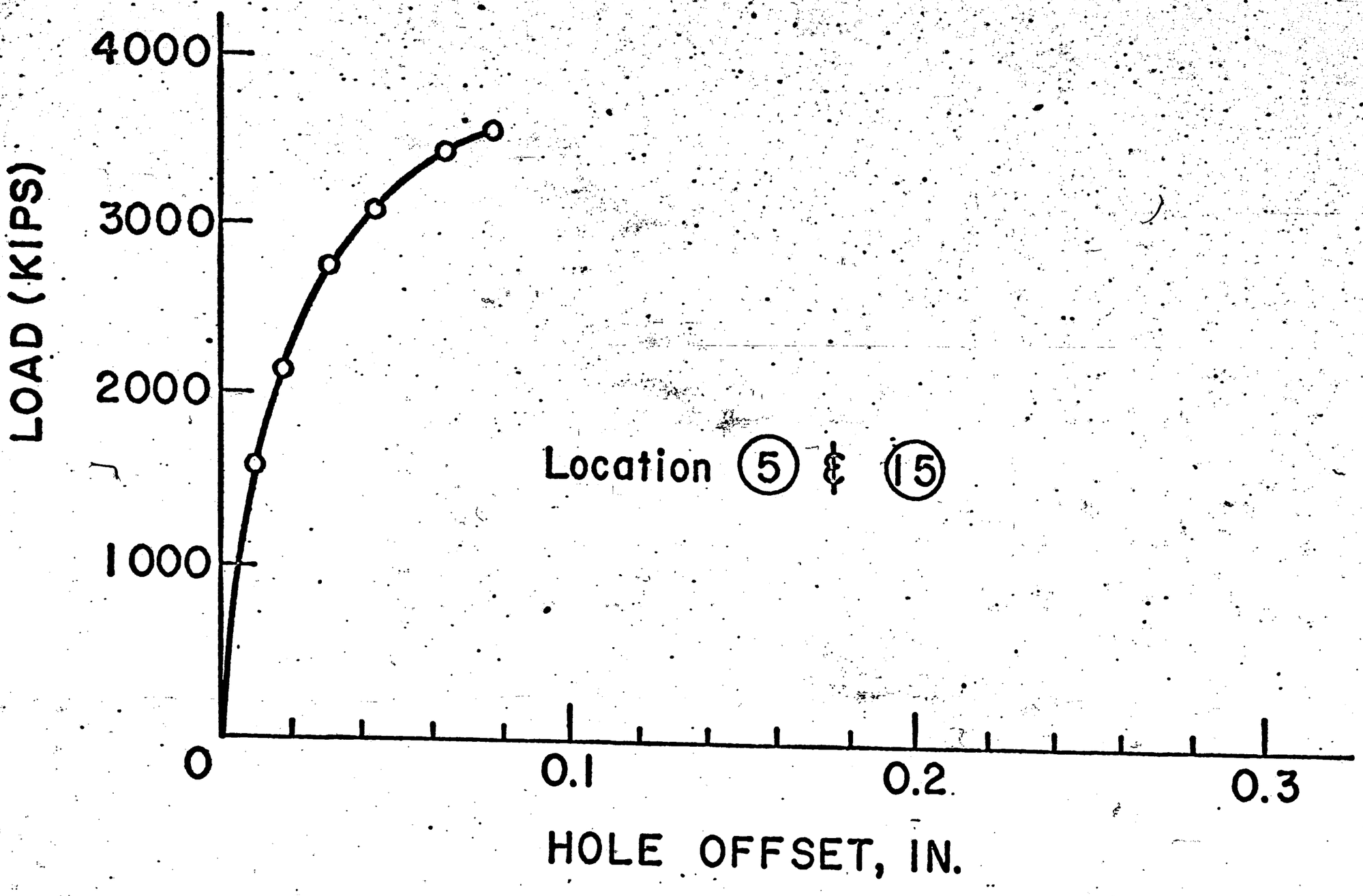

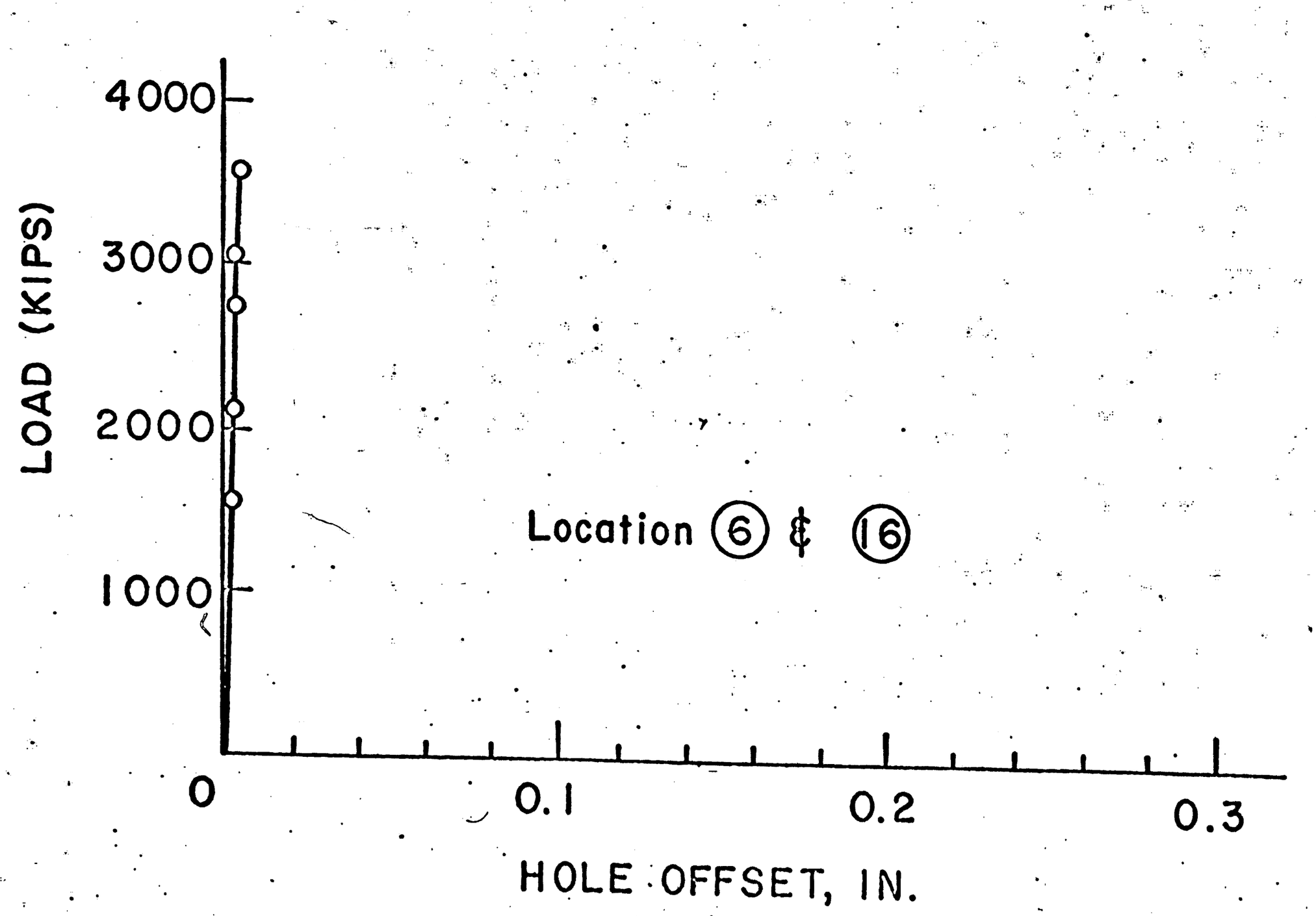

FIG. 21(c) LOCAL DEFORMATION OF LARGE BOLTED JOINT

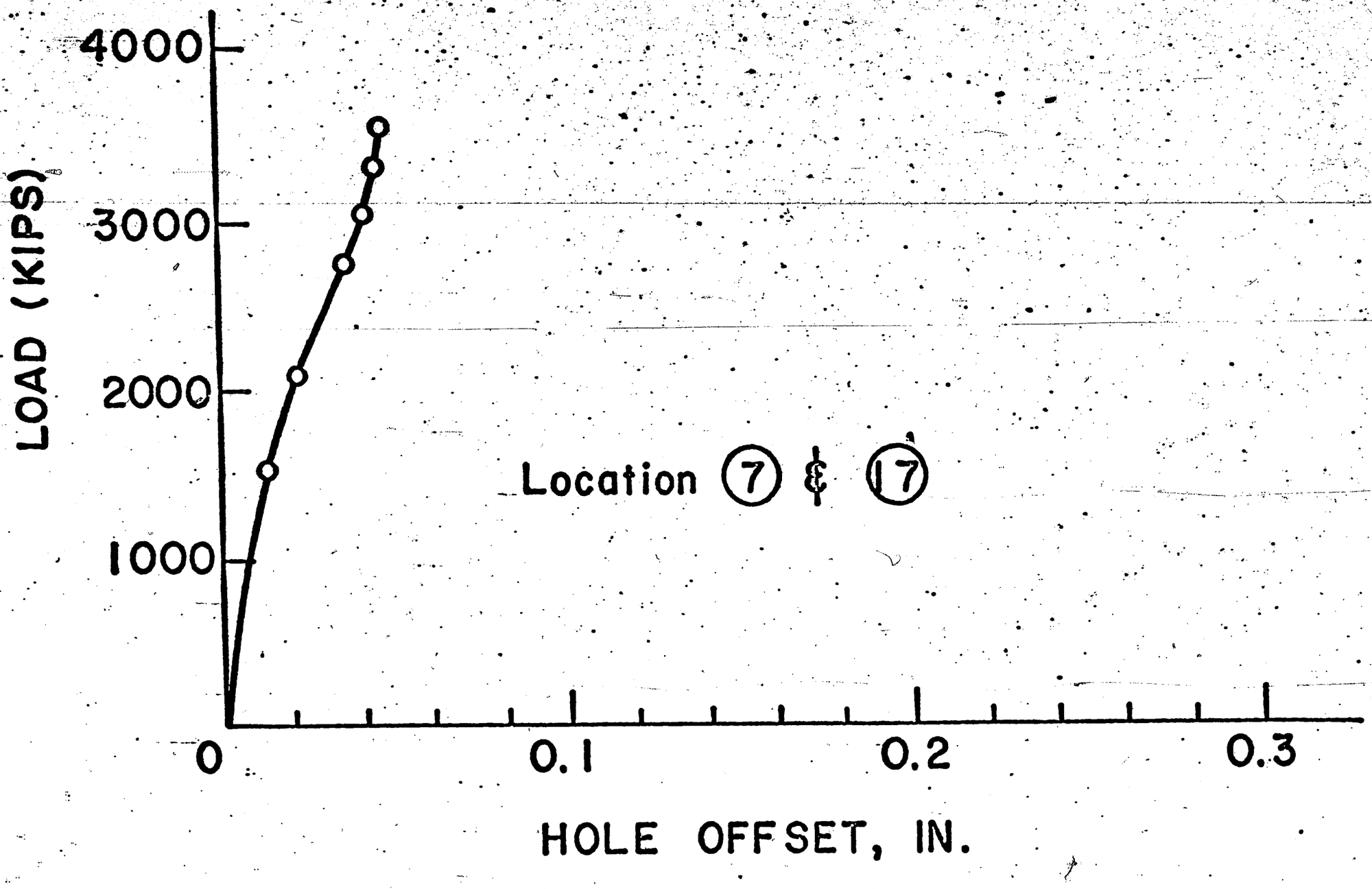

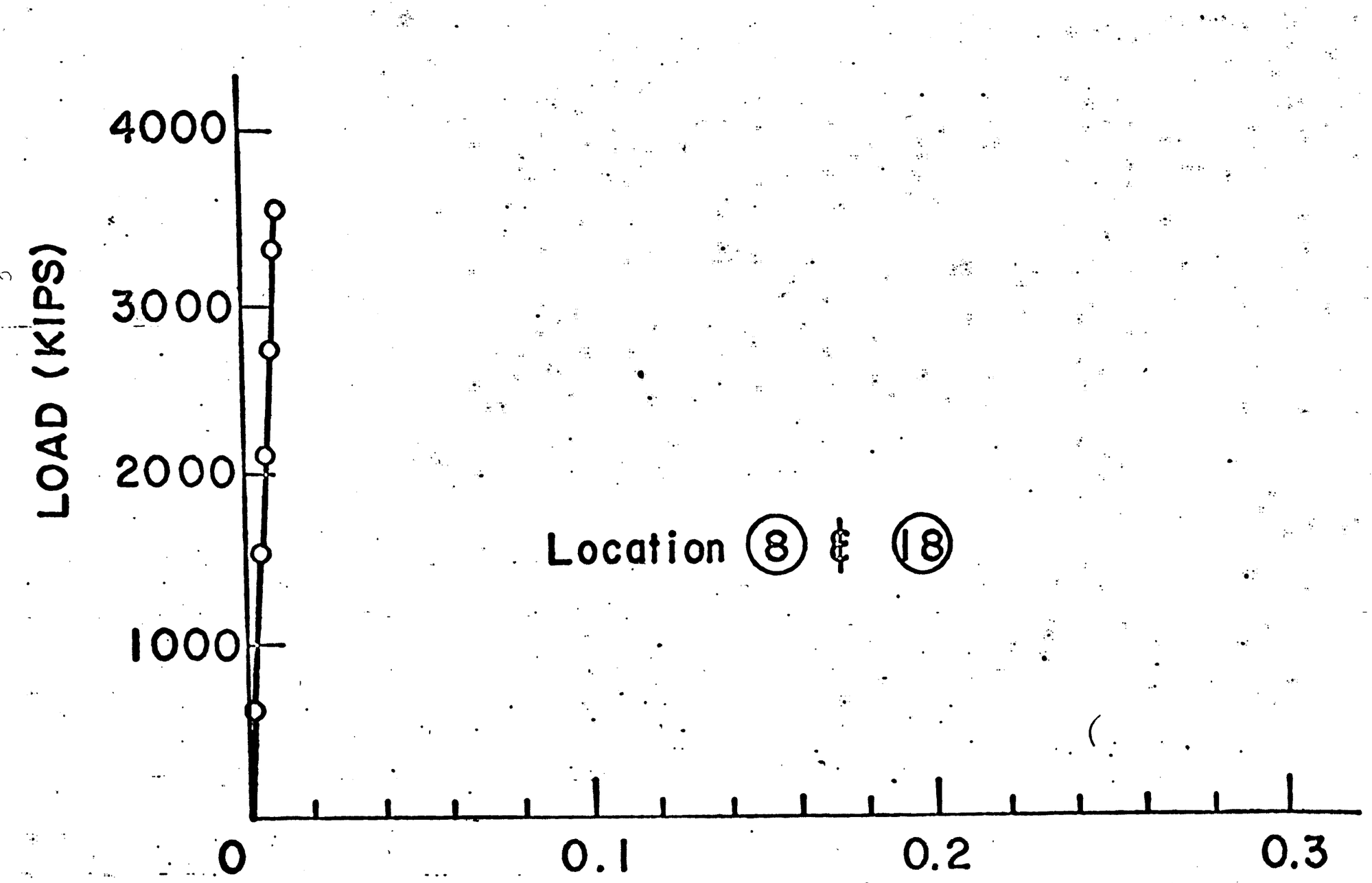

FIG. 21(d) LOCAL DEFORMATION OF LARGE BOLTED JOINT

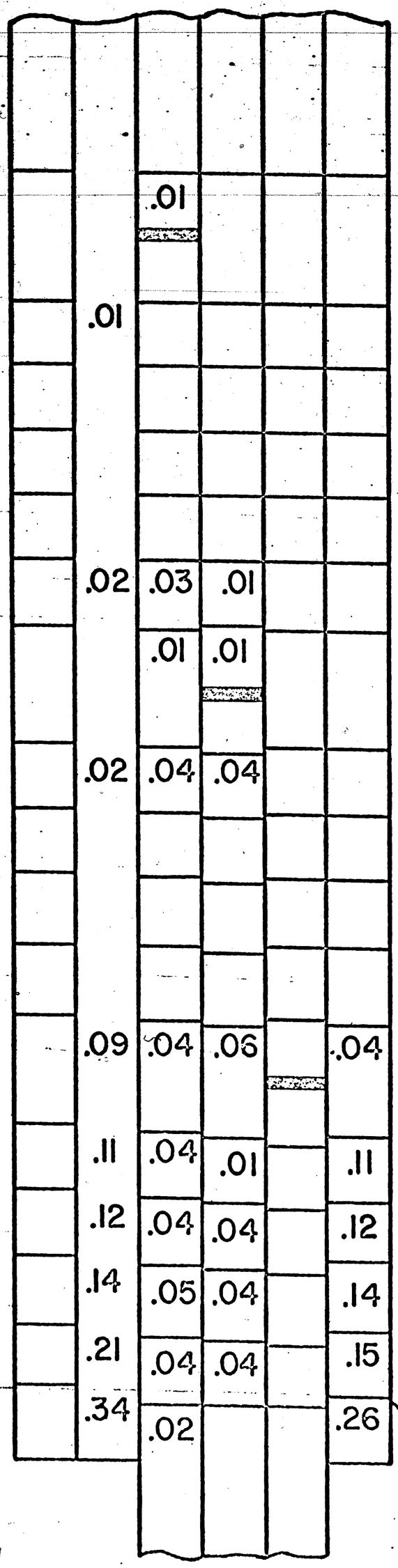

P = 3550^k

FIG. 22 HOLE OFFSETS IN MODIFIED BOLTED JOINT

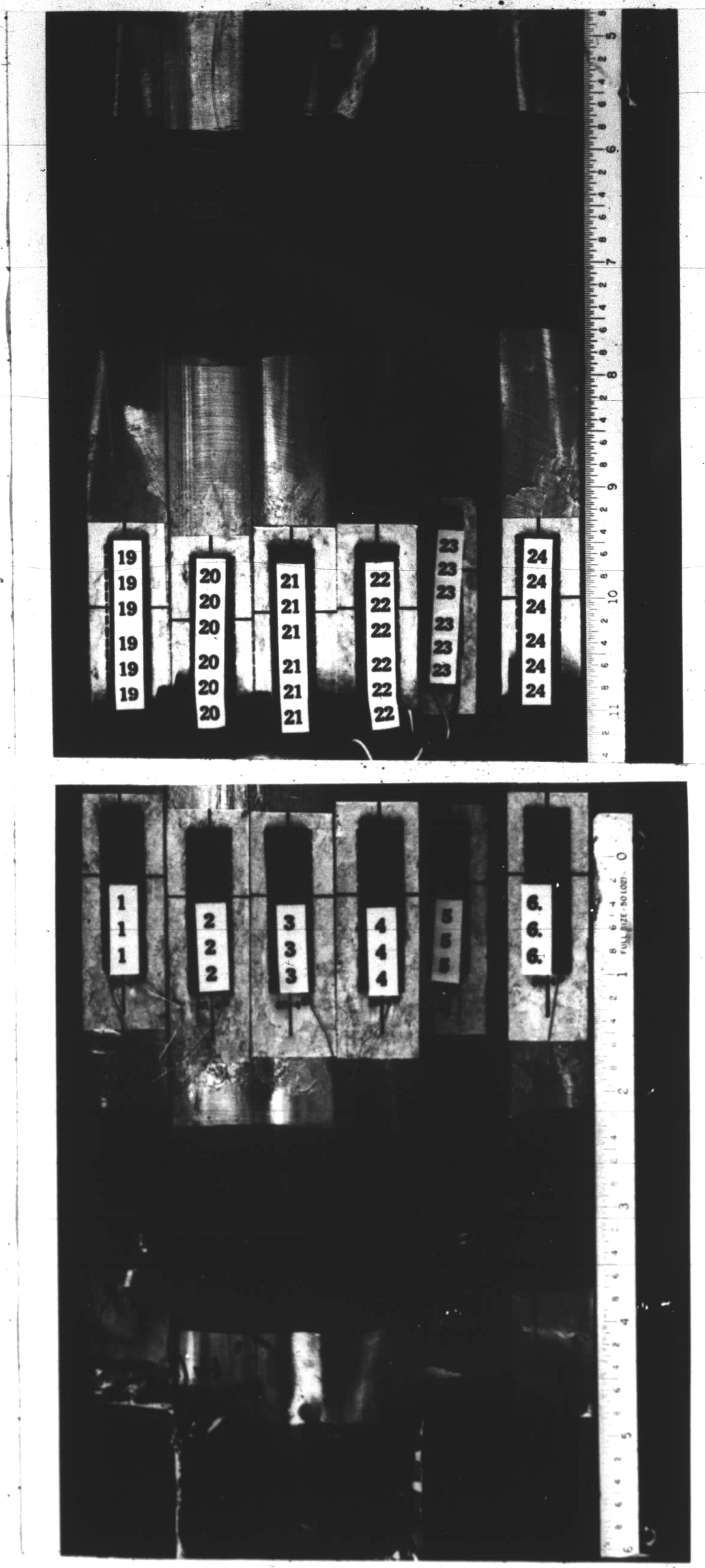

FIG. 23 SCRIBE LINES AFTER FAILURE IN MODIFIED BOLTED JOINT

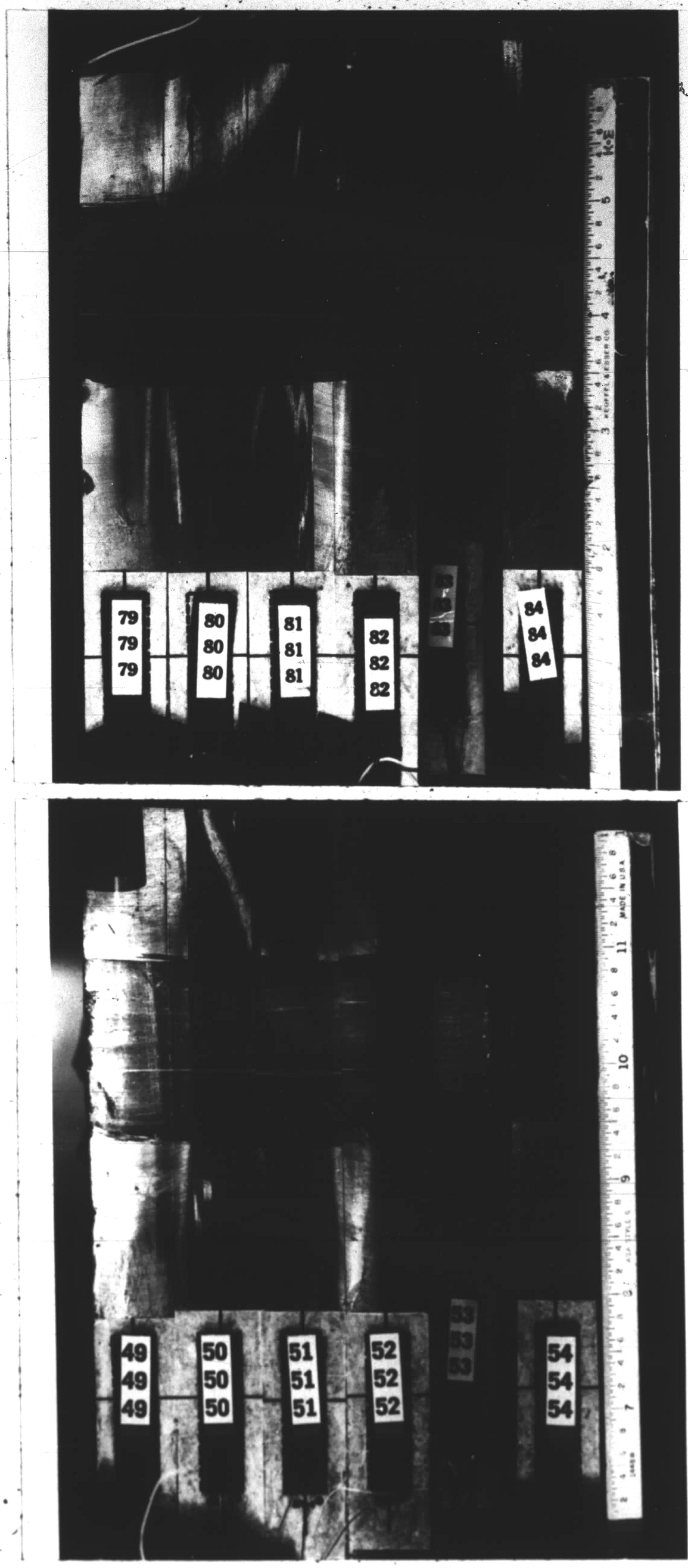

FIG. 24 SCRIBE LINES AFTER FAILURE IN MODIFIED BOLTED JOINT

BOLTED JOINT

353 (396)	286 (282)	190 (170)
489 (508) ○	298 (508)	273 (508)
509 (508)	353 (508) ○	279 (508)
527 (508)	315 (508)	329 (508) ○
235 (53)	291 (107)	332 (161)
268 (59)	320 (119)	450 (177)

( ) : Assumed Plate

Loads At 1524 Kips Design Load

FIG. 25 COMPARISON OF THE MEASURED AND ASSUMED LOAD DISTRIBUTION IN MODIFIED BOLTED JOINT

FASTENER NUMBER

PLATE NO.	①	②	③	④	⑤	⑥	⑦	⑧	⑨	⑩	⑪	⑫	⑬	⑭	⑮	⑯
①		64	126	221	305	353	342	290	273	280	300	266	219		188	256	194
②	489	403	336	270	136		67	199	250	273	296	281	248		226	231	260
③	509	469	413	358	352	353	304	271	235	132		79	167		243	262	286
④	527	533	499	416	341	315	298	267	266	292	317	294	274		249	129	
⑤		15	38	119	187	235	259	236	228	267	294	284	274		280	301	337
⑥		40	112	140	203	268	254	261	272	280	317	320	342		338	345	447

P = 1524 kips

FIG. 26 MEASURED LOAD DISTRIBUTION IN MODIFIED BOLTED JOINT AT LOAD LEVEL OF 1524 kips

FASTENER NO.

PLATE NO.	①	②	③	④	⑤	⑥	⑦	⑧	⑨	⑩	⑪	⑫	⑬	⑭	⑮	⑯
①		75	159	303	420	514	452	428	388	400	406	380	310		277	294	299
②	687	578	493	375	161		93	248	338	382	412	400	344		322	338	340
③	688	642	600	519	514	507	447	381	316	158		81	283		338	366	404
④	705	722	683	598	547	442	440	370	355	394	457	429	355		327	164	
⑤		17	39	103	200	290	315	315	322	354	390	377	350		368	430	445
⑥		46	106	182	238	327	333	338	361	392	415	413	438		448	488	592

P = 2080 Kips

FIG. 27 MEASURED LOAD DISTRIBUTION IN MODIFIED BOLTED JOINT AT LOAD LEVEL OF 2080 kips

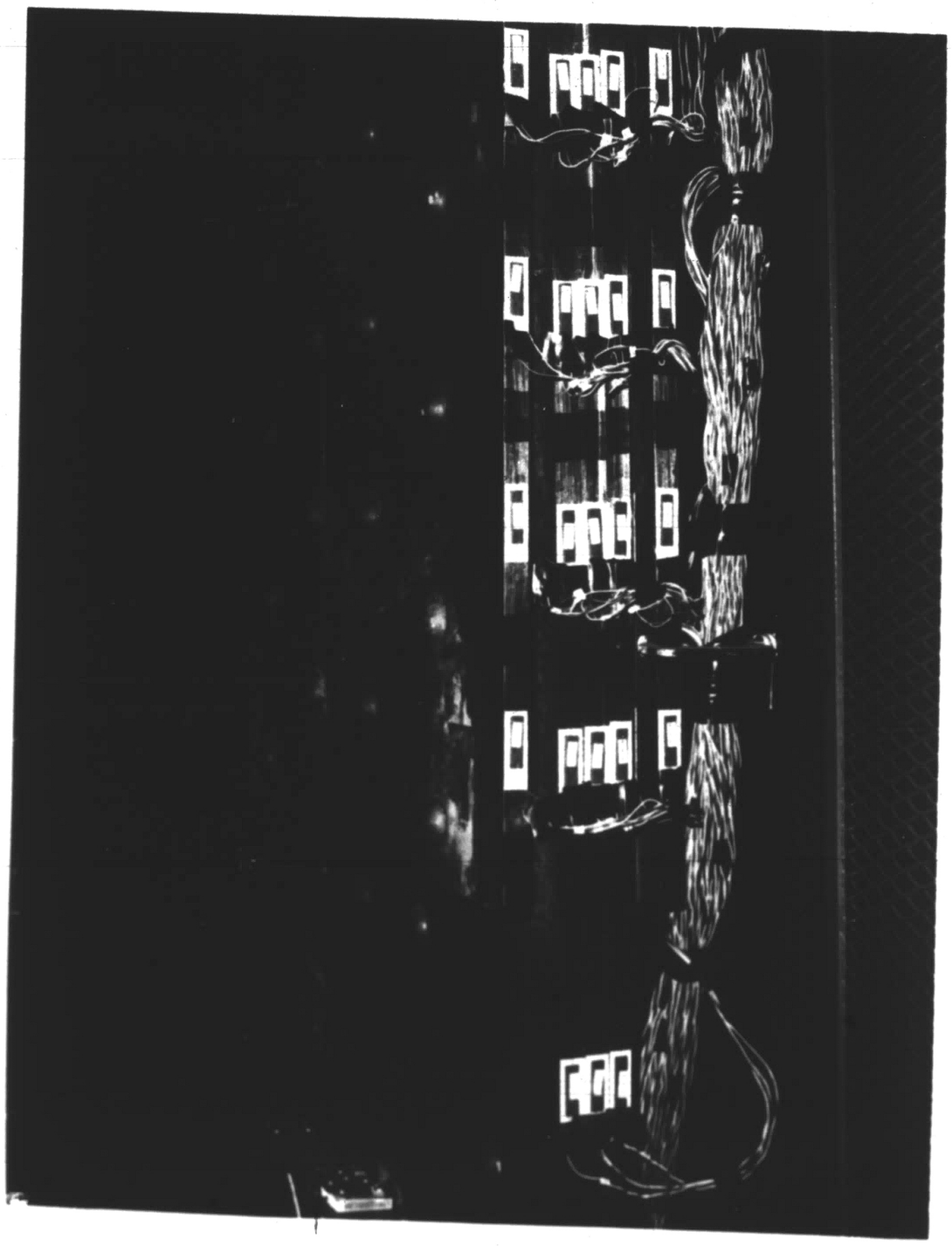

FIG. 28 MODIFIED RIVETED JOINT AFTER FAILURE

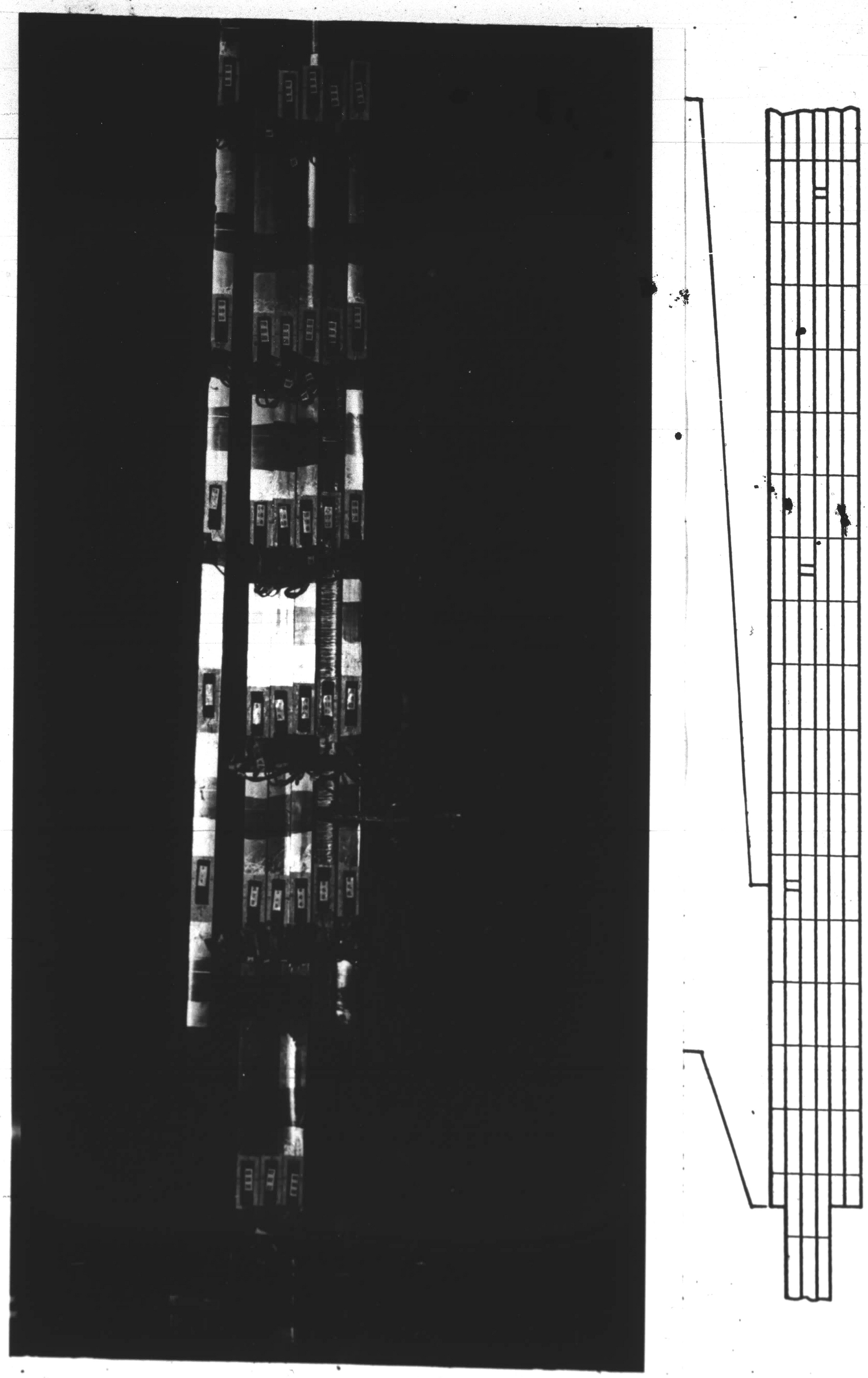

FIG. 29 MODIFIED RIVETED JOINT AFTER FAILURE - PORTION I

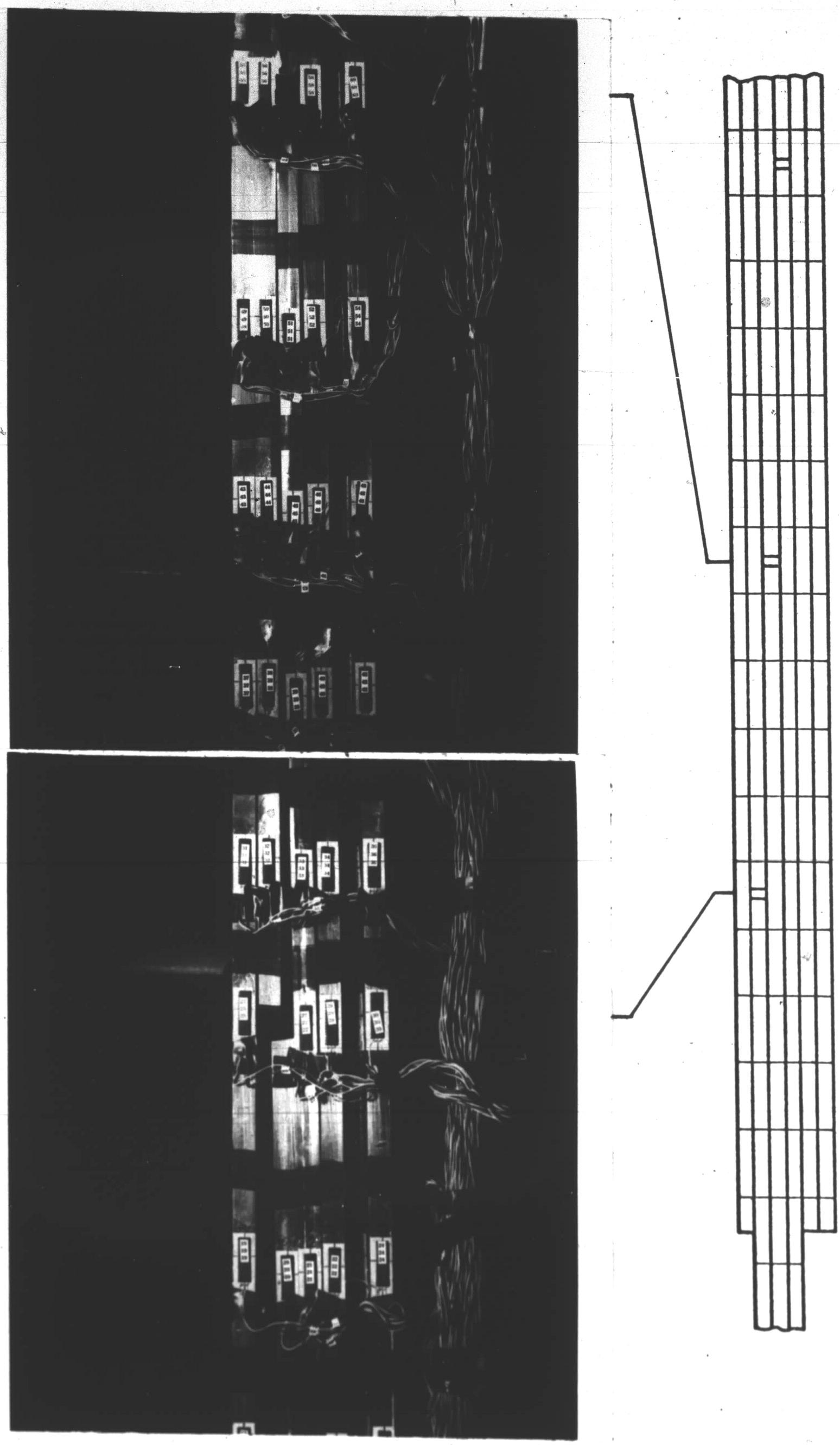

FIG. 30 MODIFIED RIVETED JOINT AFTER FAILURE - PORTION II

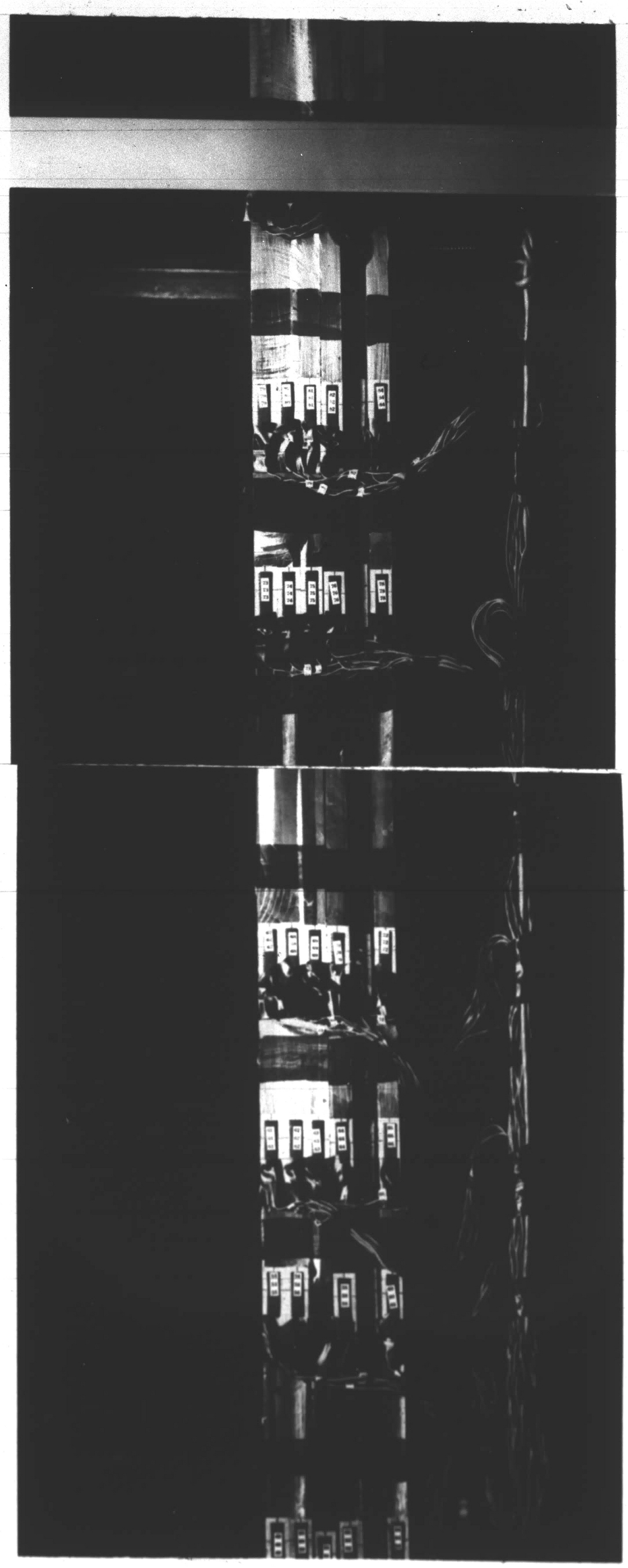

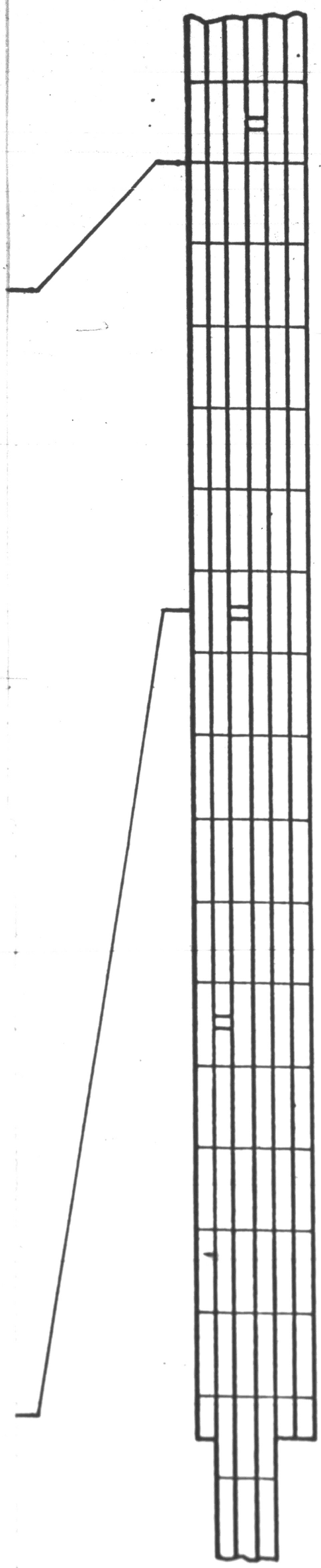

FIG. 31 MODIFIED RIVETED JOINT AFTER FAILURE - PORTION III

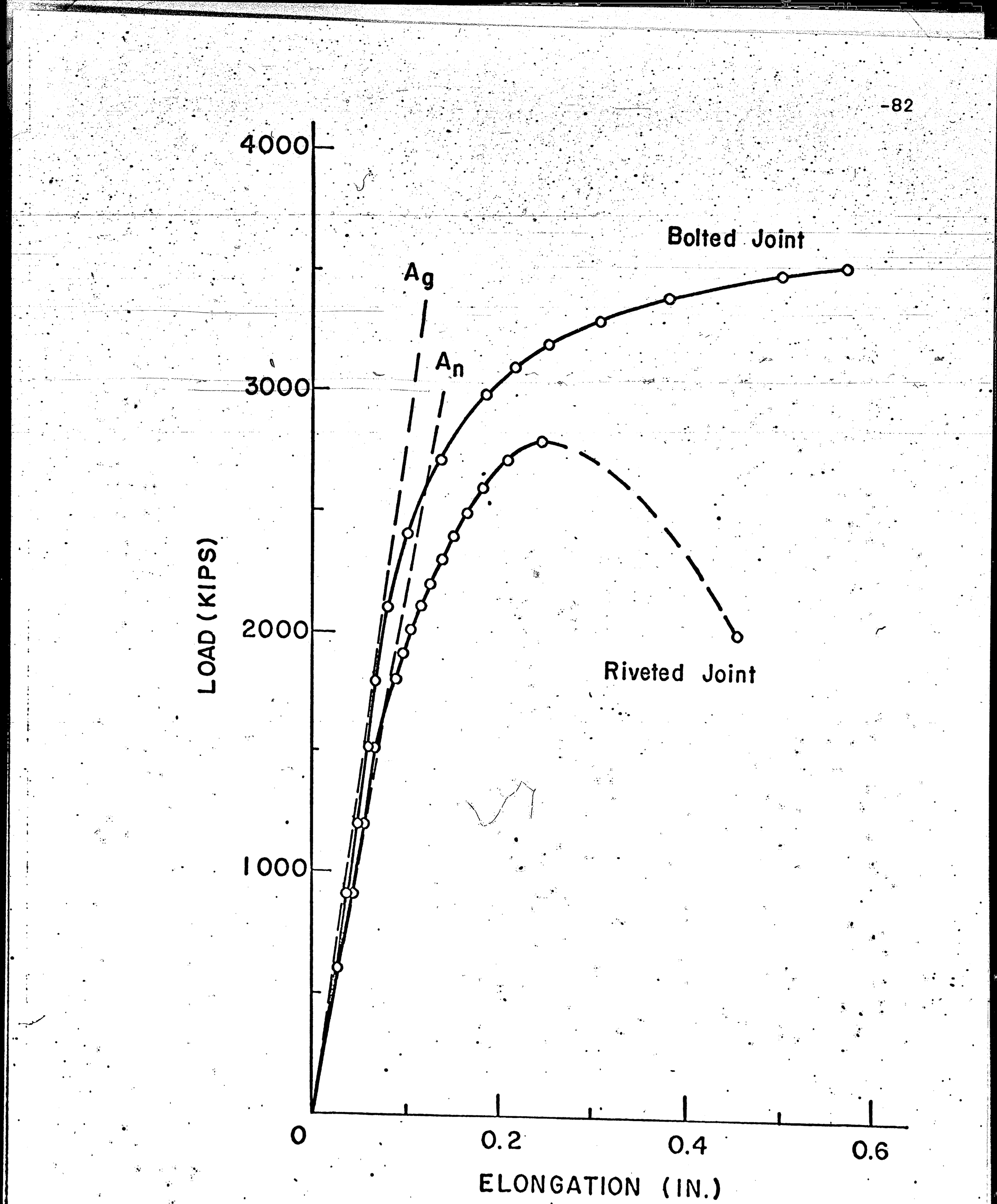

FIG. 32 COMPARISON OF LOAD-DEFORMATION CURVES OF MODIFIED BOLTED AND RIVETED JOINTS

FASTENER NUMBER

PLATE NO.	1	2	3	4	5	6	7	8	9	10	11	12	13	14	15	16
1		37	123	202	264	320	348	262	276	303	325	315	261		271	292	263
2	512	426	338	233	107		42	224	252	287	338	320	306		271	283	274
3	511	514	478	483	498	488	436	366	270	116		52	167		261	290	306
4	501	521	498	473	472	452	404	366	318	324	344	312	283		211	100	
5		12	39	65	93	130	153	162	216	262	252	257	245		246	269	298
6		14	48	68	90	134	141	144	192	232	265	268	262		264	290	383

P=1524 kips

FIG. 33 MEASURED LOAD DISTRIBUTION IN MODIFIED RIVETED JOINT

PLATE NO.	FASTENER NUMBER																
	①	②	③	④	⑤	⑥	⑦	⑧	⑨	⑩	⑪	⑫	⑬	⑭	⑮	⑯
①		83	196	291	387	461	478	395	392	408	443	420	384		384	411	363
②	711	565	441	301	145		82	190	320	375	458	435	428		379	387	386
③	585	663	650	648	644	614	565	490	320	158		81	218		354	393	430
④	683	678	670	631	612	603	535	530	528	470	505	455	323		274	138	
⑤		41	53	100	143	196	212	242	262	294	329	334	363		330	363	416
⑥		50	70	109	149	206	213	233	258	295	345	355	364		359	388	485

P = 2080 kips

FIG. 34 MEASURED LOAD DISTRIBTUION IN MODIFIED RIVETED JOINT

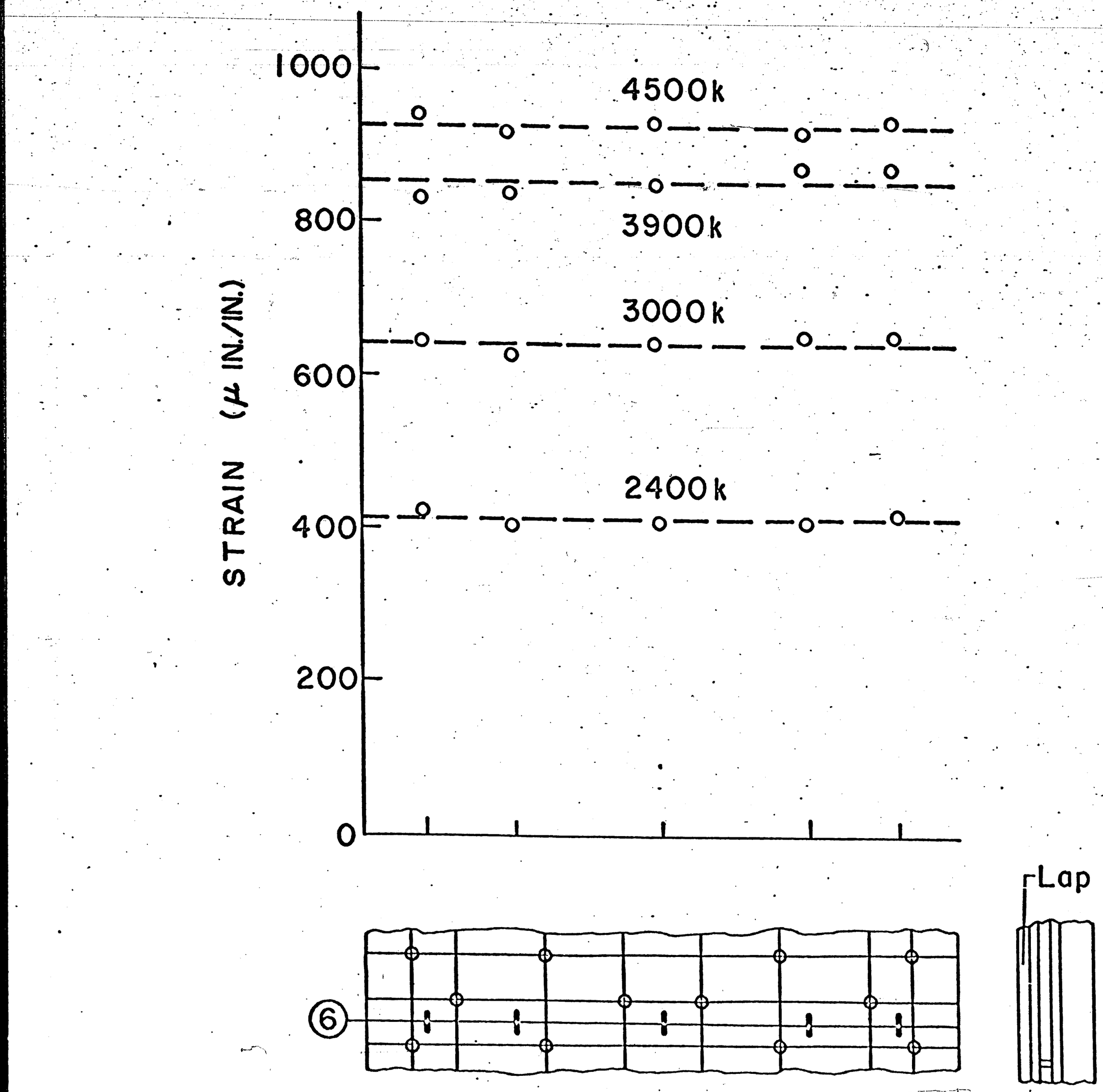

FIG. 35 STRAIN DISTRIBUTION ACROSS LAP PLATE
OF SIMULATED BOLTED BRIDGE JOINT AT SEVERAL LOAD LEVELS

PREVIOUS TEST

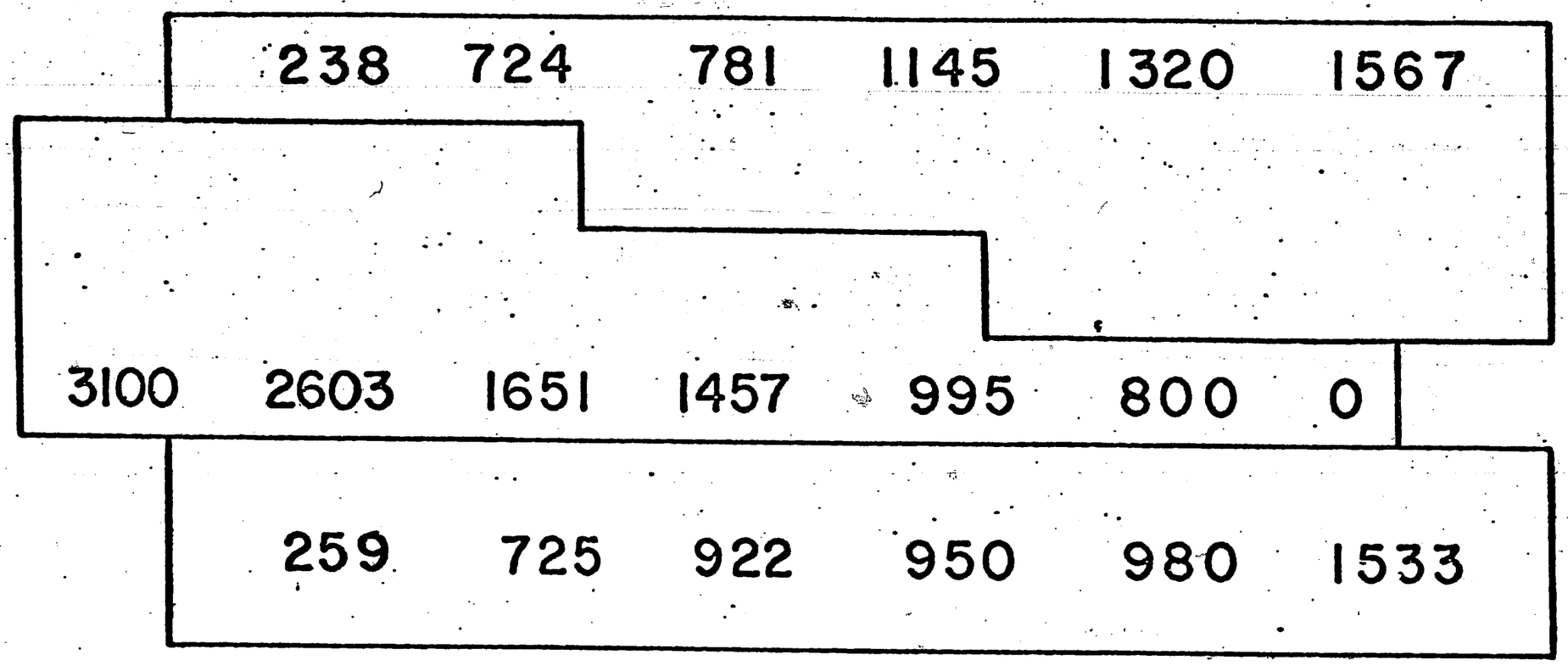

BOLTED JOINT Load in Kips

$\alpha \approx 0.50$

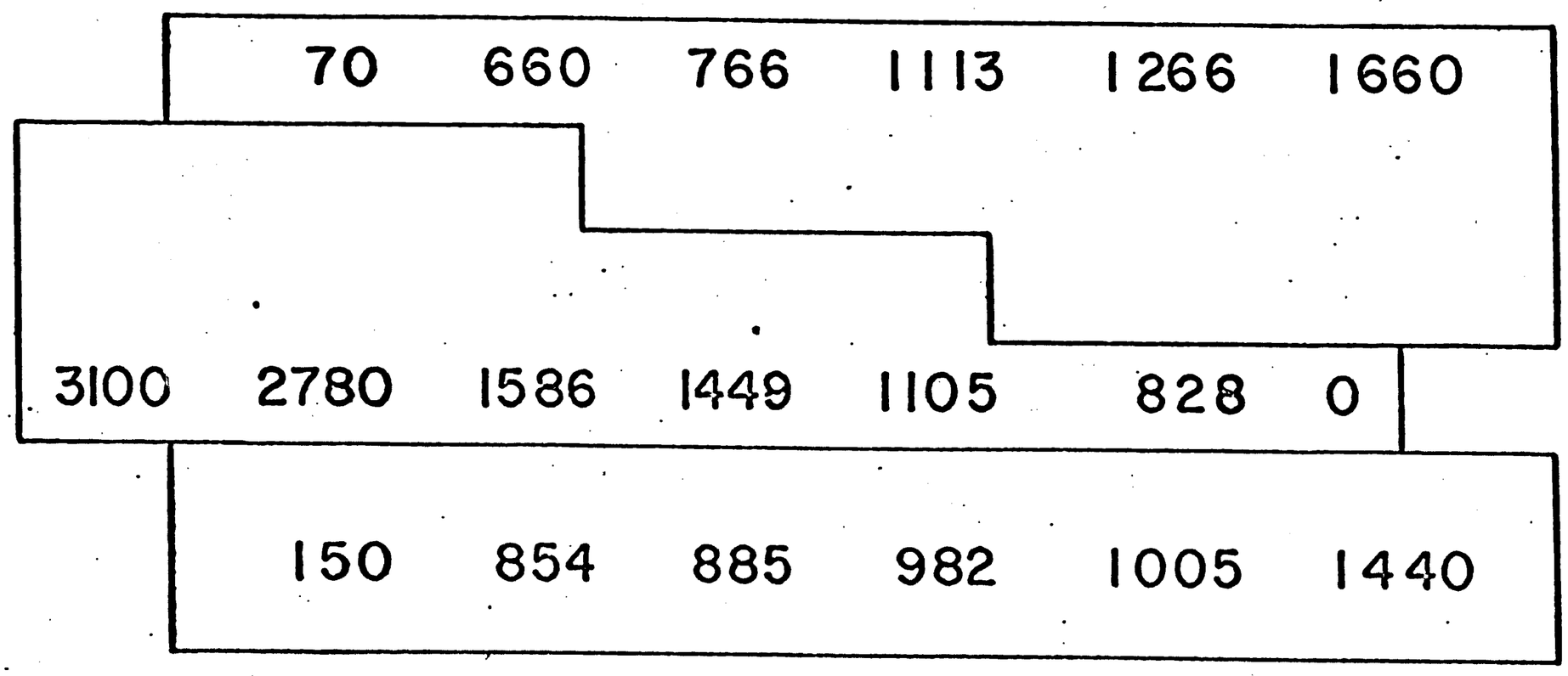

RIVETED JOINT Load in Kips

$\alpha \approx 0.54$

FIG. 36 INTEGRATED PLATE FORCES MEASURED AT THE DESIGN LOAD LEVEL - 3100 kips IN SIMULATED BRIDGE JOINTS

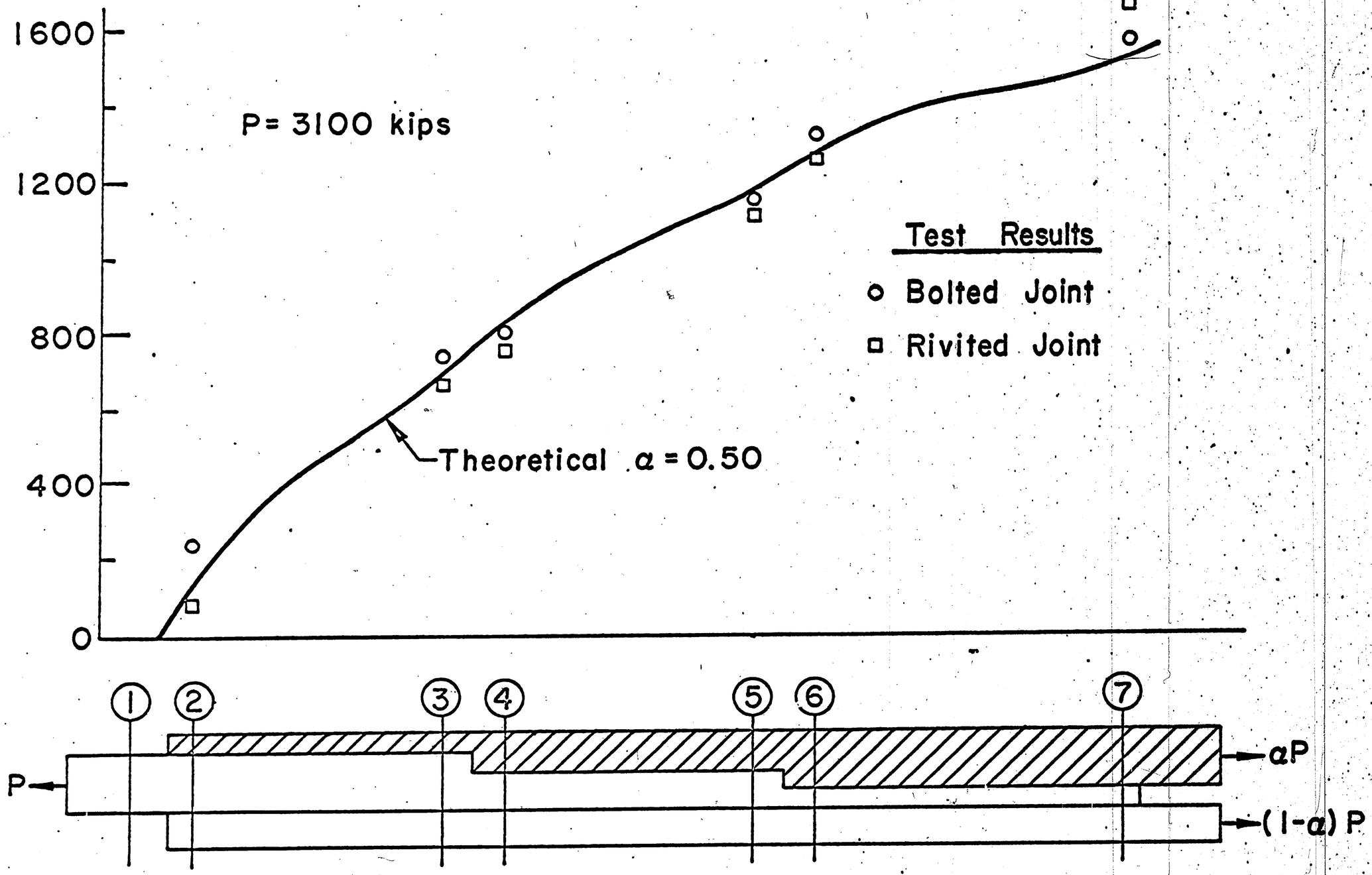

FIG. 37 COMPARISON OF THEORETICAL AND EXPERIMENTAL LOAD PARTITION IN SIMULATED BIRDGE JOINT (Top Plate)

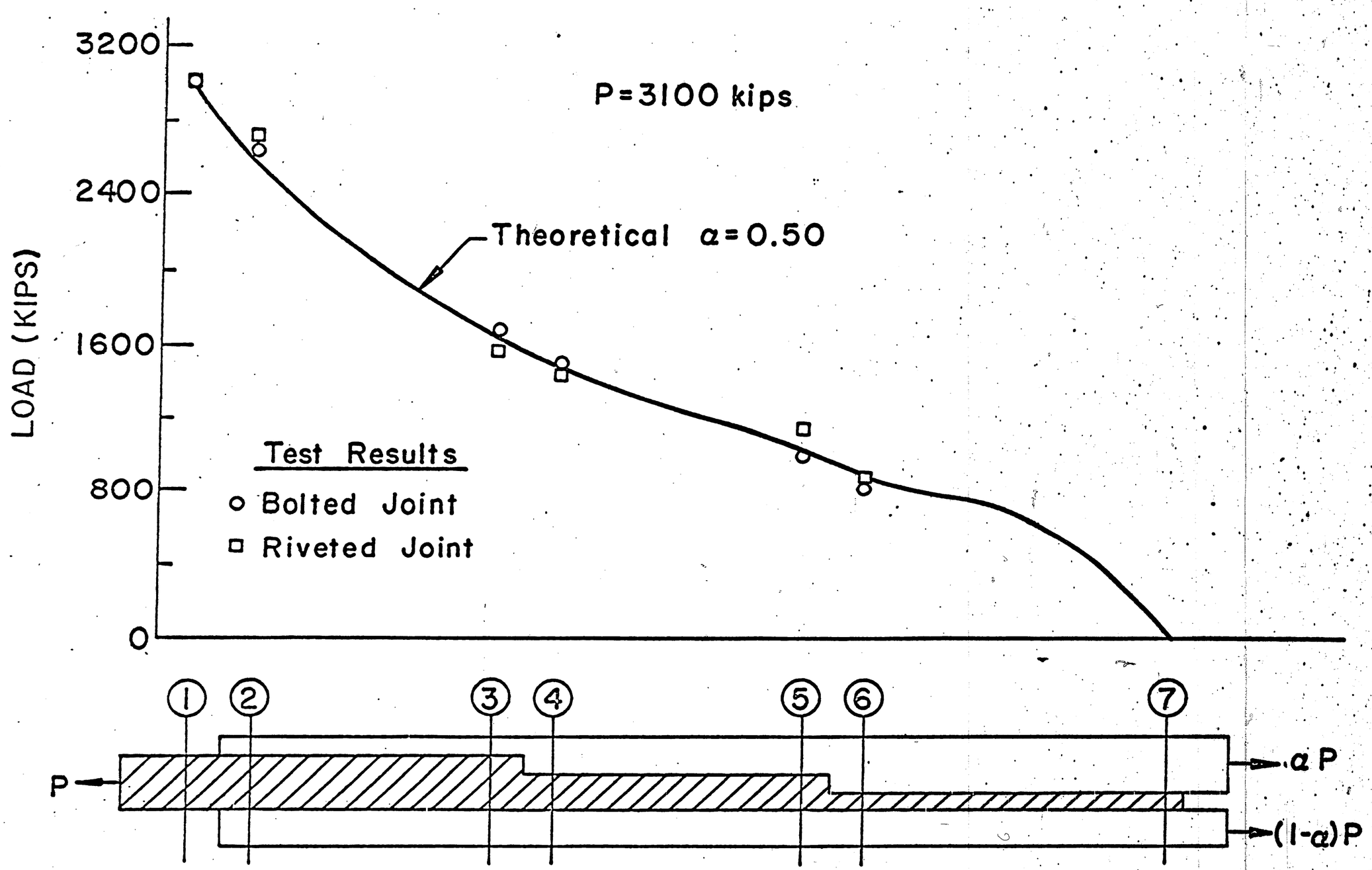

FIG. 38 COMPARISON OF THEORETICAL AND EXPERIMENTAL LOAD PARTITION IN SIMULATED BRIDGE JOINT (Middle Plate)

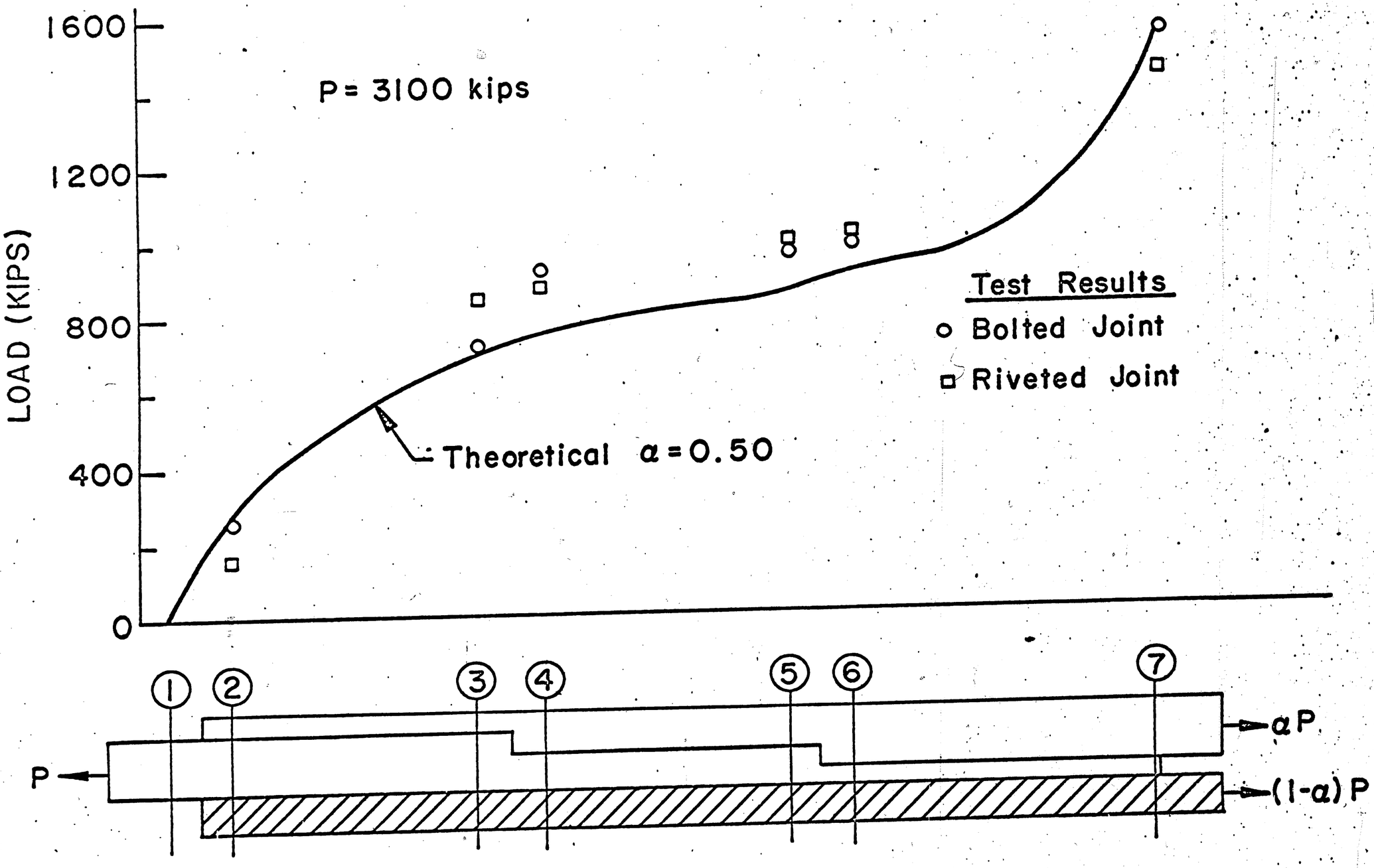

FIG. 39 COMPARISON OF THEORETICAL AND EXPERIMENTAL LOAD PARTITION IN SIMULATED BRIDGE JOINT (Bottom Plate)

FASTENER NO.

PLATE NO.	①	②	③	④	⑤	⑥	⑦	⑧	⑨	⑩	⑪	⑫	⑬	⑭	⑮	⑯	
①	0	75	159	303	420	514	545	676	726	783	818	861	937		937	998	1043	αP
②																		
③																		
④	2080	1942	1776	1492	1222	949	887	751	671	552	457	429	355		327	164	0	
⑤	0	63	145	285	438	617	648	653	683	746	805	790	788		808	918	1037	(1-α)P
⑥																		

P = 2080 Kips

α ≈ 0.50

FIG. 40 INTEGRATED PLATE FORCES IN MODIFIED BOLTED JOINT MEASURED AT A LOAD LEVEL OF 2080 kips

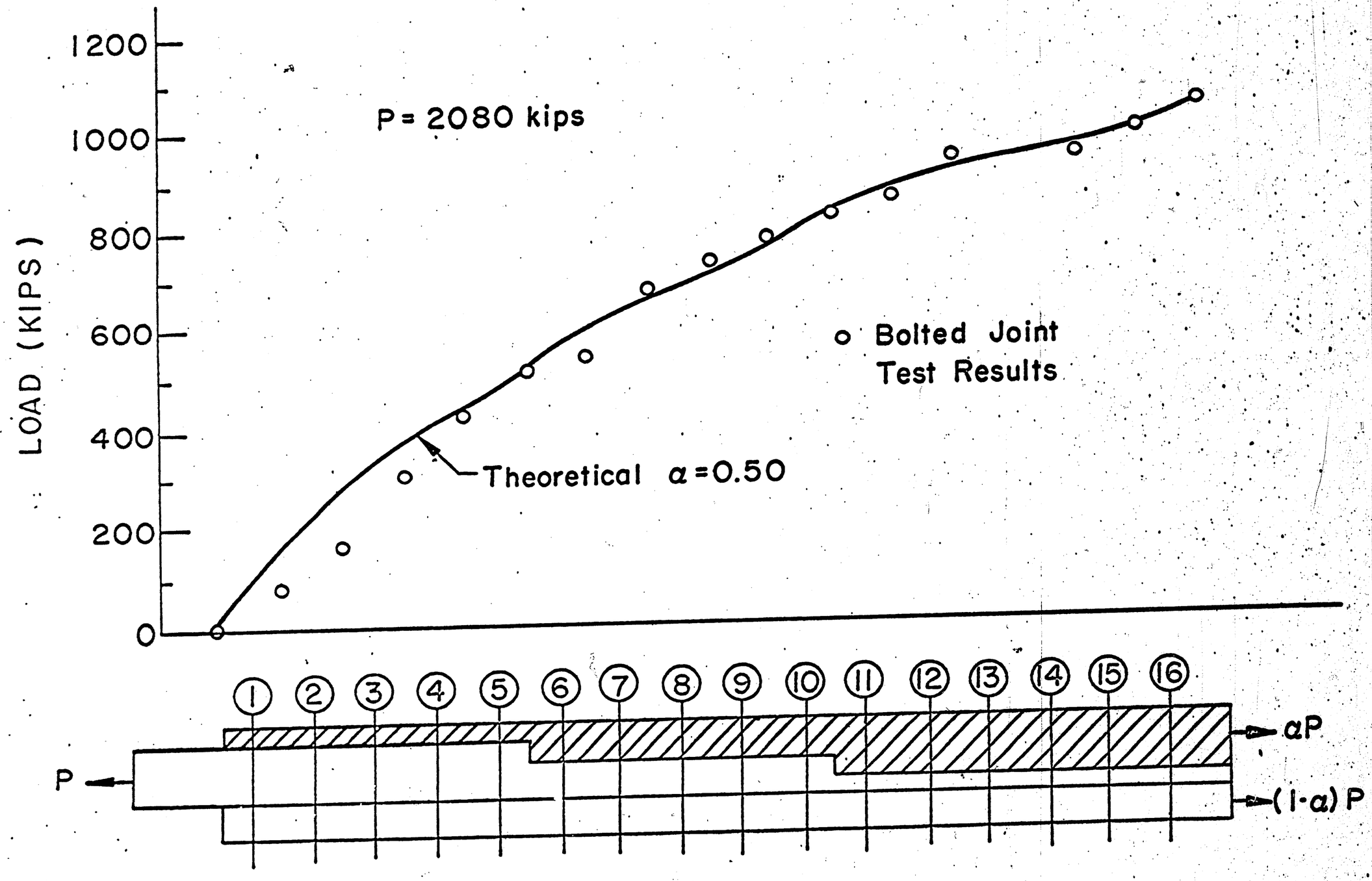

FIG. 41 COMPARISON OF THEORETICAL AND EXPERIMENTAL LOAD PARTITION IN MODIFIED BOLTED JOINT (Top Plate)

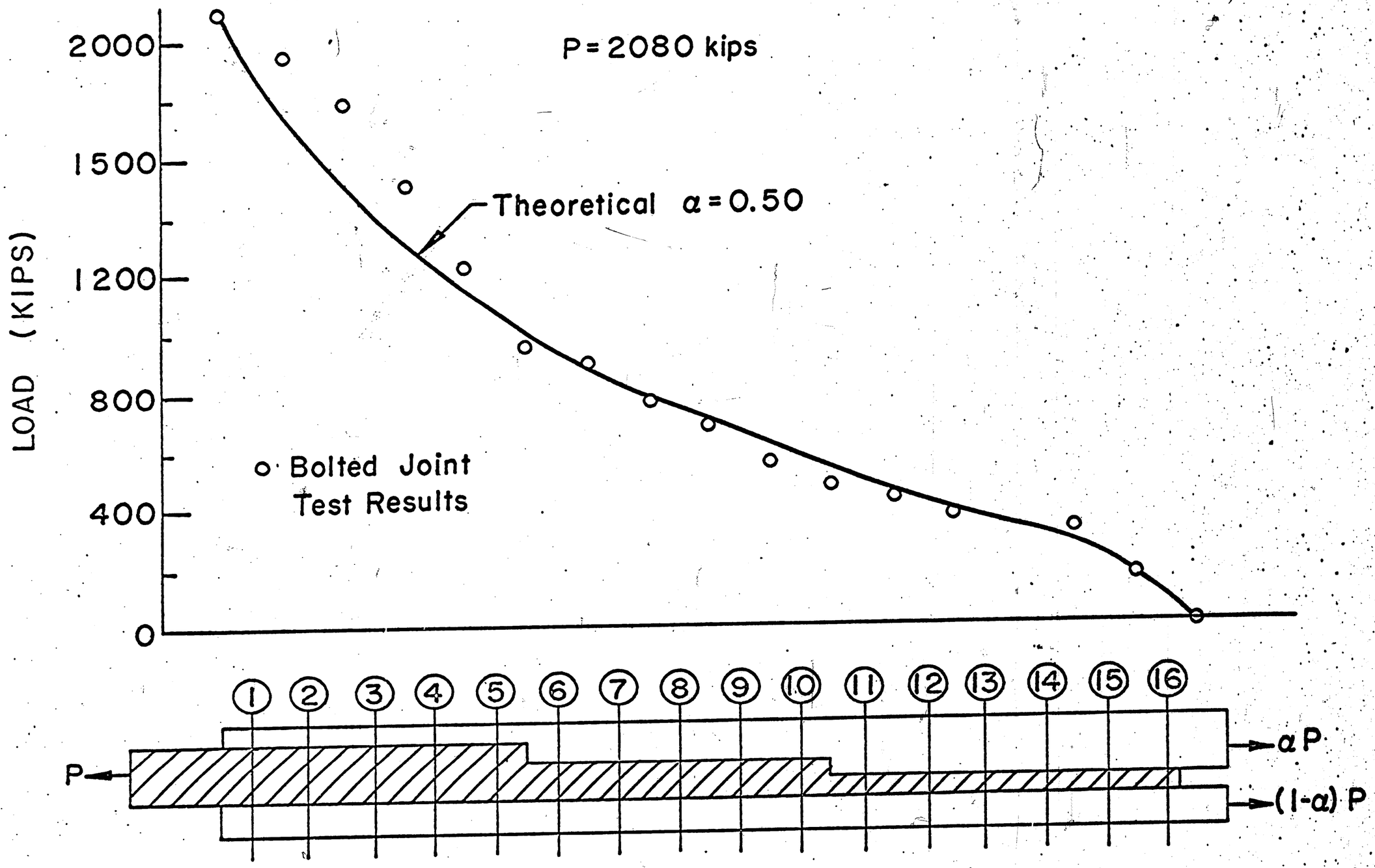

FIG. 42 COMPARISON OF THEORETICAL AND EXPERIMENTAL LOAD PARTITION IN MODIFIED BOLTED JOINT (Middle Plate)

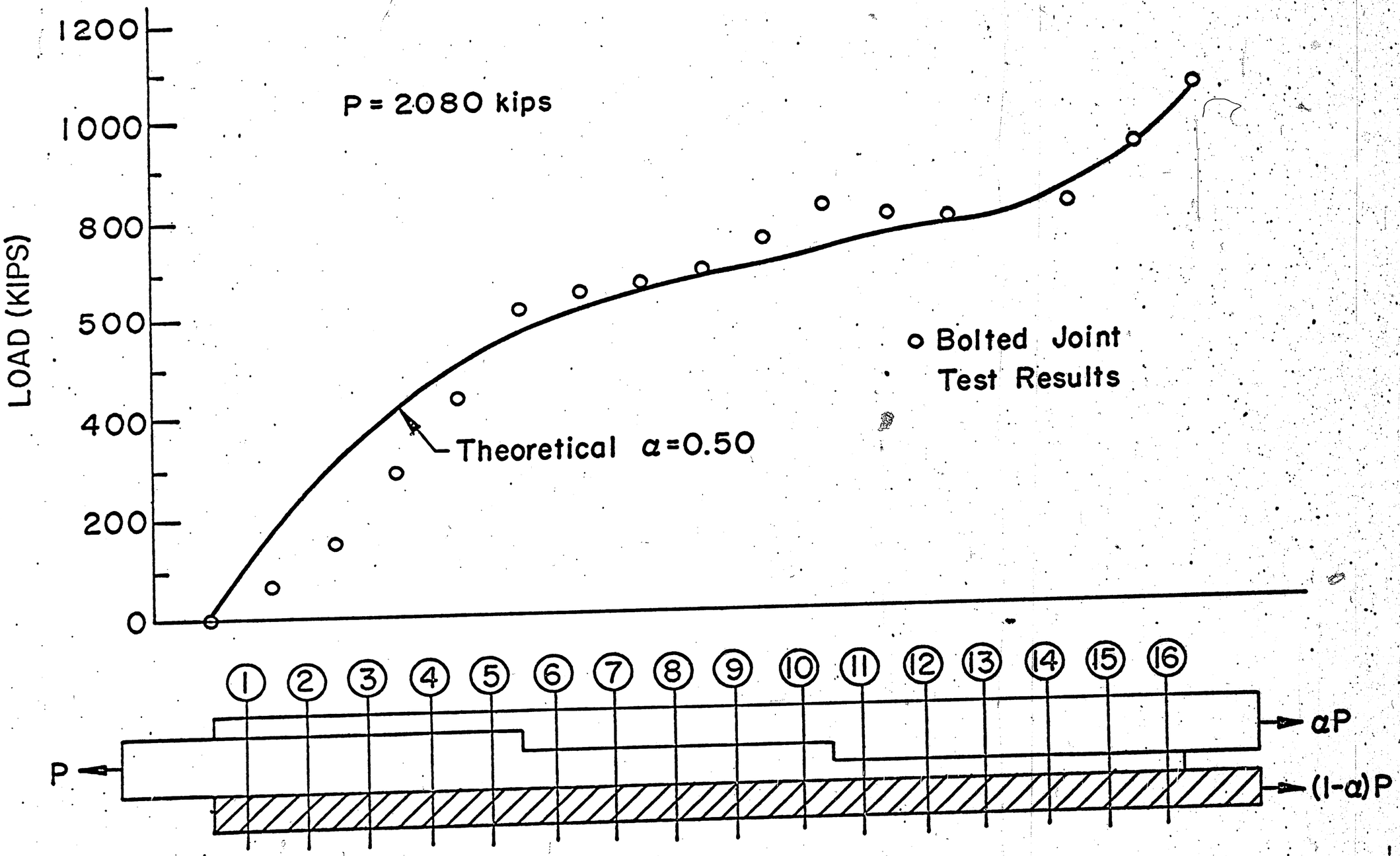

FIG. 43 COMPARISON OF THEORETICAL AND EXPERIMENTAL LOAD PARTITION IN MODIFIED BOLTED JOINT (Bottom Plate)

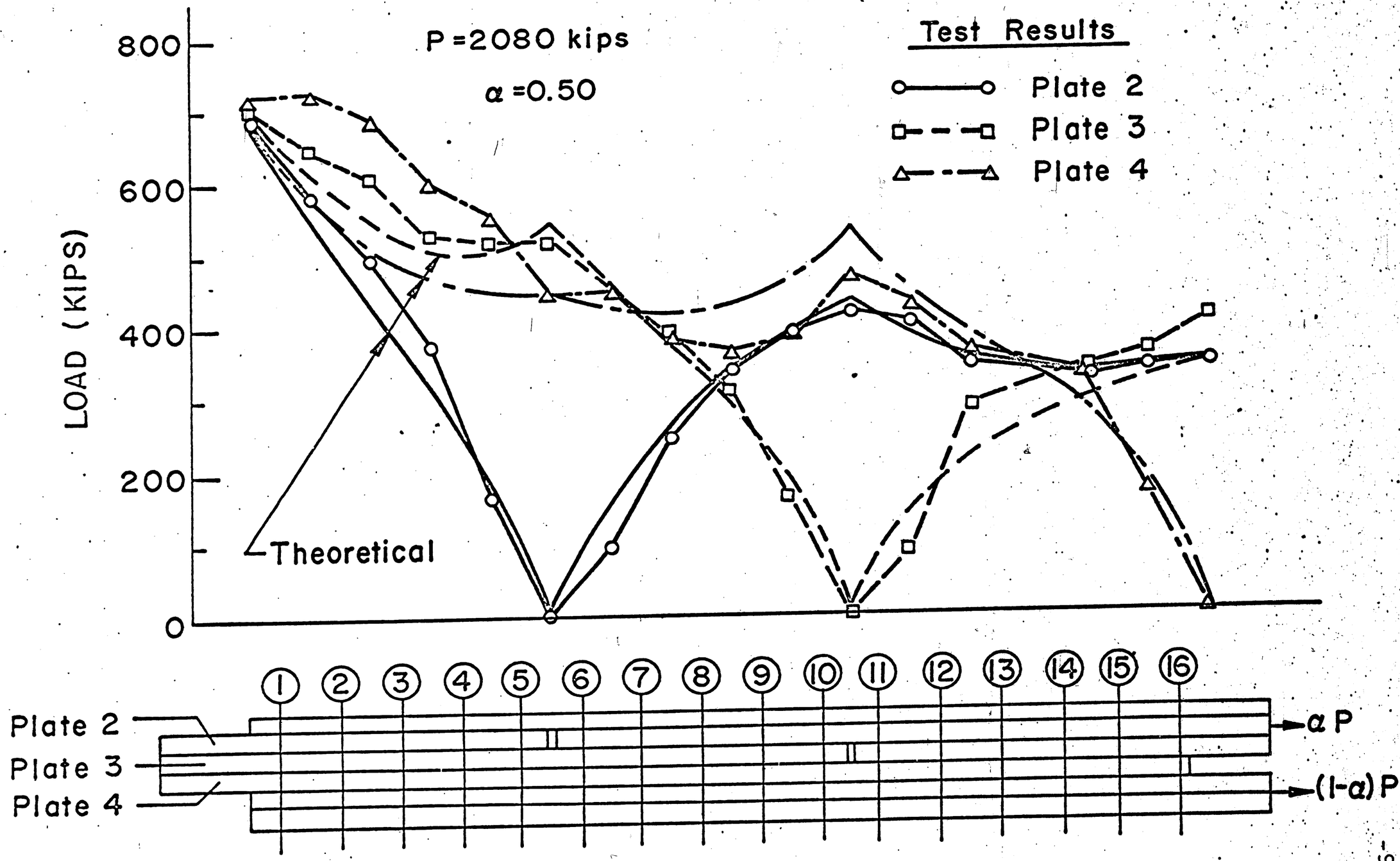

FIG. 44 COMPARISON OF THEORETICAL AND EXPERIMENTAL LOAD PARTITION FOR THE THREE MAIN PLATES IN MODIFIED BOLTED JOINT

REFERENCES

1. Yoshida, N. and Fisher, J. W.
LARGE SHINGLE SPLICES THAT SIMULATE BRIDGE JOINTS, Fritz Laboratory Report 340.2, Lehigh University, 1968

2. Davis, R. E., Woodruff, G. B. and Davis, H. E.
TENSION TESTS OF LARGE RIVETED JOINTS, Transactions, ASCE, Vol. 105, p. 1193, 1940

3. Armovlevic, I.
INANSPRUNCHNAHME DER ANSHLVSSNIETEN ELASTISCHER STABE, Zeithschrift fur Architekten und Ingenieure, Vol. 14, Heft, 2, p. 89, 1909

4. Batho, C.
THE PARTITION OF LOAD IN RIVETED JOINTS, Journal of the Franklin Institute, Vol. 182, p. 553, 1916

5. Bleich, F.
THEORIE UND BERECHNUNG DER EISERNEN BRUCKER, JULIUS SPRINGER, Berlin, 1921

6. Hrennikoff, A.
THE WORK OF RIVETS IN RIVETED JOINTS, Transactions, ASCE, Vol. 99, pp. 437-489, 1934

7. Vogt, F.
LOAD DISTRIBUTION IN BOLTED OR RIVETED STRUCTURAL JOINTS IN LIGHT-ALLOY STRUCTURES, U. S. NACA Tech. Memo No. 1135, 1947

8. Fisher, J. W. and Rumpf, J. L.
ANALYSIS OF BOLTED BUTT JOINTS, Transactions, ASCE, Vol. 91, No. ST5, 1965

9. Fisher, J. W.
BEHAVIOR OF FASTENERS AND PLATES WITH HOLES, Transactions, ASCE, Vol. 91, No. ST6, 1965

10. Fisher, J. W. and Beedle, L. S.
CRITERIA FOR DESIGNING BEARING-TYPE BOLTED JOINTS, Proceedings, ASCE, Vol. 91, ST5, October 1965

11. Fisher, J. W., Kulak, G. L. and Beedle, L. S.
BEHAVIOR OF LARGE BOLTED JOINTS, Highway Research Record No. 147, Washington, D. C., 1966

12. Foreman, R. T. and Rumpf, J. L.
STATIC TENSION TESTS OF COMPACT BOLTED JOINTS, Proceedings ASCE, Vol. 86, No. ST6, June, 1960

13. Tate, M. B. and Rosenfeld, S. J.
PRELIMINARY INVESTIGATION OF THE LOADS CARRIED BY INDIVIDUAL BOLTS IN BOLTED JOINTS, Technical Note No. 1051, National Advisory Committee for Aeronautics, Washington, D. C., 1946

VITA

Ulise C. Rivera was born on July 18, 1942 in Banes, Oriente, Cuba, the third child of Ernesto and Armelinda Rivera.

He received his primary education at Escuela Los Amigos in Cuba and Northeast Catholic High School in Philadelphia, Pennsylvania.

He received his Bachelor of Science Degree in Civil Engineering from Drexel Institute of Technology in Philadelphia in June 1967.

He entered graduate school in September 1967 in the Department of Civil Engineering, Lehigh University where he studied toward a Master of Science Degree and worked as a half-time research assistant in Fritz Engineering Laboratory.